THE CATALYTIC ACTIVITY OF ANODIC OXIDES ON ALUMINUM

by

Teresa Catherine Madeleine

Dissertation submitted to the graduate faculty of
Virginia Polytechnic Institute and State University
in partial fulfillment
of the requirements for the degree of

Doctor of Philosophy

in

Chemistry

Approved:

J.G. Dillard, Chairman

J.T. Taylor

J.P. Wightman

H.C. Dorn

G.L. Long

December, 1988

Blacksburg, Virginia

THE CATALYTIC ACTIVITY OF ANODIC OXIDES ON ALUMINUM

by

Teresa Catherine Madeleine

Committee Chairman: John G. Dillard
Department of Chemistry

(ABSTRACT)

The dehydration of isopropanol over anodic oxides was studied. The catalytic activity of the anodic oxides prepared in phosphoric, sulfuric, and oxalic acid was compared to the activity of γ-Al_2O_3. The effect of various thermal treatments on the catalytic activity was examined. IR spectroscopy proved useful for the study of the effect of thermal treatment on the acidity of the oxides. X-ray photoelectron spectroscopy (XPS) was employed to examine the oxide surfaces both before and after use as a catalyst.

The acidity of the oxides was studied by various methods and related to the activity of the oxides. The acidity of the oxide surfaces was studied by the adsorption of pH indicators on the oxide surfaces. The adsorption of gaseous bases, ammonia and pyridine, was studied by IR spectroscopy and temperature programmed desorption mass spectrometry. It was thus possible to differentiate between Lewis and Brønsted acid sites and to determine the quantity of the acid sites on the various oxides.

ACKNOWLEDGMENTS

The author would like to make the following acknowledgments:

Dr. John Dillard for his encouragement and guidance during graduate school.

Dr. Jim Wightman, Dr. Larry Taylor, Dr. Harry Dorn and Dr. Gary Long for their help as members of her committee.

Dr. Karl Wefers of The Aluminum Company of America for his help and guidance.

Alcoa and CIT for the author's stipend and additional support during her stay in graduate school.

The NSF and Commonwealth of Virginia for the funds for the purchase of many of the instruments used in this study.

Jim , Larry , and Dave of the electronics shop and Fred of the machine shop for all the help with maintenance and building of equipment.

Jack for his help with gas chromatography used in this study.

John for his help with the maintenance of the FTIR during the completion of this project.

Frank for help with the XPS analysis used in this study.

John Dillard's research group for their friendship and help.

The author's parents, and the

author's husband, for all their help, encouragement and support.

DEDICATION

This dissertation is dedicated to my parents

for their love, support and encouragement.

TABLE OF CONTENTS

List of Figures

List of Tables

Chapter 1

INTRODUCTION

Anodized aluminum has been used for corrosion protection and decorative purposes, as a porous substrate for coatings and adhesives, for insulation in multilevel large scale integrated circuits, and in other semiconductor devices(1). Recently, anodized aluminum has been used as a catalyst in the dehydration of alcohols and the isomerization of butenes(2-18). It has been shown that anodic aluminum oxides are more active than γ-Al_2O_3 in the dehydration of alcohols(13). In the study of anodized aluminum as a catalyst, only Yamada and Itabashi(16) have compared anodic oxides prepared under different conditions. However, no studies have been reported where the activity of γ-Al_2O_3 was compared with the activity of anodized aluminum prepared in different electrolyte solutions and anodized for different lengths of time. There have been no studies of the x-ray photoelectron or infrared spectroscopic characterization of anodic oxides in conjunction with studies of the catalytic properties of the oxides.

Anodized aluminum has a porous structure which can be reproducibly prepared. The pore structure of the anodic

oxide can be tailored by the anodization conditions(8). The ability to tailor-make the oxide makes the anodic oxide an ideal catalyst for model reactions.

Transition aluminas(γ-Al_2O_3 and α-Al_2O_3) are extensively used as catalysts in the dehydration of alcohols(19-63). The transition aluminas contain Lewis and Brønsted acid sites produced by dehydroxylation or anion additions, both of which have been reported to act catalytically(19-22) in the dehydration of alcohols. The dehydrogenation of alcohols results from the presence of basic sites(64-70). Acid sites are typically characterized by the adsorption of pH indicators(72-78) and of gaseous bases(28,79-95). The nature of adsorbed bases is studied by infrared spectroscopy(28,79-88) and temperature programmed desorption mass spectrometry(89-95). Acidic sites on anodic aluminum oxides are thought to be present and have a strong influence on the adhesive, electrical, and passivation properties in non-catalytic applications(1). It has been speculated that the acidic sites have a strong influence on the catalytic properties of anodic aluminum oxides(12-18). There have been no attempts to quantify experimentally or to determine the nature of the acid sites on anodic aluminum oxides or to relate the catalytic properties of the oxides to their surface properties. No reports have investigated the

effect various pretreatments have on the catalytic activity of anodic aluminum oxides or the mechanism by which alcohols are dehydrated over anodic aluminum oxides.

In the first part of this dissertation, the catalytic activity for the dehydration of isopropanol by sulfuric, phosphoric, and oxalic acid anodic aluminum oxides and by γ-Al_2O_3 is compared. The roles of pore size, anodizing electrolyte, acid sites, and surface area are discussed to account for differences in activity observed among the anodic oxides and γ-Al_2O_3. The effect of various thermal pretreatments on the activity of anodic aluminum oxides is examined. The effect of a thermal pretreatment was measured by IR spectroscopy. To determine if the length of the pore is important, the activity of oxides of various thicknesses was also investigated. To determine if the incorporated electrolyte is affected under the extreme conditions of the catalytic reaction, (i.e. by loss or migration of the electrolyte) x-ray photoelectron spectroscopy(XPS) was used to study anodized aluminum surfaces.

The second part of this dissertation characterizes the acid sites on the anodic oxides. Since the dehydration of alcohols is an acid catalyzed reaction, it is important to understand how the pretreatment conditions affect the acidity of the oxide. The effect of thermal pretreatments on the acidity of the anodic oxides was studied first by

the adsorption of pH indicators. The adsorption of pH indicators is a qualitative method for detecting changes in the overall acidity. The adsorption of ammonia and pyridine on the Lewis and Brønsted acid sites of anodic oxides was studied by transmission infrared spectroscopy. It was not possible to study the acidity of oxalic acid anodized aluminum by infrared(IR), since the IR absorption bands due to oxalate incorporation into the oxide occur in the same region as the bands due to adsorbed ammonia and pyridine. To complete the investigation, temperature programmed desorption mass spectrometry was used to study the desorption of pyridine from sulfuric, oxalic, and phosphoric acid anodic aluminum oxides and unanodized aluminum.

Chapter 2

HISTORICAL

A. STRUCTURE OF ANODIZED ALUMINUM

Anodization refers to the use of a "valve" metal, such as aluminum, as an anode in an electrolytic cell. The type of anodic oxide film produced depends on the solubility of the oxide film in the electrolyte. When the oxide is not soluble, a nonporous or barrier oxide film is produced; however, when the oxide is soluble, a porous oxide film is formed(96). The porous oxide film consists of a thin barrier layer underneath a thicker porous oxide layer. The thickness of the porous layer is dependent on the length of the anodization, the current density, and the solubility of the oxide film in the electrolyte solute. The conditions that affect the solubility of the oxide film include the temperature, the pH and the concentration of the solution. The thickness of the barrier layer is dependent on the anodization voltage and independent of the length of the anodization.

A number of investigators have discussed the structure of anodic oxides on aluminum. After studying phosphoric acid anodic aluminum oxide by transmission electron microscopy, Keller, Hunter and Robinson(97) proposed the structure shown in Figure 1. The model consisted of star-

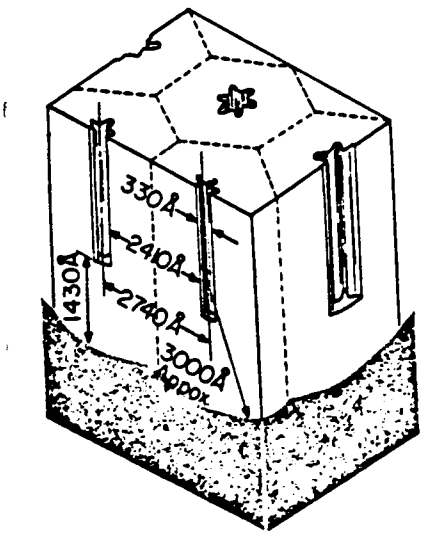

Figure 1. Structure of anodic aluminum oxide proposed by Keller, Hunter and Robinson(97).

shaped pores which were in the center of the hexagonal shaped oxide cell and perpendicular to the aluminum metal. The pore diameter was dependent on the electrolyte used. The thickness of the barrier layer and the cell width were dependent on the anodization voltage. In a similar study, Wood, O'Sullivan and Vaszko(98) studied sections of phosphoric acid anodic aluminum oxide by electron microscopy and confirmed Keller's model in principle; however, they found no evidence for the star-shaped pores. Franklin and Stirland(99) studied the optical anisotropy of anodic aluminum oxide films. They found the pores were not completely perpendicular to the metal substrate, as previously thought. The axis of the pores slanted toward the metal surface and the degree of axis slant was dependent on the substrate grain orientation.

Csokan(100) reported that hard anodization (films formed at low temperatures) of aluminum produced an irregular pore distribution. The pores were twisted, bent and distorted. The pores at the surface of the oxide appeared to have a fibrous structure whose size, shape and orientation varied considerably. Ginsberg and Wefers(101) also observed a fibrous type structure after a hard anodization. The oxide consisted of hollow fibers standing vertically with respect to the aluminum surface.

Murphy and Michelson(102) proposed a colloidal gel

model, which consisted of three layers: (1) an inner, compact, anhydrous form of alumina; (2) an intermediate, transition region, where the conversion of the inner anhydrous region to an outer region of high hydration was seen; (3) an outer region, consisting mainly of hydrated oxide. Murphy and Michelson suggested that the outer layer possessed the precursors of the pores, which they observed upon electron optical examination. A few authors (102,103) assumed that the electric field strength present during the anodization was sufficient to draw hydroxide ions and water molecules in the direction of the barrier layer, causing the barrier layer to become hydrous in localized regions, decreasing the barrier layer thickness. At the same time, the electric field at the interface caused the migration of protons away from the barrier layer,thereby deprotonating or dehydrating the oxide in this region. Murphy and Michelson(102) used these two opposing actions to explain the dependence of the barrier film thickness on the applied formation voltage. Bogoyavlenski(104) proposed a model in which the film was composed of micelles of $Al(OH)_3$ gel-like material oriented vertically to the aluminum surface by the electric field. These micelles were separated by pores through which further material required for growth was transported. Shreider(105) also suggested the films were composed of a gel-like $Al(OH)_3$. The model proposed by

Shreider was essentially the same as the model proposed by Keller, Hunter, and Robinson(97), except for the composition of the film. Diggle et al.(96) pointed out that the models proposed by Murphy and Michelson(102) and Bogoyavlenski(104) lacked experimental verification, while a cylindrical pore model had some experimental verification from direct microscopic measurements.

B. PORE FORMATION THEORIES

Many theories have been proposed to account for porous oxide film formation, including those proposed by Setoh and Miyata(106,107) involving nascent oxygen, Wernick(108) involving peptization of an $Al(OH)_3$ gel, Baumann's(109) oxide kernel theory, and Akahoni's theory(110) involving vaporization of the electrolyte and melting of aluminum.

Pore formation is not a simple matter; there are a number of factors that can affect the actual pore formation. Evidence for electrolyte involvement in pore formation was reported by Barrett(111), Hunter and Towner(112), and Dunn(113). Kissan(114) suggested porous film preparation required either di- or trivalent anions. Murphy(115) believed that both protons and anions were involved in the formation of porous films. Morfopoulos and Parruva(116) and Yokata(117) showed, through electrokinetic studies, that protons and hydroxide ions were the controlling ions for alumina film formation. Murphy(115)

showed that pore density decreased with decreasing pH of the electrolyte solution. Tajima et al.(118) suggested that the electrolyte anions underwent discharge during oxide film formation. These discharged anions then replaced oxygen atoms in the lattice. Dunn(113) reported the tendency for non-pore forming electrolytes to form pores over long anodizing periods. Brock and Wood(119) suggested that hydration played an important role in pore formation, since no pores were observed for anodic oxides produced in nonaqueous borate solutions while pores were observed for preparations in aqueous borate solutions. Franklin(120) believed that the difference between porous and non-porous films was due to the pH of the solution. Keller, Hunter and Robinson(97) suggested there were "weak" spots in the barrier layer where enhanced dissolution of the barrier layer occurred. Hoar and Mott(103) proposed an electric field assisted process where OH^- ions from the dissolution of alumina migrated through the barrier layer to the metal-oxide interface, combining with Al^{3+} to produce the barrier oxide layer. Hoar and Yakalom(121) thought the importance of the proton in the initiation process was due to proton entry into the barrier layer at low electric field strength. These sites of entry then became points of high local current density with high dissolution rates and pore formation.

C. CATALYSIS

In addition to the work reported in the literature concerning the growth mechanism of anodic oxides, there have been a number of reports on the use of anodic aluminum oxide as a catalyst. Ruckenstein et al.(2-10) and Skoulikidis(11) carried out initial studies on the use of both porous and non-porous oxide films as catalysts. Only the results of the experiments over the porous oxides will be discussed. Ihm and Ruckenstein(2) studied the dehydration of isopropanol over oxalic acid anodized aluminum oxide films. The oxide layer was removed from the aluminum metal in a mercury chloride solution and calcined at temperatures between 550°C and 700°C prior to use as a catalyst. Water and propene were the reaction products detected between 300°C and 390°C. It was shown that reactions over anodic oxide catalysts have smaller activation energies than over other alumina catalysts.

Rai and Ruckenstein(3) discussed a method of anodizing a sheet of aluminum with parallel cylindrical pores, open at both ends. This was achieved by placing two sheets of aluminum foil in intimate contact so the barrier layer was located in one piece of foil and the other piece of foil possessed open pores and no barrier layer. Rai and Ruckenstein(3) impregnated oxalic acid anodized aluminum with Ag^{o} or MoO_3 and showed transmission micrographs of

each sample. They suggested that the films would be ideal for systematic studies of heterogeneous catalysis, since these materials could be tailor-made with defined pore geometries; however, no catalytic results were reported.

Ihm and Ruckenstein(4) compared nitrogen adsorption and transmission electron microscopy for the measurement of the pore size distribution on oxalic acid anodized foil containing parallel cylindrical pores. The results of the characterization of the pore size distribution are shown in Table 1. They compared the values obtained by N_2 adsorption, using three different equations to compute the pore size distribution; the Kelvin, Cohan, and Broekhoff-deBoer equations. The Broekhoff-deBoer method for the desorption branch of an open cylindrical pore gave the best agreement with the electron microscopy measurements(Table 2).

Chu and Ruckenstein(8) proposed various procedures for obtaining oxides containing parallel cylindrical pores of uniform diameters. The authors showed that the size and density of the pores could be controlled by selecting appropriate preparative conditions. Pores larger than 60Å were obtained by anodizing 2.5 μm thick aluminum sheets in a 5 or 10 weight percent sulfuric acid solution at 0°C at various voltages between 20V and 40V, followed by etching for several minutes in a 48 weight percent phosphoric acid

TABLE 1

Pore Characteristics of Oxalic Acid Anodic Oxides on Aluminum as Determined by TEM(4)

	ANODIZING VOLTAGE (V)				
	50V	45V	40V	35V	30V
Diameter, Dp(nm)	128	116	104	92	80
Density x 10^9 (number of pores/cm^2)	4.6	5.8	7.2	9.6	13

TABLE 2

Ratio of the pore volume and the surface area V_p/s (cm^3/m^2) x 10^2 given by various methods(4)

ANODIZING VOLTAGE (V)	TEM	Broekhoff -DeBoer*	Kelvin	Broekhoff -DeBoer**	Cohan
40	2.6	2.0	1.6	1.5	0.9
45	2.9	2.9	2.2	1.9	1.3
50	3.2	3.3	2.0	2.4	1.4

* Desorption

** Adsorption

solution. Higher pore densities were obtained by lowering the applied voltage. Pores with radii less than 60Å were obtained by anodizing 30-60 mm. thick aluminum films, prepared by vapor deposition, in a 5 weight percent sulfuric acid bath at 0°C.

Skoulikidis(11) compared Ihm and Ruckenstein's(2) work on porous oxides as catalysts to similar work he had carried out. Skoulikidis indicated that he and his co-workers had first shown the superiority of electrolytically prepared aluminum oxides as a catalyst with the dehydration of formic acid over sulfuric acid anodized aluminum. The authors studied the influence of (a)the current density of preparation, (b)the thickness of the oxides, and (c)the doping of the oxides, by direct anodic oxidation of suitable aluminum alloys. Skoulikidis (11) reported that $Al_2O_3 \cdot 3H_2O$ formed on the catalyst surface via reaction with H_2O produced in the dehydration of formic acid. Water sealed the pores of the anodic oxides without affecting the rate or the activation energy of the reaction.

Hönicke(12-15) studied the formation of anodic oxides in sulfuric acid, and their activity as catalysts in the dehydration of isopropanol, the isomerization of the individual isomeric n-butenes, and the partial oxidation of 1,3-butadiene. The activity of sulfuric acid anodized aluminum was compared to the activity of α- and γ-Al_2O_3 in

the dehydration of isopropanol and the isomerization of butenes(12,13). Hönicke found that the anodic aluminum oxide structure could be reproduced, the pore diameter and oxide thickness could be varied and preselected within certain ranges by applying certain conditions of anodization(12). In the dehydration of 2-propanol to propene(13), the reaction rate, based on the surface area for the anodized aluminum(oxide + Al), was thirty times larger than that on γ-Al_2O_3. In the isomerization of the individual isomeric n-butenes, anodic aluminum oxide was more active than γ-Al_2O_3. The higher reaction rate was attributed to the presence of acid sites produced by the incorporation of SO_4^{2-} anions and water during anodic oxidation in sulfuric acid (14,16-18); however, their presence was never experimentally verified.

Hönicke(14,15) discussed the partial oxidation of 1,3-butadiene over V_2O_5/Al_2O_3/Al-coated catalysts. In these studies fresh sulfuric acid anodized aluminum wire was immediately immersed in an impregnation solution of NH_4VO_3 and oxalic acid at a pH of 4.5 and temperature of 70°C. In the study, a large number of products were formed at low conversion levels. Hönicke suggested this was due to the uniform texture of the V_2O_5/Al_2O_3/Al-coated catalyst system. He reasoned that the unbranched short pores of uniform pore lengths allowed a rapid transport of

intermediates into the bulk gas phase. He then chose to test whether the selectivity of individual products could be influenced by the variation of the texture of the catalysts,in particular the pore lengths,and hence the variation of the intrinsic residence times(15). The catalyst with the longest pores showed the highest activity and the catalyst with the shortest pores showed the lowest activity. These differences in activity could have been caused by different specific surface areas, by different average vanadium content, and/or by different ratios of catalytically active vanadium surface area to mass of vanadium of the three catalysts. Once the results were adjusted for surface areas the activity sequence of the catalysts reversed, the catalyst with the shortest pores showed the highest activity and the catalyst with the longest pores showed the lowest activity. The calculated activity of the catalyst was then adjusted for vanadium content. After adjusting for surface area and vanadium content, it was concluded that the activity of the catalysts was only dependent on the vanadium content. It was also found that the catalyst with the shortest pores provided the highest selectivity, and the catalyst with the longest pores provided the lowest selectivity. Hönicke proposed the following explanation for the dependence of the product selectivity on the pore length of the

consecutive reaction of type:

A->B->C (Figure 2)

In the first step reactant A was converted into the intermediate B both in a short pore with length lp_1 and in a long pore with the length lp_2. In the short pore(lp_1) no further reaction of B took place due to its limited residence time. Therefore, B migrated out of the pore into the gas phase. In the long pore(lp_2), intermediate B was converted to the final product C due to the enhanced intrinsic residence time of B.

Yamada and Itabashi(16) studied the catalytic activity of sulfuric acid, oxalic acid, and phosphoric acid anodized aluminum in the dehydration of cyclohexanol. The physical and chemical properties of the oxides were determined using electron microscopy, x-ray diffraction, the B.E.T. adsorption method, differential thermal analysis, and IR spectroscopy. The authors found that the surface area increased with increasing calcination temperature. The IR results showed that water and the anion in which the oxidation was carried out were present in the films. By heating the samples to 1,000°C and monitoring the desorption products by GC, it was found that SO_2 gas was generated between 800°C and 900°C and water was released from 70°C up to 200°C for sulfuric acid anodized aluminum.

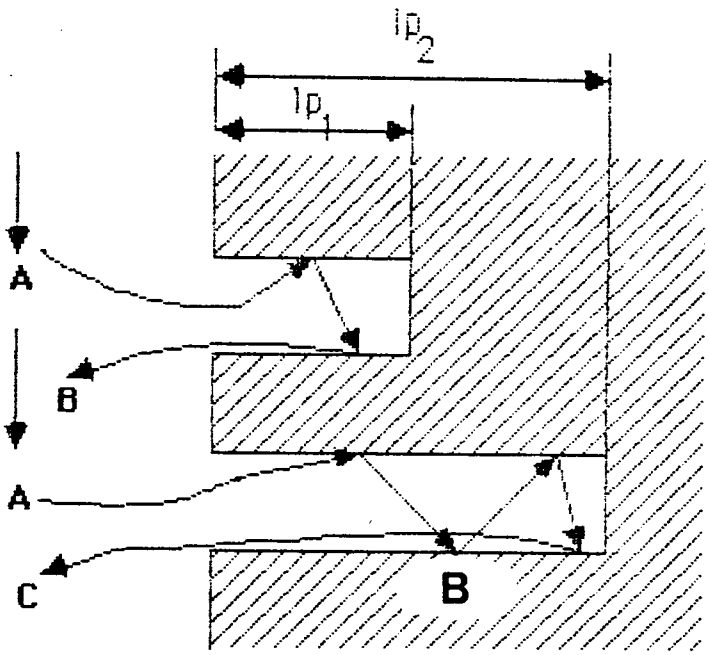

Figure 2. Hönicke's(15) reaction model.

For phosphoric acid anodized aluminum, only water was generated below 1,000°C. From their results for the dehydration of cyclohexanol over acid anodized aluminum, Yamada and Itabashi(16) found the following order of reactivity: sulfuric> oxalic> phosphoric; which coincided with the order of the specific surface areas. The authors also found that the measured amounts of anion in the film were 16-18% as SO_3, 9-11% as $C_2O_4^{2-}$, and 6-7% as PO_4^{3-}. Therefore, they concluded that the activity corresponded to specific surface area and the amount of anion in the film.

Miller and Moskovits(17) employed the electrochemical technique of anodization and electrodeposition(18) in catalyst preparation. They studied a supported iron catalyst which was used in the Fischer-Tropsch synthesis. The electrochemically developed catalysts did not require as much pretreatment as catalysts prepared by other methods. The only pretreatment necessary was alkali addition. A reduction in hydrogen, CO, or CO/H_2 was not necessary. The authors studied the effects of varying potassium content, and the influence of the basicity of the potassium pretreatment solution upon the catalytic activity. They found that the nature of the alkali pretreatment solution had little effect on the activity of the catalyst, and product selectivity was solely dependent on the potassium content. The absence of hydrocarbon

formation on untreated catalysts, and the high level of alkali necessary to attain reasonable activity was due to the substantial amount of alumina support present in the catalysts.

D. CHARACTERIZATION OF ANODIC OXIDES ON ALUMINUM

Though there has been little work characterizing the anodic oxides used as catalysts, there have been a few independent studies attempting to characterize anodic oxides. The techniques used to characterize the oxides have included TEM, IR spectroscopy, ESR spectroscopy and X-ray photoelectron spectroscopy (XPS).

By the measurement of electrical properties, Emmer, Hajek, and Repa(122) studied the surface adsorption of water vapor on hydrated layers of Al_2O_3 macerated in different ion solutions. Sulfuric acid anodized aluminum was sealed in boiling water and then macerated in solutions of H_2SiO_3, NaH_2PO_4 and Na_2WO_4. Structural changes of Al_2O_3 layers after the hydrothermal treatment and maceration were studied by means of TEM; their surface morphology was revealed by ordinary replication techniques. The dependence of leakage current through the Al_2O_3 layer on the pressure of water vapor was studied together with its time and temperature variations. TEM showed that the surface part of the hydrated Al_2O_3 layers was composed of fine, loosely connected platelets and needles, identified

by diffraction as crystallites of pseudoboehmite. No substantial differences in morphology were visible on electron micrographs of the layers treated in different maceration solutions. From the electrical measurements it was determined that the best stabilization of surface properties was achieved if a solution of NaH_2PO_4 was used. The leakage current rose only slightly with increasing temperature in the region of low pressures of water vapor. On the contrary, the steep decrease of sample current with increasing temperature was observed at high surface coverage; this trend was reversed again as the sample temperature increased further. The authors believed that the observed dependency of sample current on pressure and temperature was caused by the adsorption of water vapor on the surface of the layers. The shape of the measured curves suggested that this process corresponded to a model of polymolecular adsorption.

Kudo and Alwitt(123) examined sections of hydrous oxide films on aluminum by transmission electron microscopy. The films were prepared by reaction with boiling water followed by subsequent anodic oxidation of these surfaces. Two well defined layers were evident: an inner layer of uniform density and thickness, and an outer fibrillar layer of varying thickness. The thickness of both layers increased with longer reaction time. These results gave the first

visual evidence of the incorporation of pseudoboehmite into the barrier oxide during anodic oxidation.

O'Sullivan, Hockey, and Wood(124) studied the nature of freshly prepared and hydrothermally treated anodic oxide films by infrared spectroscopy and by electron microscopy. Their objective was to use infrared spectroscopic methods, including isotopic exchange techniques, to examine changes in both the chemical structure and permeability that occurred in the films during hydrothermal treatment. Upon deuteration, all the hydroxylic species were exchanged to their corresponding isotopic analogues; proving that the hydroxyl groups or ions retained by the film after evacuation at room temperature were situated on the exterior surfaces of oxide particles or crystallites. Upon hydrothermal treatment, the films retained greater quantities of molecular water after evacuation under ambient conditions, an effect which increased with the time of the treatment. This was evidence that changes in the crystallite arrangement were due to trapping of water in the film structure. The hydrothermal treatments reduced the quantity of exchangeable species within the film. These films were sealed throughout; if the pores were only plugged at the exterior surface, removal of the barrier layer would lead to a large increase in isotopic exchange, which it did not. The IR spectroscopy results indicated

that the freshly prepared anodic film was a relatively open array of amorphous, largely anhydrous, alumina crystallites, the surface of which contained hydroxyl groups or ions. The hydrothermal treatment of the oxide array did not induce changes in the bulk composition. Pore plugging, initially most rapid at the surface, eventually extended through the entire film, retarding the removal of molecular water during evacuation and also exchange during deuteration.

Dorsey(125) used infrared spectroscopy to study different oxide coatings and concluded that a difference between a barrier layer and a porous oxide layer existed. The barrier layer absorption was limited to the 1000-900 cm^{-1} region due to Al<->OH bending, while the porous layer showed bands above 1000 cm^{-1} or below 900 cm^{-1}, due to AlO<->H stretching (3660 cm^{-1}-2940 cm^{-1}), Al<->O stretching (1696 cm^{-1}-1345 cm^{-1}) and Al<->OAl stretching (below 900 cm^{-1}). Dorsey(126) used infrared spectroscopy to analyze quantitatively the amount of porous and barrier layers prepared in eight dicarboxylic acid electrolytes. The film formed only at low temperature, and dissolved in the electrolyte at higher temperatures in acids which readily formed stable complexes (oxalic or malonic) and showed a high dissolving effect on the anodic film. Tartaric acid, a weaker complexing agent, required a higher temperature to

produce a similar dissolving action. Other acids, which were not complexing agents under these conditions, produced only barrier layers. The author also found that the barrier layer apparently underwent a change as the porous overlayer formed. When a porous coating was formed in conjunction with the barrier layer, the barrier layer infrared band(1000-900 cm^{-1}) shifted toward higher frequencies. The frequency shift corresponded to a reduction in the reduced mass of the barrier layer. Dorsey interpreted this as a reduction in polymer weight, indicating the breaking up of a high polymer of aluminum oxide to give a series of lesser polymers. This reduction in polymer weight appeared to be independent of the anodizing temperature and was influenced by increasing amounts of the porous layer Al=O bond.

Belov et al.(127) applied thermal analysis to the study of water-sealed anodic aluminum oxide films formed in solutions of various electrolytes. The authors showed that anodic aluminum oxides differed in their tendency to hydrate, depending on the nature of the anodizing electrolyte in which they were formed. Regardless of the nature of the anodizing electrolyte, heating of all the anodic aluminum oxides to 1000°C, resulted in the loss of water and the conversion of the amorphous oxides into γ-Al_2O_3. The temperature of the conversion(shown in Table 3)

Table 3

Conversion of Anodic Oxides to γ-Al_2O_3

Anodizing Electrolyte	Temperature of Crystalline Change
$C_6H_5(OH)COOH \cdot SO_3H$	910° C
$H_2C_2O_4$	915° C
$NH_2 \cdot SO_3H$	920° C
CrO_3	850° C
$H_2CrO_4 + H_2SO_4$	970° C
H_3PO_4	940° C
Na_2CO_3	925° C
NaOH	925° C
H_2SO_4	970° C

of anodic oxides to γ-Al_2O_3 depended on the nature of the structural anion and the previous history of the amorphous Al_2O_3.

The surfaces of oxide films produced in a boric acid-borate solution were studied by Konno, Kobayashi, Takahashi, and Nagayama(128) by x-ray photoelectron spectroscopy. The authors studied the distribution of the anion in the film using both chemical dissolution in sulfuric acid and ion sputter etching. The borate ions were present throughout the oxide film and at the oxide/metal interface. The oxides also had a higher degree of hydration and a higher concentration of borate at the surface of the oxide, compared to deeper into the oxide. A similar study on sulfuric acid anodized aluminum was carried out by Treverton and Davies(129), using XPS to study ion etched d.c. and a.c. anodic films. The authors found that sulfate in the oxide films was reduced to sulfide upon ion-etching. No chemical differences were observed when comparing the d.c. and a.c. anodic films.

E. THE DECOMPOSITION OF ALCOHOLS OVER ALUMINA

There have been a number of IR and mechanistic studies involving the dehydration and dehydrogenation of alcohols over alumina. Knözinger(19) reviewed studies of the dehydration of alcohols over alumina. Widely differing views are held concerning the mechanism of the

heterogeneously catalyzed dehydration of alcohols on aluminum oxide. An oxonium-carbonium ion mechanism similar to that assumed for liquid-phase reactions in acidic media was supported by several authors(20-23) for the dehydration of alcohols on solid surfaces. A proton from the surface was assumed to add to the OH group of the alcohol in the adsorption step. This process was explained by the formation of strongly polarized hydrogen-bonds(24). Pines and Haag(25) showed that this mechanism was valid for the dehydration of 2-butanol. The participation of surface protons or OH groups was supported by the need for water at the contact surface(26,27). For an oxonium ion to be formed by proton addition, the surface of the aluminum oxide must contain Brønsted acid sites; Parry(28) found only Lewis acid sites in IR studies on aluminum oxide with adsorbed pyridine. Any Brønsted acid sites present were only weakly acidic(29), so that ionic addition of protons to alcohols was not very likely.

Eucken(30) and Wicke(31) postulated a hydrogen exchange mechanism, in which the alcohol molecule was adsorbed in such a way that it approximated, as closely as possible, the structure of the product molecule. A covalently bound adsorption complex in the form of a surface alkoxide was postulated for the dehydration of ethanol(32-34). The dissociation of this surface compound yielded ethylene,

whereas the condensation of two adjacent alkoxide groups led to ether formation. Topchieva et al.(34) believed that the active sites were surface OH groups, forming surface compounds of an alkoxide type. Alkoxide structures were detected in the IR spectra of some alcohols adsorbed on aluminum oxide (35,36). Vasserberg et al.(37) suggested a free-radical mechanism for the dehydration of isopropanol. Since free-radical mechanisms proceed preferentially in apolar media, and the surfaces of metal oxides are polar(37), this route was rather unlikely(19).

Wolkenstein(39,40), Garner(41) and Hauffe(42) described the dehydration and dehydrogenation of alcohols in terms of the electron theory of semiconductors. The first two authors postulated a rate-determining step over n-type conductors(basic solids) where the alcohol was an electron acceptor for the dehydrogenation and a rate-determining step over p-type conductors(acidic solids) where the alcohol was an electron donor for the dehydration. Hauffe(42) regarded the rate-determining step in the dehydrogenation of ethanol as the desorption of acetone.

Pines and Pillai(43) and Schwab et al.(44) suggested neighboring-group effects and reaction at preferred sites on the catalyst to explain preferential trans-elimination in the dehydration of menthol and neomenthol. Watanabe et al. (45) interpreted the fact that the principal product in

the dehydration of 2-endo- and 2-exo-bornanol was camphene as meaning that this reaction resulted from a concerted trans-elimination in which the hydroxyl group was attracted by an acidic surface center and the proton by a basic center. Watanabe et al.(45) also assumed that trans-elimination was preferred in the dehydration of primary aliphatic alcohols. This conclusion was based on the distribution of primary products in the dehydration of 1-butanol(25), isobutanol, and 2-phenyl-1-propanol(46), with and without ^{14}C-labeling(47). The effects of neighboring groups were also taken into account.

Pines and Manassen(47) concluded that both acidic and basic sites take part in the dehydration of alcohols on aluminum oxide. They reported that a carbonium ion mechanism appeared to be favored in the dehydration of tertiary alcohols and a concerted mechanism in the case of primary or secondary alcohols.

Jain and Pillai(48) proposed an adsorbed phase substitution-elimination mechanism that also included ether formation. If aluminum oxide was assumed to have electrophilic and nucleophilic sites on its surface, there would also be two types of adsorbed alcohol molecules, i.e. carbonium ions[1] and alkoxide ions[2]. A nucleophilic attack by [2] on the positively charged C atom of [1] led to ether formation, while the abstraction of a β-proton

from the carbonium ion[1] by the alkoxide[2] led to olefin formation. According to this view, the catalyst gave the reacting molecules the required polarity and fixed them in the correct arrangement. The adsorbed phase resembled a polar medium in which nucleophilic substitution and elimination competed.

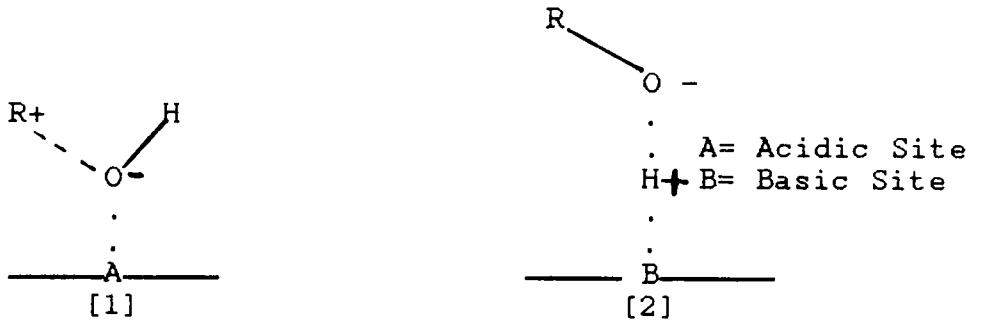

The dehydration of simple alcohols on γ-Al_2O_3 led mainly to ethers, olefins, and water. Balaceanu and Jungers(49) studied the dehydration of methanol and ethanol up to about 200°C. In the dehydration of ethanol, ethylene was formed as a secondary product with reformation of ethanol; ethylene was also formed directly at higher temperature. Stauffer and Kranich(50), on the other hand, reported that primary aliphatic alcohols up to n-hexanol were dehydrated to the ether and the olefin in independent parallel steps.

Knözinger and Köhne(51,52) studied the product distribution as a function of catalyst temperature and contact time for the dehydration of some unbranched and

branched aliphatic alcohols over alumina. They observed, for primary alcohols containing two to six carbon atoms, reactions corresponding to steps (1) to (4). As the temperature rose, primary olefin formation from alcohol and secondary olefin formation from ether started in the same temperature range and steadily became more important. Step (2) was favored at low temperatures.

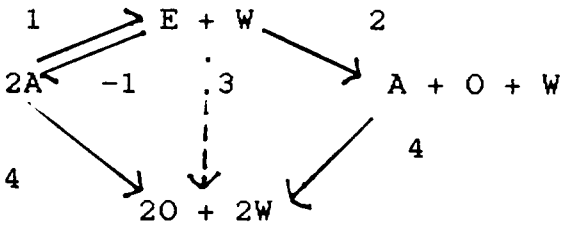

E= ether
W= water
O= olefin
A= alcohol

The dehydration of isopropanol led to the formation of propylene, and yielded only small quantities of isopropyl ether(52).

Jambor and Beránek(53) studied the kinetics of parallel dehydrogenation and dehydration of 2-propanol at 350°C on a series of oxides (ThO_2, TiO_2, La_2O_3, Cr_2O_3, ZrO_2 and MgO). They observed that the prevailing reaction on metal(II) oxides was dehydrogenation, while on metal(IV) oxides it was dehydration. Metal(III) oxides showed medium selectivity. A number of authors believed that dehydration was favored over oxides with small, highly-charged cations,

while dehydrogenation was associated with larger, more polarizable cations such as alkaline earth ions (27,30,54-57). Moffat(58) concluded that the dehydrogenation mechanism over hydroxyapatite (calcium phosphate) catalysts involved the transfer of the alcoholic proton to the basic site and the α-hydrogen to the acid site of the catalyst.

Kibby and Hall(59) pointed out that the acid and base sites cannot be the same for both reactions because of different poisoning characteristics. They suggested that the acid sites in the dehydrogenation over hydroxyapatite catalysts were the catalyst cations or the protons of HPO_4^{2-} groups, while the basic sites were the OH^- or PO_4^{3-} groups. They proposed that the dehydration mechanism could be pictured as a nearly concerted elimination involving an acidic and basic site(60):

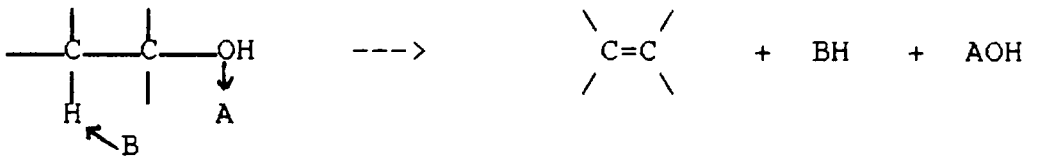

A= Acidic Site
B= Basic Site

while one could conceive of the dehydrogenation reaction as:

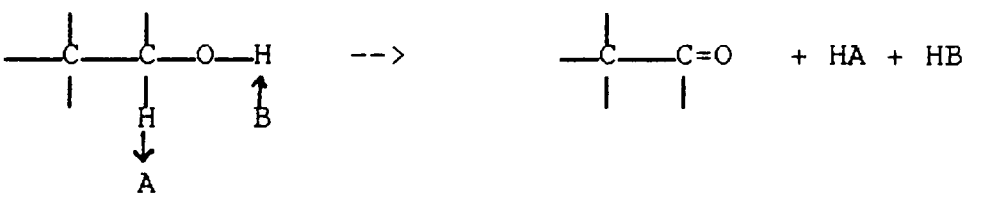

In the dehydration, the C-O bond was cleaved and the β-hydrogen was discharged to the basic site. In dehydrogenation, the alcoholic proton was discharged to the basic site and the α-hydrogen to the acid site.

Tada et al.(61) studied the dehydration and dehydrogenation of sec-butanol over a zinc phosphate catalyst. The catalyst showed very high selectivity for dehydrogenation when calcined at 650°C and a high selectivity for the dehydration when calcined at 300°C. From the results of poisoning experiments it was shown that the dehydration needed acidic sites and the dehydrogenation required basic sites.

Davis(62) studied the conversion of 2-octanol to octenes and 2-octanone over alumina after various pretreatments and concluded that alumina was sensitive to the pretreatment. Hydrogen pretreated oxides were highly selective to dehydrogenation and the oxygen pretreated oxides were highly selective to dehydration products. The authors concluded that the dehydrogenation occurred over basic sites and the dehydration over acidic sites.

Pepe et al.(63) studied the catalytic behavior of copper/alumina catalysts for isopropanol decomposition. The authors used the decomposition of 2-propanol as a means for investigating the activity and selectivity toward

dehydrogenation as a function of the copper concentration and oxidation state. Addition of copper to alumina resulted in dehydrogenation activity. These results also showed that a reducing treatment produced an increase in the dehydrogenation activity. The Cu(0) species was responsible for the dehydrogenation of isopropanol.

F. THE SURFACE STRUCTURE OF γ-Al_2O_3

In the simplest model, the surface centers of aluminum oxide are regarded as incompletely coordinated aluminum and oxygen ions; the surface was assumed to be completely free of OH groups(19). Other models took into account cation defects and strained sites, which resulted from the dehydration of the originally hydrated surface(64,65). Peri(66) investigated water adsorption on γ-Al_2O_3 by IR. From the IR results he developed a detailed model based on a few assumptions:

1. The oxide was in the form of a defect spinel lattice.

2. Ionic surfaces were generally bound by anions, which were more readily polarizable than cations.

3. The [100] face of γ-Al_2O_3 was preferentially exposed. Oxides of this type characteristically adsorb water, which led to the formation of OH groups.

4. Water was liberated from a hydrated surface by the condensation of two hydroxyl groups on exposed oxygen ions.

The remaining hydroxyl groups acquired different acidic properties defined by their immediate surroundings.

5. Aluminum ions in the second atomic position lost their full coordination and became accessible from the surface through oxygen vacancies (Figure 3).

Knözinger and Ratnasamy(67) further refined Peri's (66) model and discussed five types of hydroxide groups on transition alumina surfaces, shown in Figure 4. The various hydroxide groups have different chemical properties. Type III sites exhibit the highest acidity, while types IA and IB were the most basic.

G. IR STUDIES OF THE STRUCTURE OF ADSORBED ALCOHOLS

Three surface compounds were proposed for the adsorption of alcohols, as discussed below.

1. MOLECULAR ADSORPTION OF ALCOHOLS

Greenler (35), Treibmann and Simon (36), and Kagel (68) found that alcohols were readily desorbed from γ-Al_2O_3 at room temperature. NMR studies showed that the hydroxyl group of the alcohols interacted directly with the γ-Al_2O_3 surface(69,70). Kagel(68) assumed that structures [3] and [4] were both present.

Knözinger et al.(71) proposed a structure such as [5], which was more stable and heat-resistant than the singly hydrogen-bonded structures [3] and [4].

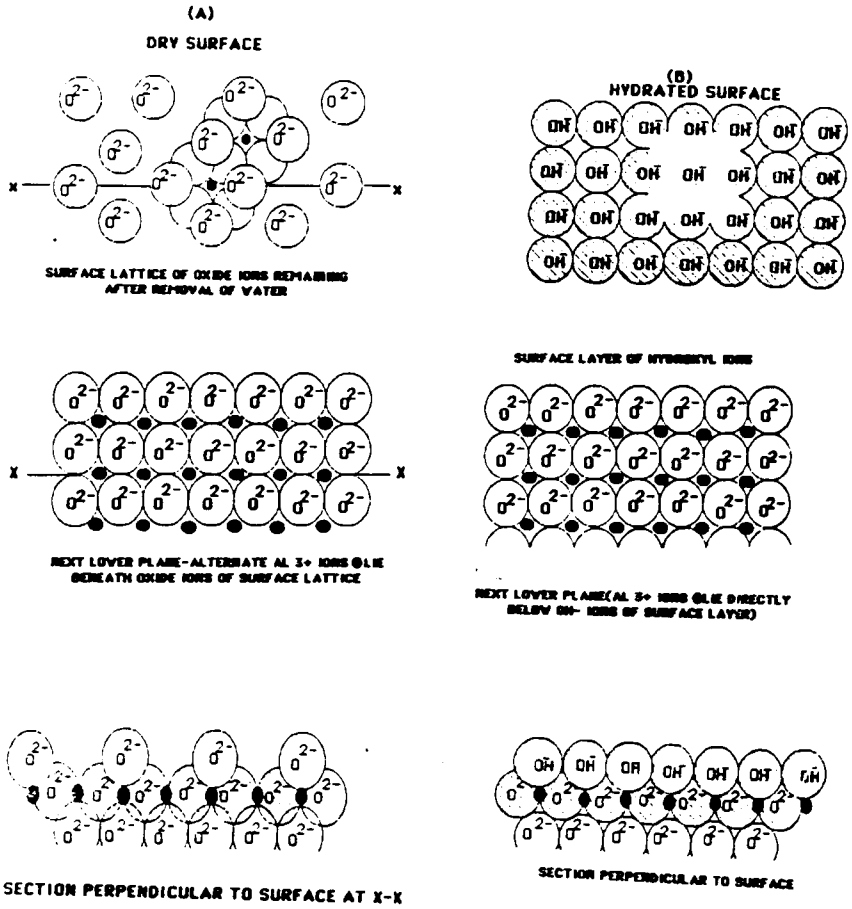

Figure 3. Peri's(66) model of the γ-Al_2O_3 surface.

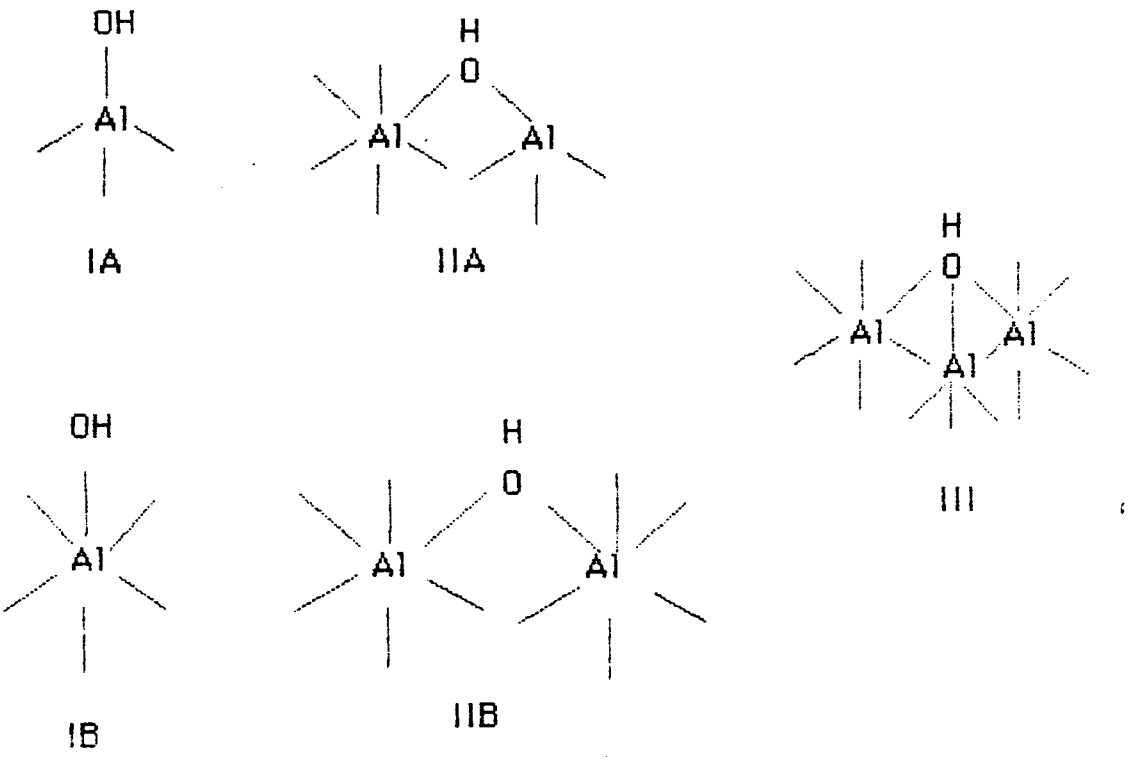

Figure 4. Five types of hydroxide groups on the surface of γ-Al_2O_3, proposed by Knözinger and Ratnasamy(67).

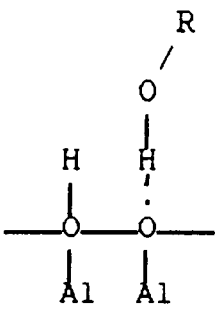

[3]

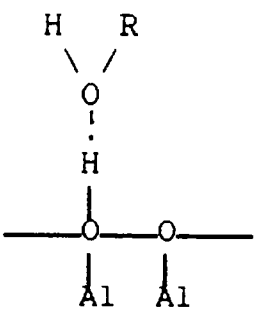

[4]

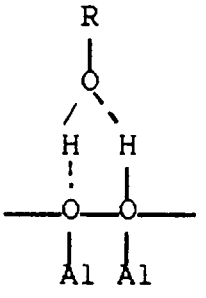

[5]

2. ALKOXIDE STRUCTURES

A comparison of the IR spectra of adsorbed alcohols on γ-Al_2O_3 with those of solid alkoxides showed the presence of surface alkoxide groups on adsorption of methanol(35), ethanol (35,36), n-propanol (36,68), isopropanol(36), and n-butanol(68). In Peri's(66) model of the aluminum oxide surface, there were two possible routes for the formation of alkoxide by dissociative adsorption:

a. A hydroxyl proton from the alcohol would split off to form a surface OH group with γ-Al_2O_3, while the alkoxide residue occupied an oxygen vacancy on the surface (Lewis acid site).

b. The C-O bond of the alcohol would break, the resulting OH^- group filled an oxygen vacancy on the surface, while the carbonium ion added to an adjacent oxygen ion(66).

3. CARBOXYLATE STRUCTURES

Oxidation of methanol(35), ethanol(35,36) and n-butanol(19,68) during adsorption on aluminum oxide above about 170°C yielded carboxylate structures. Knözinger(19) reported carboxylate-type surface compounds as a result of the adsorption of isobutanol and benzyl alcohol on γ-Al_2O_3 above about 120°C. Treibmann and Simon(36) concluded that the adsorption of isopropanol on γ-Al_2O_3 occurred by the formation of an acetate structure resulting from the break down of the carbon skeleton of the alcohol molecule. Carboxylate structures were observed in IR spectra up to 400°C and the adsorption of water did not change the absorption bands. In view of the high stability of carboxylates, the carboxylate structure would hardly be important as an intermediate in surface reactions, up to 250°C. However, Knözinger concluded that the dehydrogenation of ethanol at temperatures above about 300°C would proceed by a carboxylate structure. Knözinger(19) argued that olefin formation began with adsorption complex [5]. He believed that the rearrangement of [5] occurred in two ways. With strongly polarized

hydrogen-bonds, structure [5] would approximate an oxonium ion and change by charge migration into a carbonium ion, which allowed the formation of an olefin by subsequent transfer of a proton to an adjacent surface oxygen ion. A concerted E2-type mechanism would also be possible, with simultaneous rupture of the C-H and C-O bonds of the alcohol. According to Pines et al.(47), it was assumed that tertiary alcohols, which form relatively stable tertiary carbonium ions, were dehydrated to olefins by an ionic mechanism, and the other aliphatic alcohols by a concerted mechanism.

H. ACID-BASE PROPERTIES

The structural models and the proposed mechanism for the dehydration of alcohols indicate that acidic sites on the surfaces of aluminas are important. It is necessary to characterize the acid sites on the surfaces of catalysts. There are a number of methods for the determination of the acidic properties of a catalyst, including the adsorption of indicators(72-78), the IR spectroscopic study of the adsorption of gaseous bases(79-88), and the thermal desorption of adsorbed gaseous bases(89-95).

1. ADSORBED INDICATORS

Hammet and Deyrup(72) defined the ability of acids to donate a proton to a neutral base:

$$H_0 = -\log a_{H^+} f_B / f_{BH^+} \quad [1]$$

where a_{H^+} was the activity of the hydrogen ion and the f's, the activity coefficients for a neutral base, and its conjugate acid. Lewis and Bigeleisen(73) pointed out that the measurement of the ability of a solvent to convert a base to its conjugate acid could be extended as well to media containing "Lewis acids" (electron acceptors) rather than proton donors. If the base formed a complex on the surface with a Lewis acid, the H_0 function would have the following meaning:

$$H_0 = -\log a_A f_B / f_{AB} \quad [2]$$

where a_A was now the activity of the Lewis acid or electron acceptor.

Walling (74) first studied the adsorption of indicators onto solid surfaces as a measure of surface acidity. Walling indicated that if the Lewis definition of acid strength was applicable to surfaces, the acid strength of any surface would be readily measurable by the observation of the color of indicators adsorbed upon it. Some restrictions for this technique were given.

a. The indicators had to be restricted to those in which the basic form was uncharged and which were converted to their conjugate acids by simple proton addition.

b. They had to be adsorbed by the surfaces under

study.

c. The acid form of the indicator had to be more highly colored than the basic form.

d. The solvent from which the indicator was adsorbed may also be adsorbed on, and alter, the acid properties of the surface under study.

e. Simple visual comparison of the colors of adsorbed indicators permitted only a semi-quantitative determination of acid strengths.

f. The indicator method was limited to white or light-colored surfaces.

Benesi(75) studied the acidity of catalyst surfaces by adsorbing indicators. He concluded that the use of Hammett indicators in measuring acid strengths of solid surfaces could furnish useful information not readily obtainable by other means.

Yamanaka and Tanabe(76) measured the basicity of various solids by titrating with trichloroacetic acid using a series of Hammett indicators. When a solid had no acid sites for which $H_0 \leq pk_{BH^+}$, the color of the basic indicator did not change. As basic sites were neutralized by a Brønsted acid at the endpoint, the titres of Brønsted acid required for neutralization gave a measure of the number of basic sites (basicity) on the surface. The authors defined "basic strength, H_0" of basic sites as the acid strength,

H_o, of the conjugate acids. Two kinds of aluminas tested showed basicity. The basicity of γ-Al_2O_3 was higher than that of the activated Al_2O_3. ZnO, TiO_2, BaO, and B_2O_3 showed basicity.

Yamanaka and Tanabe(77) reported the use of "$H_{o,max}$", defined as the point where the strongest H_o value of the acid sites was approximately equal to the strongest H_o of the basic sites. The acidity and basicity at various acid-base strengths were measured with n-butylamine or trichloracetic acid in benzene. The authors concluded that $H_{o,max}$ would be regarded as a practical parameter to represent an acid-base property on solids which were sensitive to the surface structure. A solid with a large positive $H_{o,max}$ had strong basic sites and weak acid sites. On the other hand, a solid with a large negative $H_{o,max}$ had strong acid sites and weak basic sites.

Mason, Siriwardane, and Wightman(78) used the adsorption of colored indicators as a measure of the acidity of pretreated titanium metal before adhesive bonding. Using this method, they were able to estimate the acidity and basicity of the surfaces after thermal and aging experiments.

In order to determine whether the color changes observed are due to Brønsted or Lewis acid centers, the adsorption of ammonia and pyridine can be studied. IR

spectroscopy represents a good method for differentiating between adsorption of pyridine or ammonia on Lewis and Brønsted acid sites and for determining the relative strength of the acid centers.

2. ADSORPTION OF AMMONIA

Mapes and Eischens(79) studied the infrared spectrum of chemisorbed ammonia to determine whether the acidity of cracking catalysts resulted from Brønsted or Lewis acidity. They showed (Figure 5) the three different catalyst acid structures that had been proposed in the literature. Structure I, proposed by Thomas(80), shows the active site on cracking catalysts as Brønsted acid sites. An aluminum ion replaced a silicon ion and was bonded to four oxygens, since aluminum has a valence of +3, an added proton was required to balance the charge. Structure II, proposed by Milliken, Mills, and Oblad(81) shows the active sites on a catalyst as Lewis acid sites. Here the aluminum ion was bonded to three oxygens, leaving an electron-pair vacancy in its valence shell. Structure III, proposed by Tamele (82) and Hansford (83) showed the product formed when water reacted with Structure II. The electron-pair vacancy of aluminum was filled by the sharing of one of the free electron-pairs of oxygen in water, making one of the protons of water readily ionizable.

Ammonia adsorption resulted in an IR band at 1620 cm^{-1}

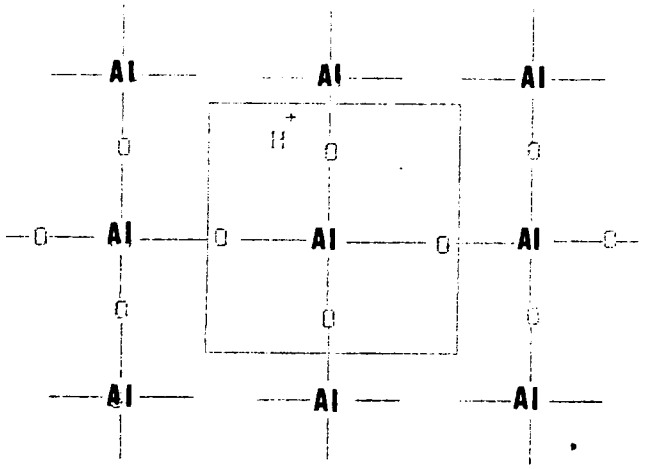

I. BRØNSTED ACID

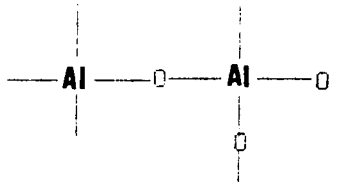

II. LEWIS ACID

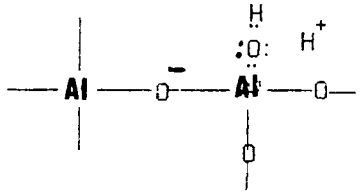

III. HYDRATED LEWIS ACID

Figure 5. Three different catalyst acid structures(80-83).

due to the N-H bending vibration of coordinatively bonded ammonia and a band at 1440 cm^{-1} due to the N-H bending vibration of the NH_4^+ structure(79). Mapes and Eischens(79) believed that when ammonia reacted with a Brønsted acid site, ammonia gained the available proton to form the ammonium ion, converting NH_3 to NH_4^+. In reacting with a Lewis acid the nitrogen in ammonia shared its free electron pair to fill the vacancy of a coordinatively unsaturated aluminum, thus maintaining the NH_3 structure. These authors found that the major active sites on these cracking catalysts were Lewis acid sites; however, there was interference with the band at 1620 cm^{-1} due to the OH bending vibration for adsorbed water.

Peri(84) studied the mechanism of the adsorption of ammonia on γ-alumina by IR, deuterium exchange, gravimetry, and mass spectrometry. He found that the adsorption of ammonia on dry γ-alumina occurred in several ways, including adsorption of molecular ammonia and formation of amide ions (NH_2^-). The formation of NH_2^- presumably required simultaneous formation of hydroxyl groups (NH_3+O^{2-} $->NH_2^-+OH^-$). The IR evidence (band at 1510 cm^{-1}) showed however, that only about one ammonia molecule in ten reacted in this way. The spectra also eliminated NH_4^+ as a major product of adsorption although small amounts could exist. Most of the ammonia was initially adsorbed

molecularly.

Tsyganenko, Pozdnyakov, and Filimonov(85) reported the results of a study in which the IR spectra of ammonia adsorbed on CoO, NiO, SiO_2, CaO, MgO, ZrO_2, ZnO, TiO_2, BeO and γ-Al_2O_3 were measured. Ammonia adsorbed in several ways:

i) hydrogen-bonding via one of its hydrogen atoms to a surface oxygen atom (or to the oxygen of a surface hydroxyl group);

ii) hydrogen-bonding via its nitrogen atom to the hydrogen of a surface hydroxyl group;

iii) coordination to an electron-deficient metal atom (Lewis acid site).

The dissociation of ammonia with the formation of surface NH_2^- (or NH^{-2}) and OH^- species, as well as a complete transfer of protons to the ammonia molecules from Brønsted sites to produce adsorbed NH_4^+ ion, were also possible. They found that ammonia adsorption depended on the hydroxyl content of the oxide. The adsorption of ammonia on Brønsted sites was found only on γ-alumina.

3. PYRIDINE ADSORPTION

Parry(28) studied the adsorption of pyridine on acidic solids by IR as a method of characterizing surface acidity. Pyridine adsorption showed that silica surfaces hydrogen bond pyridine, alumina has strong Lewis acid sites, and a

cracking catalyst has both Lewis and Brønsted acidity. Pyridine adsorption resulted in a band at 1540 cm^{-1}, due to the N-H deformation resulting from pyridinium ion formation(28). IR bands were also observed between 1440 and 1465 cm^{-1} due to changes in the "ring" vibrations of pyridine. Pyridine adsorbed on a Lewis acid site had an IR band between 1440-1447 cm^{-1} (28).

Kiviat and Petrakis(86) studied the surface acidity of transition metal modified aluminas by pyridine adsorption using IR and wide-line NMR spectroscopy. This study showed that alumina and both Co and Ni impregnated alumina, contained only Lewis acid surface sites whereas alumina impregnated with Mo, either in the presence or absence of Co or Ni, contained both Lewis and Brønsted acid sites. η-Al_2O_3 contained two Lewis acid sites, and the sites differed in strength. The authors concluded that Ni and Co interact with the MoO_3, and that the resultant species occupied specific sites upon the η-Al_2O_3 surface.

Morterra, Coluccia, Chiorino, and Boccuzzi(87) studied by IR spectroscopy the adsorption of pyridine on two different preparations of α-Al_2O_3, obtained by thermal treatment of γ-Al_2O_3 for different times. The authors concluded that weak acid sites of comparable strength were produced by a few surface OH groups and some octahedral Al^{3+} ions. Strong acid sites were produced by some

tetrahedral Al^{3+} ions, probably coming from an incomplete surface transformation of tetrahedral Al^{3+} into octahedral Al^{3+}. These strong sites were heterogeneous on preparations treated for short times, while the strong sites became much less abundant and more homogeneous on samples treated for long times.

Ward(88) studied the adsorption of pyridine on alkali and alkaline earth ion-exchanged Y-zeolites. If the calcination temperature was less than 500°C, none of the zeolites exhibited Lewis acidity. After the 650°C calcination, Lewis acidity was observed. The authors found that the alkaline earth forms were Brønsted acids while the alkali cation forms were not, and the hydroxyl groups were the Brønsted acid sites. They found that the Brønsted acidity, hydroxyl group concentration, and catalytic activity varied with cation size. The smaller the cation, the greater the polarizing effect on the Brønsted acid sites.

4. TEMPERATURE PROGRAMMED DESORPTION(TPD)

TPD is often used to study the acidity of a catalyst (89-95). In a typical experiment the catalyst is first pretreated and exposed to a gaseous base. After the excess gas is removed, the catalyst is heated to create a linear rise in temperature with time. The ideal detector is a mass spectrometer. A desorption spectrum is a record of

the concentration of desorbed gas as a function of temperature. The shape and position of the peak maxima are related to the desorption process, and therefore, provide information on how the gas was adsorbed on the catalyst(91). The detailed analysis of spectra can be complicated by experimental considerations, including diffusion, heterogeneous surfaces with a range of acid distributions, and readsorption of the desorbed gas. A review of TPD has been written by Falconer and Schwartz(90).

Scholle et al.(91) studied the acidity of the framework hydroxyl groups of H-ZSM-5 and H-boralite by means of proton magic angle spinning NMR and temperature programmed desorption of NH_3 (NH_3-TPD). Both the NMR study and NH_3-TPD study led to the conclusion that the Brønsted acidic site in H-ZSM-5 was more acidic than in H-boralite, while these sites on H-boralite in turn were more acidic than the silanol group. Hodnett and Moffat(92) studied the TPD of pyridine and water from a series of heteropoly compounds. The heteropoly acids used in the study were $H_3PW_{12}O_{40} \cdot nH_2O$(HPW), $H_3PMo_{12}O_{40} \cdot H_2O$(HPMo), and $H_4SiW_{12}O_{40}$(HSiW). The sorptive capacity of heteropoly acids toward pyridine depended strongly upon pretreatment conditions. They found that pyridine only desorbed from HPW without decomposition, provided more than one pyridine molecule per PW_{12} unit was

adsorbed. Koubek, Volf and Pasek(93) studied the adsorption of a series of aliphatic amines on γ-Al_2O_3 using a gas chromatograph. Two peaks were observed in the TPD chromatograms of all the amines studied with the exception of ammonia and methylamine. The existence of the two peaks was explained by the presence of two types of active sites on the surface of the γ-Al_2O_3. Mass spectral analysis proved that the desorption products in the region of the second peak are formed mainly by the following reactions of amines over alumina:

1. Disproportionation

$$2RNH_2 \rightleftharpoons R_2NH + NH_3$$

$$2R_2NH \rightleftharpoons R_3N + RNH_2$$

2. Deamination

$$RCH_2CH_2NH_2 \rightarrow RCH=CH_2 + NH_3$$

However, there was no evidence for the decomposition of amine in the region of the first peak. Koubek, Volf and Pasek(93) believed that the first peak was due to adsorption of amines to Brønsted acid sites and the second peak was due to the adsorption of amines to the Lewis acid sites. Mieville and Meyers(94) reported a method that employed the second, higher-temperature peak as an index of catalyst acidity; t-butylamine was the chosen adsorbent. Takahashi, Iwasawa, and Ogasawara(95) studied the behavior of n-butylamine and pyridine adsorbed on silica-alumina

catalysts by thermal desorption chromatography. The results showed two types of adsorption sites for n-butylamine one as a Brønsted acid, and the second as a strong Lewis acid site. The Lewis acid sites resulted in the decomposition of n-butylamine. For pyridine, one peak was observed due to adsorption on Lewis acid sites, the pyridine was desorbed without decomposition. It was concluded that the Brønsted acid sites were not strong enough to adsorb pyridine.

I. JUSTIFICATION OF STUDY

There has been much discussion in the literature concerning the use of transition aluminas in the dehydration of alcohols (19-54); however, only in the last few years have there been any reports of the use of anodic oxides as catalysts(2-18). Until now it has only been shown that anodic oxides formed in sulfuric acid are more active as catalysts than γ-Al_2O_3. No attempts have been made to understand why the anodic oxides are more active.

The purpose of this study has been to correlate the catalytic properties with the surface properties of anodic aluminum oxides; specifically,

1) Study anodic oxides prepared in various electrolytes as catalysts in the dehydration of isopropanol and compare the activity of these oxides with the activity of γ-Al_2O_3.

2) Study the effect of various thermal pretreatments on

the catalytic activity of anodized aluminum.

3) Relate the surface acidity of the oxides to their catalytic activity.

4) Propose a mechanism for the dehydration of isopropanol over anodized aluminum.

This research is unique in that it studies anodic oxides prepared in different electrolyte solutions and under different conditions as catalysts and relates the catalytic properties of the anodic oxides to their surface and bulk characteristics.

Chapter 3

EXPERIMENTAL

A. CATALYSTS

1. ANODIC ALUMINUM OXIDE

Anodic aluminum oxide samples were prepared from 0.01 cm cold rolled aluminum (99.99%) sheets. Samples (14 cm x 11 cm) were cleaned with acetone, etched one minute in 5% (w/w) sodium hydroxide at 90°C, and chemically desmudged at room temperature in a 50% (w/w) aqueous HNO_3 acid solution. The aluminum was then anodized in either a 15% (w/w) H_2SO_4 acid solution at 23°C for 10 minutes or 20 minutes; a 15% (w/w) H_3PO_4 acid solution at 28°C, or a 3% (w/w) $H_2C_2O_4$ acid solution at 23°C for twenty minutes at 1.29 A/dm^2.

An idealized pore structure of anodic aluminum oxide is shown in Figure 6. The pore diameter, surface area, and the oxide thickness are a function of the anodization conditions. The krypton BET(130) surface areas, pore diameters, and oxide thicknesses are presented in Table 4. The methods used to determine these properties are described later. The surface areas were calculated based on the weight of the oxide. The weight of the oxides and the coating ratios were determined gravimetrically by the following method. The aluminum to be anodized was first weighed prior to oxide formation, W_1. Aluminum was anodized for the required time and the sample was

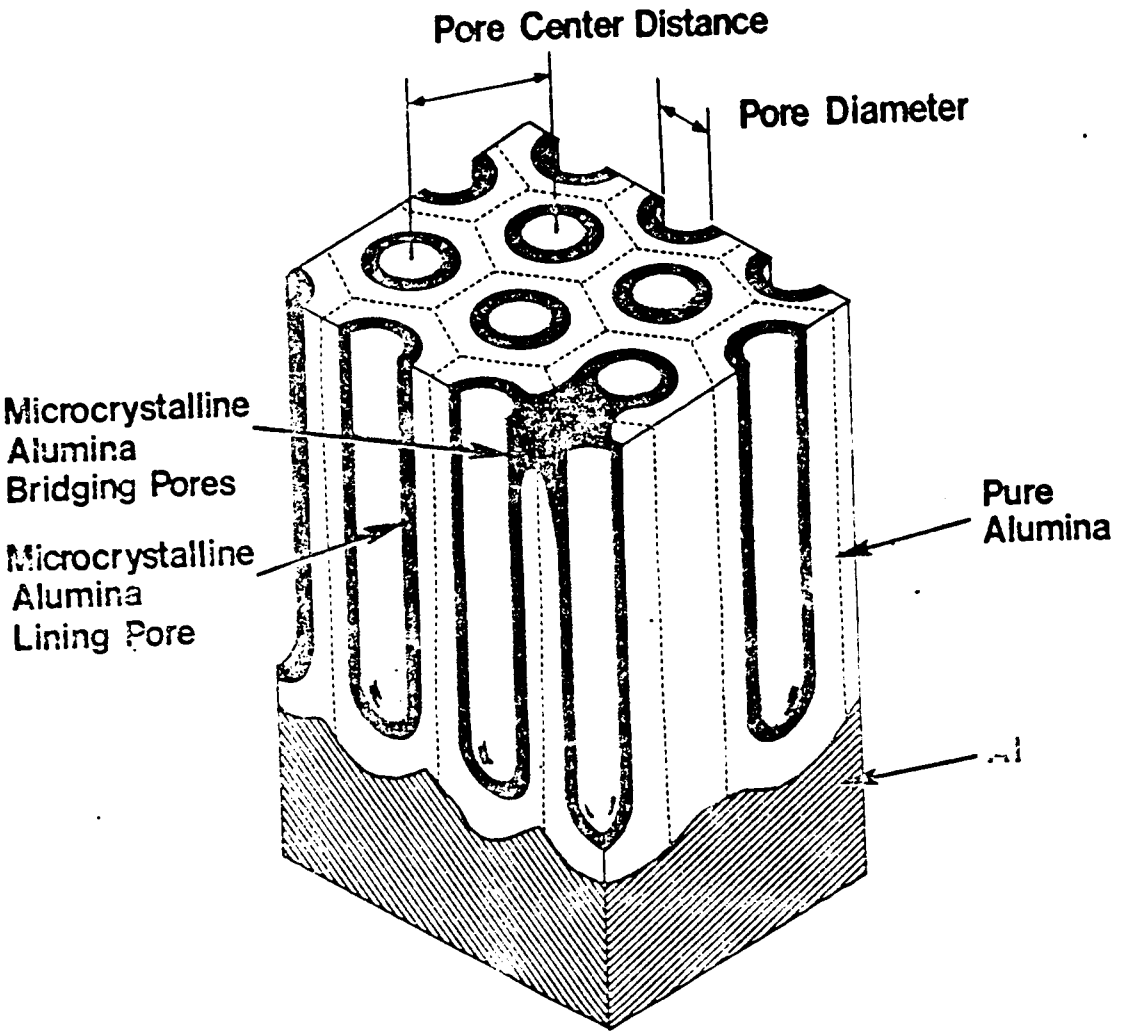

Figure 6. Idealized porous structure of anodic aluminum oxide(1).

Table 4

Oxide Thicknesses, Pore Diameters, and Surface Areas of Catalysts

Electrolyte Oxide	Anodization Time (minutes)	Oxide Thickness (μm)	Pore Diameter (Å)	Surface area m^2/g of oxide	Surface area m^2/g of anodized aluminum (oxide+Al)
H_2SO_4	20	10	*	18.5	0.12
H_2SO_4	10	3.5	*	16.0	0.08
$H_2C_2O_4$	20	8	400	5.5	0.14
H_3PO_4	20	1	500-1000	20.4	0.003
"sealed" H_2SO_4	20	10	na	3.4	0.21
γ-Al_2O_3	na	na	na	90.0	na

*unresolvable by SEM

na = not applicable

reweighed, W_2. The anodized aluminum sample was then immersed in phosphochromic acid(20g CrO_3, 35ml of concentrated H_3PO_4 and 70 ml of distilled water). Following oxide removal the aluminum was reweighed, W_3. The aluminum was repetitively immersed in the phosphochromic acid and reweighed until a constant final weight was obtained. The coating ratio was calculated from the weighings according to equation 3.

$$\text{coating ratio} = \frac{W_2 - W_3}{W_1 - W_3} \qquad [3]$$

2. γ-Al_2O_3

High purity γ-Al_2O_3 was furnished by Alcoa(131). The γ-Al_2O_3 was prepared by abrading high purity aluminum metal to remove the barrier oxide. The aluminum was activated by treatment in a 0.1 M $HgCl_2$ solution and was washed and then placed in distilled water, forming bayerite (γ-$Al(OH)_3$). Bayerite was heated at 100°C and 240 lbs. of pressure in a Parr reactor for two hours, hydrothermally converting bayerite to boehmite (γ-AlOOH). Boehmite was thermally activated by ramping the temperature at 10°C/minute to 525°C for two hours, forming γ-Al_2O_3. The nitrogen BET surface area (130) of γ-Al_2O_3 is presented in Table 4.

3. "SEALED" SULFURIC ACID ANODIC ALUMINUM OXIDE

Aluminum anodized for 20 minutes in 15% H_2SO_4 was placed in distilled water, maintained at 90°C for 24 hours. The Kr BET surface area of "sealed" sulfuric acid anodic aluminum oxide is given in Table 4.

B. REFERENCE COMPOUNDS

The following compounds were used as standards for XPS measurements:

Aluminum sulfate [$Al_2(SO_4)_3 \cdot 18H_2O$], aluminum phosphate [$AlPO_4$], sodium oxalate [$Na_2C_2O_4$] and aluminum carbide [$Al_4C_3$] were obtained from Alfa Chemical Company and were used as received. γ-Aluminum oxide [γ-Al_2O_3] was obtained from Alcoa(131) and dried 24 hours at 400°C under a 20 ml/min flow of helium before use.

C. CATALYTIC REACTIONS

The catalytic experiments were carried out in the apparatus diagramed in Figure 7. A helium stream saturated with isopropanol flowed at a rate of 20 ml/min over the catalyst, which was packed in a quartz flow reactor. The reactor was connected on line to a Valco sampling valve, and in series with a Perkin-Elmer Sigma 3B gas chromatograph equipped with a thermal conductivity detector. The reactor was loaded with either 0.5 grams of anodic aluminum oxide strips, 0.5 grams of sealed sulfuric acid anodic aluminum oxide strips, 0.5 grams of unanodized

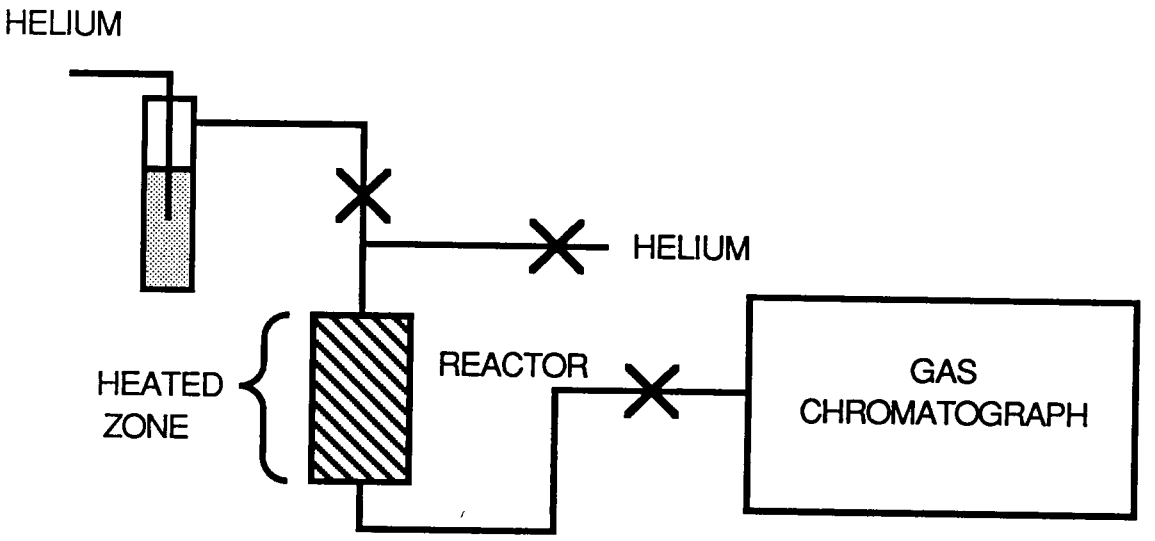

Figure 7. Schematic of flow reactor.

aluminum, or 0.2 grams of γ-Al_2O_3. The total surface area in the reactor during catalytic reactions is listed in Table 5.

Separation of hydrocarbons was accomplished using an 8 ft x 1/4 in glass column packed with Porapak QS. Helium was used as the carrier gas at a flow rate of 30 ml/min. A column temperature of 150°C, and a detector temperature of 200°C were used. The chromatographic response to the products and reactants was determined by injecting known amounts of the respective materials into the gas chromatograph. The peak areas were used to obtain a standard calibration curve. Data acquisition was carried out using a Perkin-Elmer LCI-100 Laboratory Integrator. The reaction products were identified by mass spectrometric analysis. The GC separated products were passed through a cold trap maintained at -93.9°C. The trapped reaction products were analyzed using an UTI 100 quadrupole mass analyzer.

1. PRETREATMENT SURVEY

Three different pretreatments of anodic oxides were compared:

a. Anodic aluminum oxide was heated to the reaction temperature under an isopropanol flow of 20 ml/min. It took 30 minutes for the reaction temperature to be reached. The reaction was then continued for three

Table 5

Total Surface Area of Catalyst Used in Reactions

Electrolyte	Anodization Length (minutes)	Surface area of catalyst (m^2)
H_2SO_4	20	1.10
H_2SO_4	10	0.60
$H_2C_2O_4$	20	0.40
H_3PO_4 "sealed"	20	0.03
H_2SO_4	20	0.40
γ-Al_2O_3	na	18.00

na = Not applicable

hours.

b. Anodic aluminum oxide was held at the reaction temperature under a helium flow of 30 ml/min for two hours. The isopropanol flow of 20 ml/min was then started and the reaction was carried out for three hours.

c. Anodic aluminum oxide was held at the reaction temperature under a helium flow of 30 ml/min for thirteen hours. The isopropanol flow was then started and the reaction was investigated for three hours.

2. BLANKS

Unanodized aluminum strips were used as a blank in the studies. Unanodized aluminum(99.99%), 0.01cm thick was first degreased by wiping with acetone. Degreased aluminum was heated under a 30 ml/min flow of helium at the reaction temperature for 2 hours. A 20 ml/min flow of isopropanol was then initiated and the reaction was continued for 2 hours. Reactions at temperatures between 150°C and 400°C were studied.

3. γ-Al_2O_3

γ-Al_2O_3 was also studied as a catalyst in the dehydration of isopropanol. 0.2 grams of γ-Al_2O_3 of a 50 mesh powder were placed between two pieces of quartz wool and held at the reaction temperature under a helium flow of 30 ml/min for two hours. The isopropanol flow of 20 ml/min was then started and the reaction was continued for three

hours. Reaction temperatures between 150°C and 400°C were studied.

4. BROMINE ETCHED SULFURIC ACID ANODIC ALUMINUM OXIDE

15% sulfuric acid anodic aluminum oxides were placed in a 2% bromine/methanol solution and gently heated for one minute. The catalytic activity of 15% sulfuric acid anodic aluminum oxides that had been etched in a 2% bromine/methanol solution was then studied. The oxide was held at 300°C for 2 hours under a 30 ml/min flow of helium. A 20 ml/min flow of isopropanol was then started and continued for 2 hours.

5. LONG-TERM REACTIONS

The catalytic activity of a two-hour pretreated sulfuric acid anodic aluminum oxide was studied at a reaction temperature of 300°C. Sulfuric acid anodic aluminum oxide was thermally pretreated two hours at 300°C under a 30 ml/min flow of helium in a flow reactor. After the thermal pretreatment was complete, a 20 ml/min flow of isopropanol was initiated over the catalyst. The reaction was continued for 73 hours. It was possible to change helium tanks without interrupting the flow of helium or exposing the catalyst to air.

6. EFFECTS OF PORE LENGTH

The catalytic activity of twenty-minute, ten-minute, and "sealed" twenty-minute sulfuric acid anodic

aluminum oxide was compared. The anodic oxides were thermally pretreated for two hours under a 30 ml/min flow of helium at the reaction temperature. A 20 ml/min flow of isopropanol was then initiated and the reaction was continued for three hours.

D. CHARACTERIZATION OF ANODIC OXIDES ON ALUMINUM

1. X-RAY PHOTOELECTRON SPECTROSCOPY

Anodic aluminum oxide surfaces were characterized using a Perkin-Elmer PHI 5300 x-ray photoelectron spectrometer before and after use as a catalyst. The core energy levels for the aluminum 2p, oxygen 1s, carbon 1s, sulfur 2p, and phosphorus 2p were studied. Photoelectrons were generated, using a Mg anode ($h\nu$ = 1253.6 eV). The pressure in the instrument was approximately 10^{-8} torr during the measurements. The spectrometer energy scale was calibrated, using 285.0eV for the CH_n C 1s peak. This value was established using the Au $4f_{7/2}$ photopeak(84.4 eV) as a reference. The precision of the binding energy measurements is ±0.2eV. Spectra were collected using a Perkin-Elmer 7500 computer. The integrated peak intensities were evaluated by measuring the peak areas and correcting the measured area using sensitivity factors calculated from XPS measurements on γ-Al_2O_3, $AlPO_4$, $Al_2(SO_4)_3 \cdot 8H_2O$, and $Na_2C_2O_4$. The calculated O 1s, Al 2p, S 2p, P 2p, and C(oxalate) 1s sensitivity factors are listed in Table 6.

Table 6

XPS Sensitivity Factors

Al 2p	0.2
O 1s	1.0
S 2p	1.0
P 2p	0.63
C 1s*	0.47

*oxalate

The atomic ratios were calculated using standard methods (132,133).

Following any particular treatment or use in the reactor, the anodized aluminum samples were taken directly from the reactor and stored in a desiccator until they were analyzed.

2. SCANNING ELECTRON MICROSCOPY

Scanning electron microscopy was used to examine both the cross-section and the surface of anodic aluminum oxides. By examining the cross-sections it was possible to determine the oxide thickness as a function of the length of the anodization. These SEM measurements were carried out at Alcoa(134) using an ISI-40 scanning electron microscope. The anodic aluminum oxides were embedded in epoxy, polished and the edge of the embedded sample was then examined by scanning electron microscopy. The thicknesses of oxide films on aluminum anodized in 15% H_2SO_4 for 10, 15, 20, and 40 minutes; in 3% $H_2C_2O_4$ for 20, 30 and 40 minutes; in 4% H_3PO_4 for 20, 90, and 120 minutes; and in 15% H_3PO_4 for 20 minutes were measured. SEM measurements were also made on a ISI-SX-40 scanning electron microscope. Cross-sections of transparent oxide films were studied to determine the oxide thickness, by examining the edge of the oxide. Before each SEM measurement, the surfaces were sputter coated with

approximately 200Å of gold.

3. KRYPTON BET SURFACE AREA

The krypton BET surface areas for anodic oxides on aluminum were measured in duplicate using a Micrometrics Accusorb 2100E surface area analyzer. Sample bulbs were loaded using 0.2 g of anodized aluminum strips($Al+Al_2O_3$). The oxide sample was outgassed for 30 minutes at 25°C under vacuum. The isotherms were determined at liquid N_2 temperature. The anodized aluminum was exposed to 0.05 torr increments of Kr between 0.3 torr and 0.5 torr. Two computer programs were employed in conjunction with an IBM-AT computer to calculate surface areas based on the BET equation. A computer program(listed in Appendix 1) was written to calculate the volume of gas adsorbed after each adsorption step. The volume of gas adsorbed was then entered into a program provided by Micromeritics(135) to calculate the surface area by the BET equation. The cross-sectional area for Kr was assumed to be 19.5 $Å^2$/molecule. The surface areas of anodic oxides thermally pretreated for two hours at 200°C, 300°C, 400°C, and 500°C were measured.

4. NITROGEN BET SURFACE AREA

The N_2 BET surface area for γ-Al_2O_3 was measured in duplicate using a Micromeritics Accusorb 2100E(130). Approximately 0.2 grams of γ-Al_2O_3 were measured into sample bulbs. The sample was outgassed for 30 minutes at

25°C under vacuum. The γ-Al_2O_3 was exposed to 20 torr increments of N_2 between 130.0 and 210.0 torr. The cross-sectional area for N_2 was assumed to be 16.2$Å^2$/molecule.

5. SURFACE ACIDITY

The acidity of anodic oxides on aluminum was measured using three different methods: the adsorption of pH indicators; the adsorption of ammonia and pyridine measured by infrared spectroscopy; and the desorption of pyridine using temperature programmed thermal desorption mass spectrometry.

a. pH INDICATORS

Sulfuric, phosphoric, and oxalic acid anodic aluminum oxide samples were thermally pretreated in a flow reactor(Fig. 7), under a 30 ml/min flow of helium for two hours at 200°C, 300°C, 400°C, and 500°C. The oxides were then cooled to room temperature under helium, removed from the flow reactor, and the pH of the surface was tested. One drop of each pH indicator was placed on the thermally pretreated oxide surface; the color of the indicators provided an approximate measure of the acidity. The indicators used in this study are listed in Table 7 where the endpoints and the corresponding color changes are given.

PREPARATION OF INDICATORS

Orange I (Pfaltz and Bauer, Inc.), sodium

Table 7

pH Indicators

Indicator	color change	pH range
Thymol blue	red -> yellow	1.2-2.8
	yellow -> blue	8.0-9.6
Orange I	red -> yellow	1.2-2.5
Bromophenol blue	yellow -> blue	3.0-4.6
Bromocresol green	yellow -> blue	3.8-5.4
Bromocresol purple	yellow -> purple	5.2-6.8
Bromothymol blue	yellow -> blue	6.0-7.6
Neutral red	red -> amber	6.8-8.0

azo-α-naphtholsulfanilate - 0.02 grams of crystalline orange I was dissolved in 50 ml of distilled water.

Thymol Blue (Pfaltz and Bauer, Inc.), Thymolsulfonephthalein - 0.02 grams of crystalline thymol blue was dissolved in 50 ml of distilled water.

Bromphenol Blue (Arthur H. Thomas Co.), 3,3',5,5'-tetrabromophenolsulfonphthalein - 0.02 grams of crystalline bromphenol blue was dissolved in 50 ml of distilled water.

Neutral Red (Fisher),3-amino-7-dimethylamino-2-methylphenazine hydrochloride - 0.01 grams of crystalline neutral red was dissolved in 50 ml of ethanol and 50 ml of distilled water.

Bromocresol Green (Chemical Dynamics), 3,3',5, 5'-tetrabromo-m-cresolsulfonphthalein - 0.1 grams of crystalline bromocresol green was dissolved in 14.3 ml of 0.01 N NaOH and 235.7 ml of distilled water.

Bromothymol Blue (Chemalog), 3,3'-dibromothymolsulfonphthalein - 0.1 grams of crystalline bromothymol blue was dissolved in 16 ml of 0.01 N NaOH and 234 ml of distilled water.

Bromocresol Purple (Chemical Dynamics), 5,5'-dibromo-o-cresolsulfonphthalein-0.1 grams of bromocresol purple was dissolved in 18.5 ml of 0.01 N NaOH and 231.5 ml of distilled water.

b. INFRARED SPECTROSCOPY

The adsorption of pyridine and ammonia on sulfuric and phosphoric acid anodized aluminum, and of ammonia on γ-Al_2O_3 was studied as a function of pretreatment temperature by transmission infrared spectroscopy. An IR spectrum of the oxide, using two transparent windows of anodic aluminum oxide was measured before and after a thermal pretreatment using a Nicolet 5DXB FTIR equipped with a liquid N_2 cooled MCT detector. The band position assignments have a precision of ±0.5 cm^{-1}. Each spectrum was the accumulation of 1000 scans. Thermal pretreatments were carried out at 200°C, 300°C, or 400°C for two hours under a 30 ml/min helium flow in a flow reactor followed by transfer to the IR cell(Fig. 8). After the transfer, the IR cell was evacuated to 50 μm or lower and heated at 100°C for fifteen minutes to rid the samples of physically adsorbed water. The pressure was measured using an uncalibrated Hastings thermocouple gauge. The temperature was measured using a calibrated chromel-alumel thermocouple. The thermocouple temperature was calibrated using a series of melting point standards. After the thermal pretreatments, the oxides were exposed to 1 atm. of pyridine or ammonia for two hours. The sample cell was evacuated to 50 μm or better at 25°C and a spectrum of the sample was measured. Pyridine and ammonia were desorbed at 150°C and 200°C by increasing the

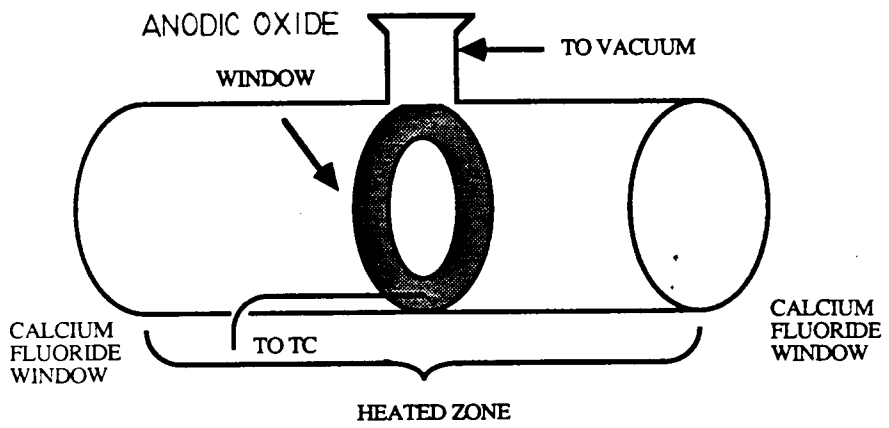

Figure 8. Schematic of IR cell.

temperature of the cell to the designated temperature while the cell was evacuated to 50 μm. The temperature was held constant for fifteen minutes, the cell was then cooled to room temperature, and the IR spectrum was measured. The IR spectrum of the pretreated oxide was subtracted from the IR spectrum of pyridine adsorbed on the anodic aluminum oxide. The area of each IR band in the subtraction spectrum was measured using the software provided by Nicolet. Before each IR measurement, the IR bench was purged with dry N_2 for 2 minutes at a flow rate of 30 ml/min to eliminate water and CO_2 from the system. Even though the adsorption of ammonia and pyridine on oxalic acid anodized aluminum was not studied by IR spectroscopy, the effect of thermal pretreatments on oxalic acid anodized aluminum windows was studied by IR spectroscopy. One oxide window was heated two hours at 200°C, 300°C, or 400°C in a flow reactor under a 30 ml/min flow of helium. The IR spectrum was measured before and after the thermal pretreatment.

i. PREPARATION OF TRANSPARENT OXIDE WINDOWS

A 1.5 cm disk of 1.0 mm thick aluminum was anodized on both sides in a 15%(w/w) H_2SO_4, 3%(w/w) $H_2C_2O_4$, or 4%(w/w) H_3PO_4 solution. One side of the disk was then mechanically abraded and placed in a solution composed of 2 ml of bromine and 100 ml of dry methanol. The solution was gently heated until the aluminum was dissolved, leaving a

transparent aluminum oxide window. The oxide window was then thoroughly rinsed in methanol. The oxide thickness was measured by SEM as described previously. The oxide thicknesses were 10±1μm.

ii. PREPARATION OF γ-Al_2O_3

High purity γ-Al_2O_3(131) was compressed into a self-supporting disk 1.5 cm in diameter and weighing 0.1 grams.

iii. MATERIALS

Gaseous anhydrous ammonia (Matheson) was used as received. Pyridine (Fisher) was degassed several times under vacuum (50μm) before use. Bromine(Fisher) was used as received. Methanol(Fisher) was dried over molecular sieve before use.

E. TEMPERATURE PROGRAMMED DESORPTION

An UTI quadrupole mass analyzer was used as a detector in temperature programmed desorption (TPD) experiments. A tungsten filament was used to heat a piece of anodic oxide on aluminum attached to an electrical feedthrough (Figure 9). The temperature of the sample was measured by a calibrated chromel-alumel thermocouple. The temperature was controlled by an Omega Model CN-210 temperature controller. A 10°C/min temperature ramp was used. Due to the porous nature of the oxides, a slow temperature ramp was chosen. In all experiments, the mass

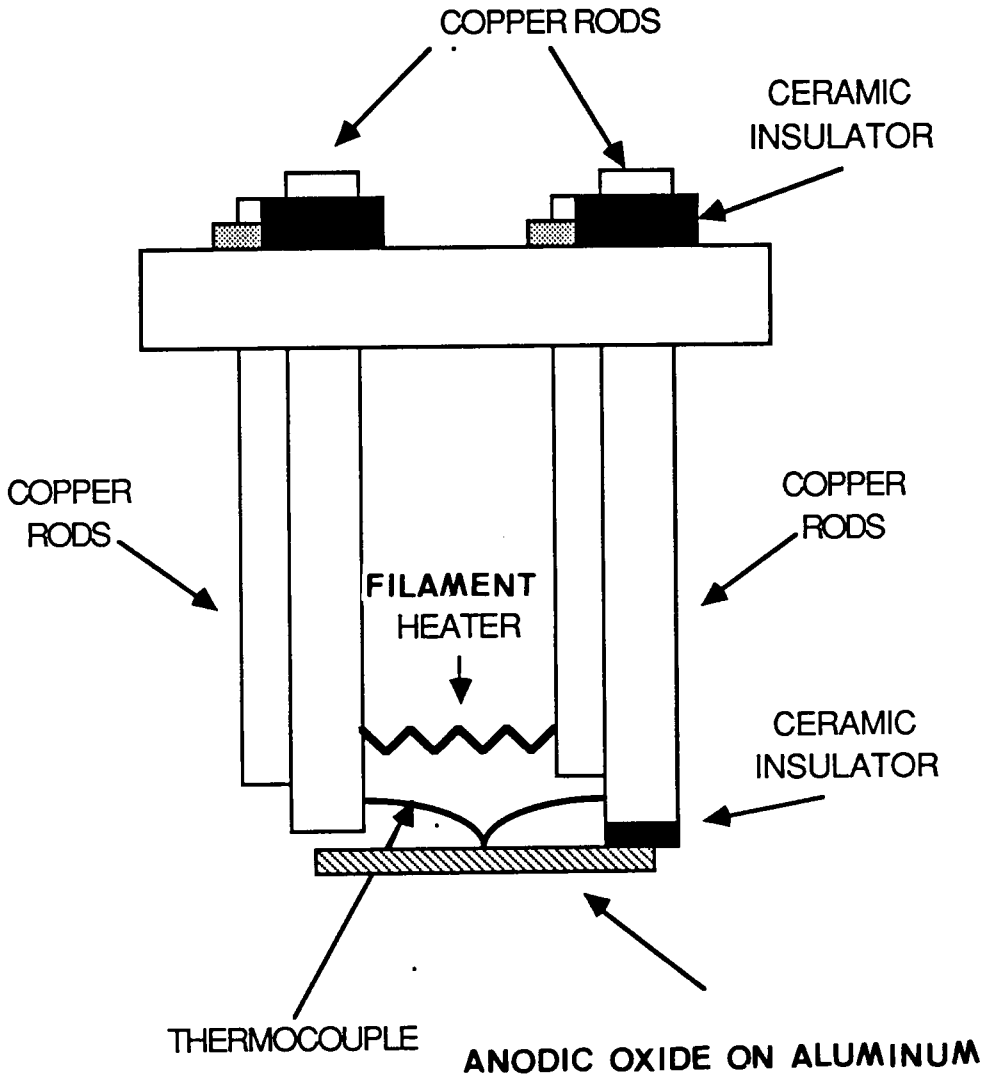

Figure 9. Schematic of the electrical feed-through used in the mass spectrometer vacuum system.

spectrometer filament emission current was 1.0 mamp, the electron energy was 70 eV, and the instrument sensitivity was between 10^{-9} and 10^{-10} amps.

The ion detector used in this study was a channeltron electron multiplier. Data collection and processing was accomplished using a Tecknivent interface and software installed on an IBM-AT computer. The software made it possible to monitor the whole spectrum(4-100m/z) or individual masses.

Anodic Oxide on Aluminum

A 3 cm x 1 cm piece of sulfuric, oxalic, or phosphoric acid anodic oxide on aluminum was placed on the feed-through, so it was electrically isolated. The feedthrough was then connected to the vacuum chamber pictured in Figure 10. The chamber was evacuated to a pressure of 4 x 10^{-7} torr. The sample was thermally treated two hours at 200°C, 300°C, or 400°C under vacuum. Once the thermal treatment was complete, the sample was cooled to 30°C, and exposed to 1 atm of pyridine for two hours. The vacuum chamber was then evacuated to 4 x 10^{-7} torr, and the sample was heated to 400°C at a rate of 10°C/minute. The pressure was measured by a ionization gauge. The desorbed gases were monitored by mass analysis as a function of temperature. A mass spectrum was collected every 10°C, the first mass spectrum was collected

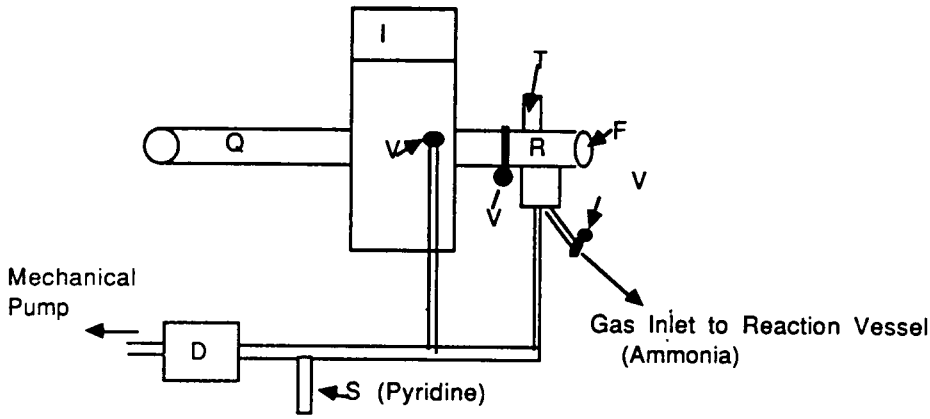

D = Diffusion Pump
F = Electrical Feedthrough
I = Ion Pump
Q = Quadrupole
V = Valve
R = Reaction Vessel
T = Pressure Thermocouple
S = Pyridine Vessel

Figure 10. Schematic of mass spectrometer vacuum system.

before heating was started. The area of each thermal desorption peak was calculated, using the software provided by Tecknivent. The baseline was drawn from valley to valley as shown in a typical thermal desorption profile in Figure 11. The precision of the area measurements was ±10%. Standard spectra of pyridine were measured at pressures of $5x10^{-7}$, $5x\ 10^{-6}$, and $1x10^{-6}$ torr and used as references for product analyses and to prepare a calibration curve for pyridine desorbed from the oxides. The pressure of pyridine was measured using the ion pump gauge output. The calibration curve for m/z 79 was linear in this region.

The partial pressure of pyridine desorbed was calculated using equation 4 with the area of the desorption peak (m/z 79), the intensity (peak height) of the m/z 79 peak in the standard spectrum, and the pressure at which the standard spectrum was measured.

$$\frac{\text{m/z 79 peak area of desorbed pyridine}}{x} = \frac{\text{m/z 79 peak height of pure pyridine}}{\text{pressure of pure pyridine}} \quad [4]$$

x= partial pressure of pyridine desorbed

The volume of the mass spectrometer was estimated. The volume of the mass spectrometer and the partial pressure of pyridine desorbed were used to calculate the number of mmoles of pyridine desorbed from the oxides.

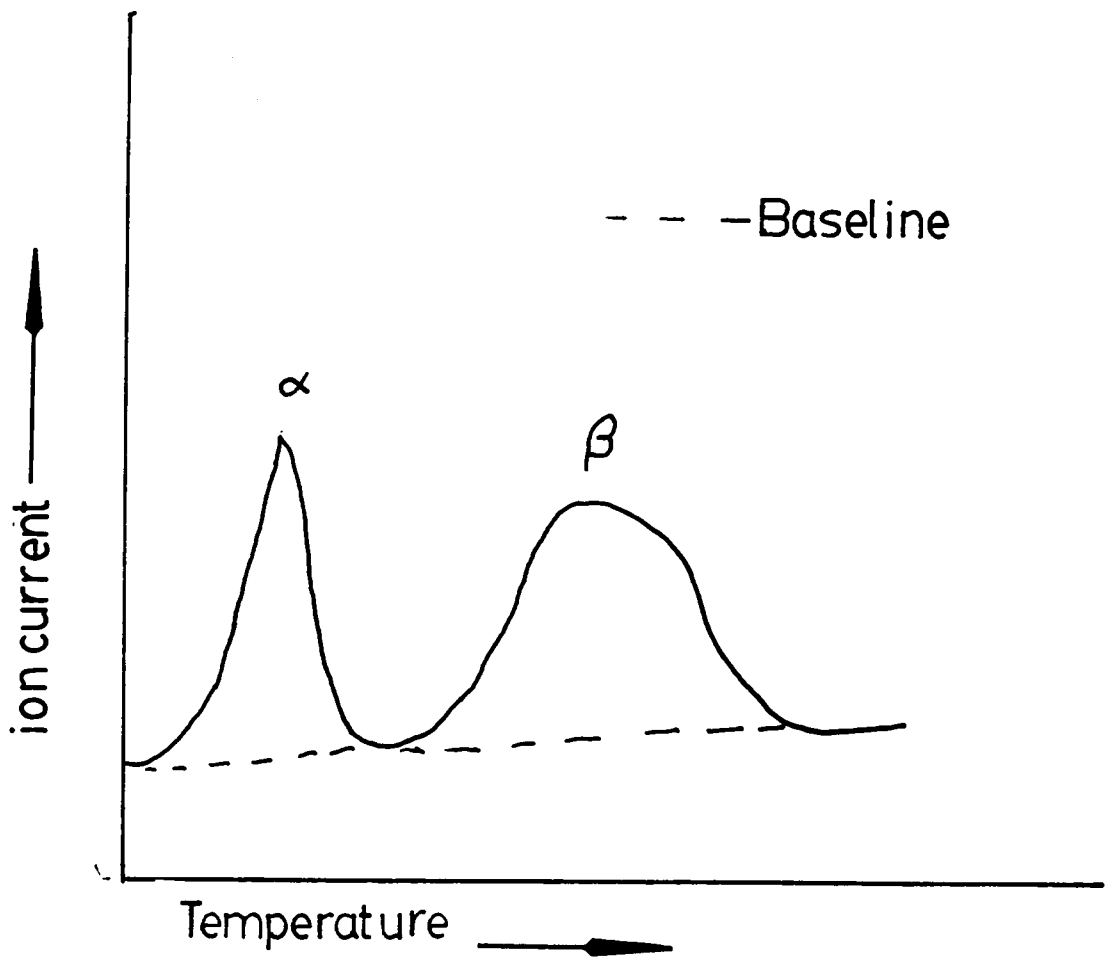

Figure 11. Typical temperature programmed desorption profile.

Chapter 4

RESULTS AND DISCUSSION

A. PORE DIAMETER

Surface area, pore size, and the oxide thickness are physical properties that are important to consider in a catalytic study of anodic oxides on aluminum. The pore diameter may determine whether the reactant molecule can diffuse into the pore, therefore increasing the surface area available for adsorption of the reactant and the residence time of the molecule on the oxide. The pore diameters of the oxides used in this study were measured from scanning electron (SEM) photomicrographs.

Shown in Figure 12a is a SEM photomicrograph of phosphoric acid anodic oxide(20 minute) on aluminum. The pores are closely packed and the pore diameter is between 500-1000Å. A one hour anodization in phosphoric acid results in pore diameters(between 500-1000Å) that are the same as after a 20 minute anodization as shown in Figure 12b, The increased time spent in the acid did not increase the pore diameter.

Similar results are obtained for oxalic acid anodized aluminum. A 20 minute anodization in oxalic acid results in the surface shown in the SEM photomicrograph in Figure 13a. The average pore diameter resulting from a 20 minute

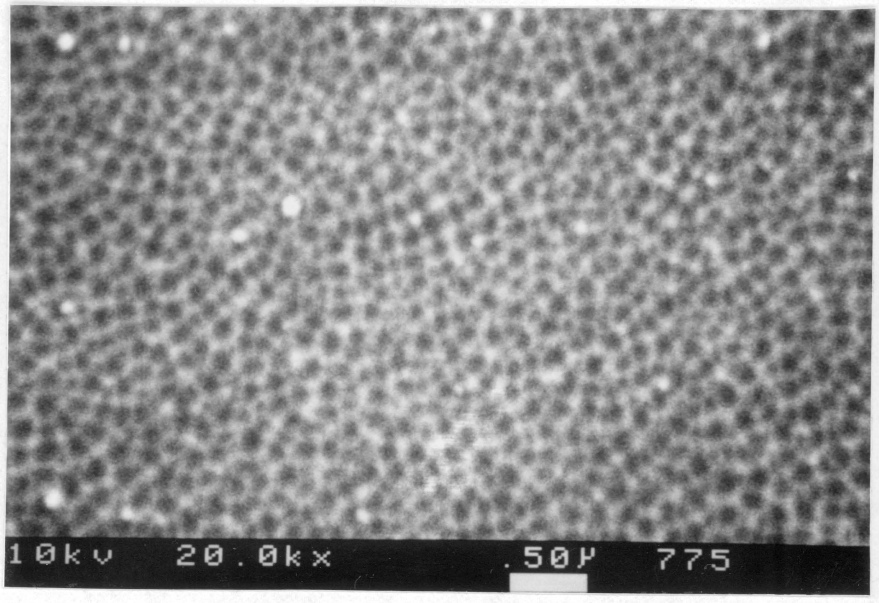

Figure 12a. SEM photomicrograph of 20 minute 4% phosphoric acid anodic oxide on aluminum.

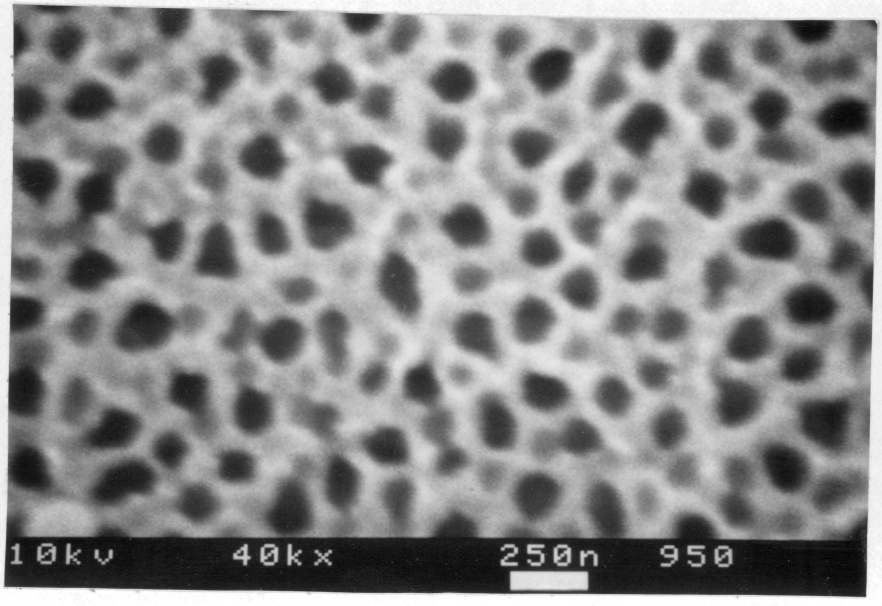

Figure 12b. SEM photomicrograph of 1 hour 4% phosphoric acid anodic oxide on aluminum.

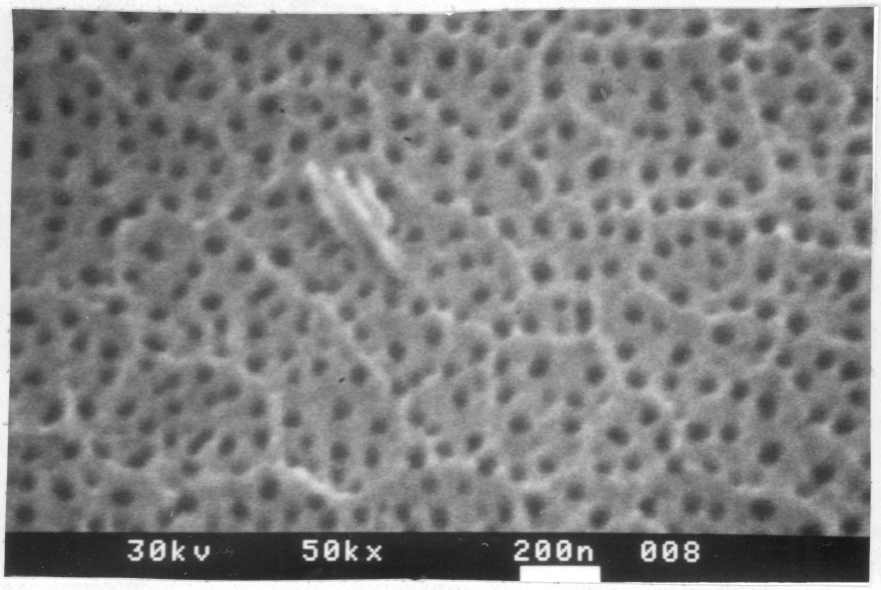

Figure 13a. SEM photomicrograph of 20 minute 3% oxalic acid anodic oxide on aluminum.

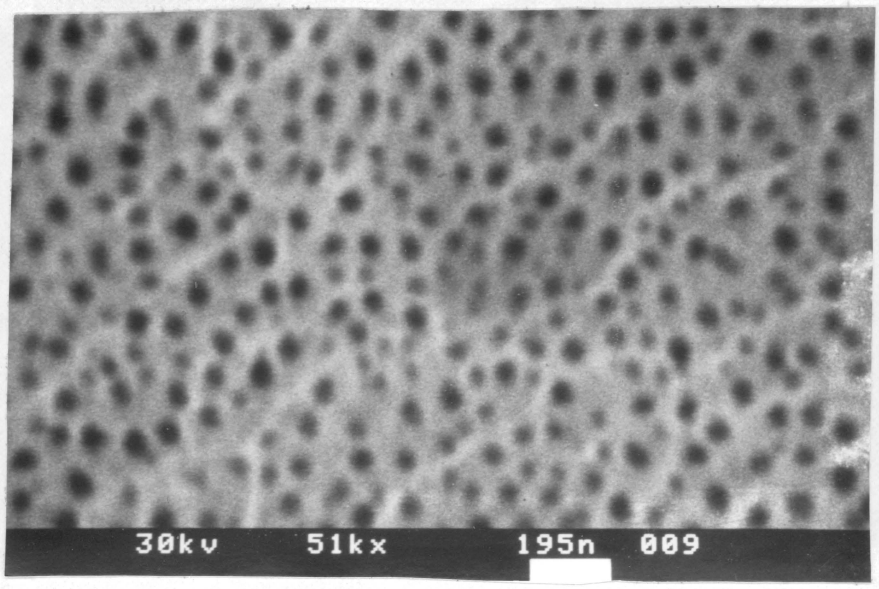

Figure 13b. SEM photomicrograph of 90 minute 3% oxalic acid anodic oxide on aluminum.

anodization in oxalic acid is about 400Å. The pores formed in oxalic acid are smaller than the pores formed in phosphoric acid since the oxide is probably more soluble in phosphoric acid, under the conditions of the anodizations. A 90 minute anodization in oxalic acid results in pores about 400Å(the same as a 20 minute anodization) in diameter as shown in Figure 13b. The anodization time has no effect on pore diameter.

A 20 minute anodization in sulfuric acid results in smaller pores. Shown in Figure 14 is a SEM photomicrograph of sulfuric acid anodized aluminum. The pores are unresolvable by SEM. The pore diameter has been reported to be about 100Å(96).

B. OXIDE THICKNESS

The thickness of the anodic oxide varies with the anodizing voltage, length of anodization, temperature of the anodization solution, and the concentration of the anodization solution. The oxide thicknesses of 15% sulfuric, 3% oxalic, and 4% phosphoric acid anodized aluminum are shown in Figure 15, as a function of the length of anodization. The oxide thicknesses were measured from SEM photomicrographs of cross-sections of the oxide films. For all the anodic oxides studied, a thicker film is favored by longer anodization. Shown in Figure 16 is a SEM photomicrograph of a cross-section of a 2 hour 4%

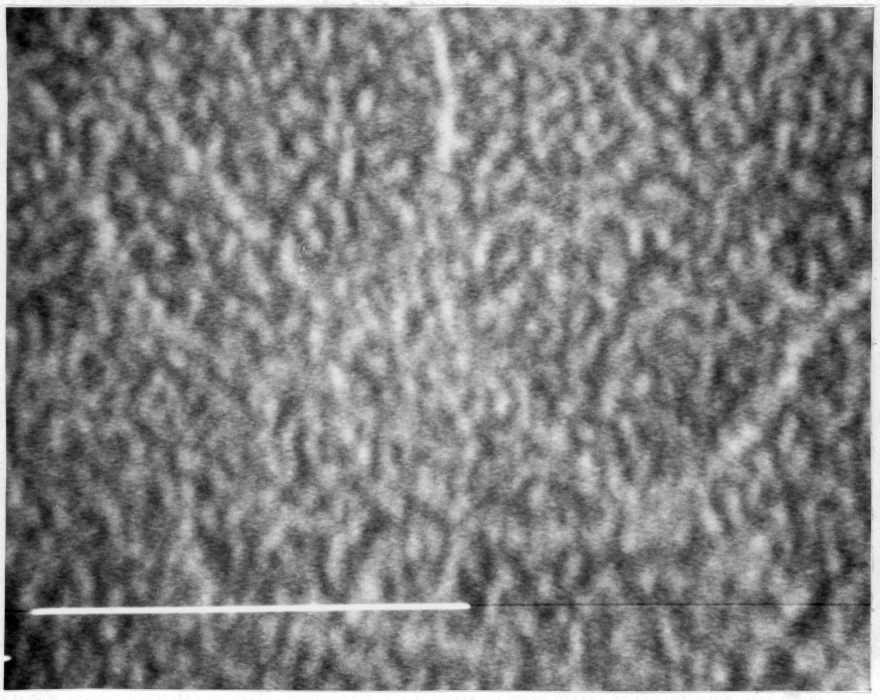

1mm = 100Å

Figure 14. SEM photomicrograph of 20 minute 15% sulfuric acid anodic oxide on aluminum.

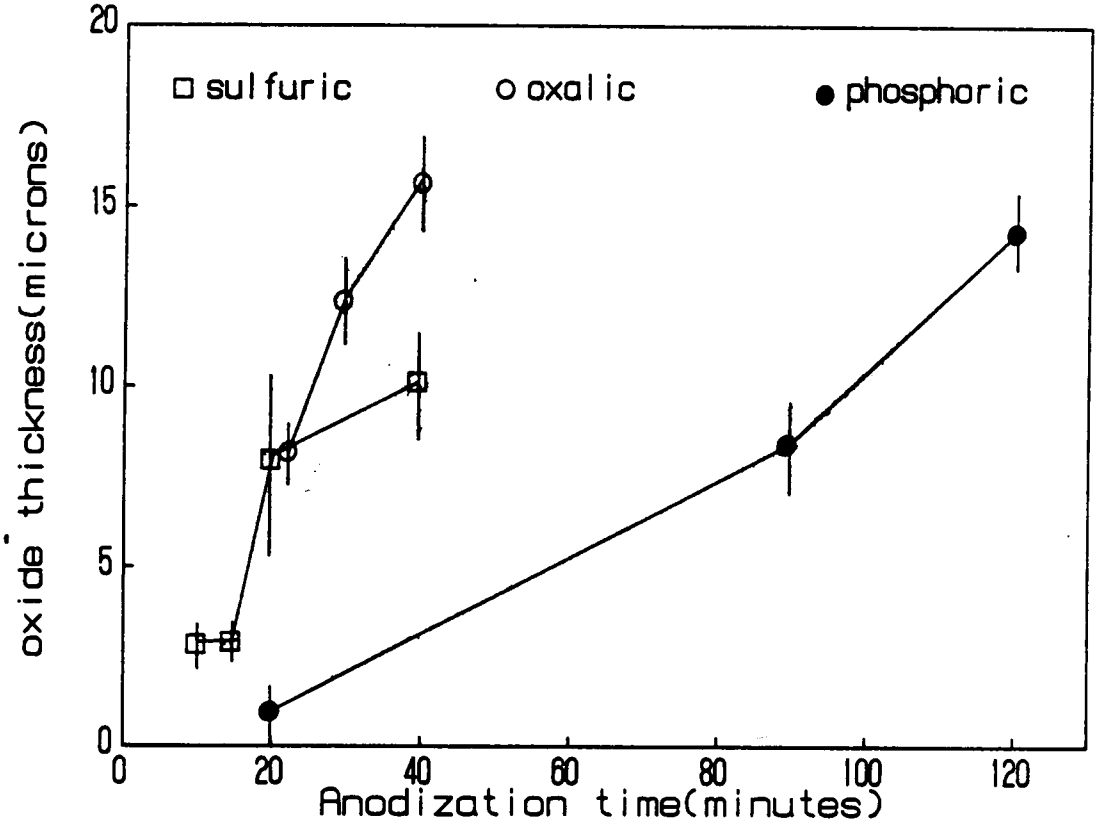

Figure 15. Thicknesses of oxides formed in sulfuric, phosphoric, and oxalic acid as a function of the length of the anodization.

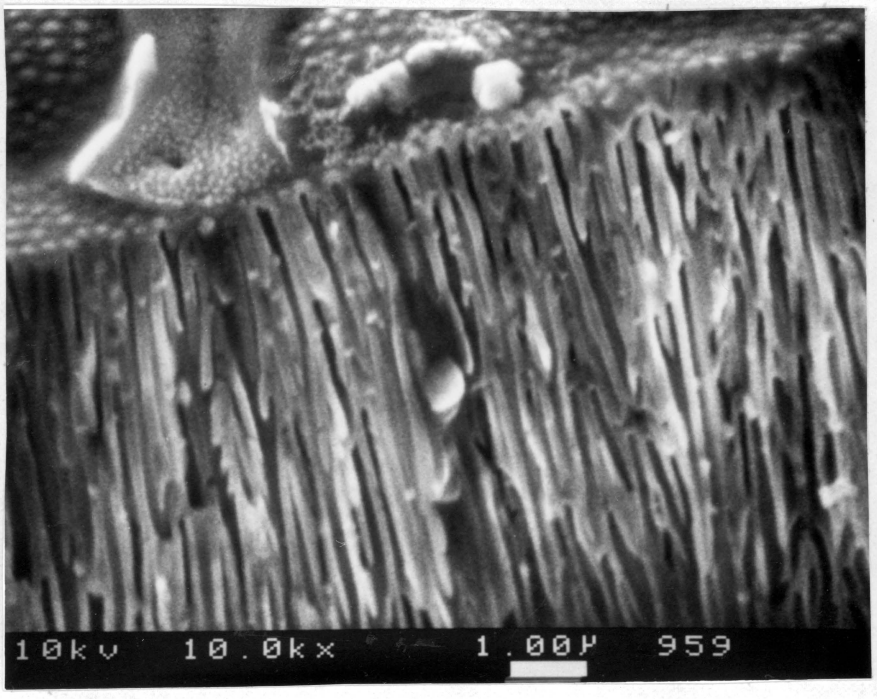

Figure 16. SEM photomicrograph of a cross-section of 4% phosphoric acid anodic oxide.

phosphoric acid anodized oxide film. The photomicrograph shows the bottom of the pores (the top of the photomicrograph) and that the pores are parallel. The oxide shown in Figure 16 was prepared by dissolving the aluminum away from the oxide in a 2% bromine/methanol solution and examining the edge of the oxide.

C. SURFACE AREAS

The surface area of a catalyst is a very important physical property to consider since this is what partially determines the amount of gas that adsorbs on the catalyst. Yamada and Itabashi(16) observed that the surface areas of the oxides formed in sulfuric, oxalic, and phosphoric acid were constant after a heat treatment between 200°C and 500°C.

In an effort to determine what effect a 2 hour thermal pretreatment had on the surface area of the anodized aluminum, the surface areas of the anodized aluminum samples were studied as a function of pretreatment temperature. The surface area results as a function of pretreatment temperature are shown in Figure 17, in which the surface areas(m^2/g of oxide) are plotted versus the pretreatment temperature(°C) for 20 minute, 10 minute, and "sealed" 20 minute sulfuric acid; 20 minute oxalic acid; and 20 minute phosphoric acid anodic oxides on aluminum. Within the error of the measurements(±25%) the surface

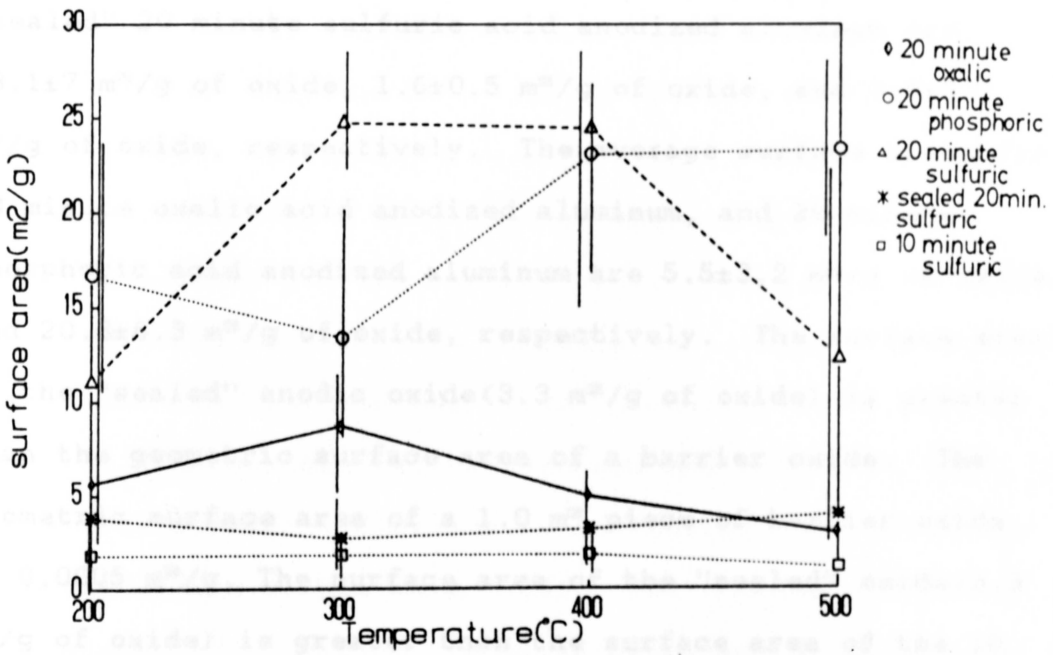

Figure 17. Surface areas(m^2/g of oxide) of 20 minute phosphoric, 10 and 20 minute sulfuric, "sealed" 20 minute sulfuric and 20 minute oxalic acid anodic oxides on aluminum as a function of thermal pretreatment temperature.

areas of all these oxides are constant after thermal treatments between 200°C and 500°C. The surface area of the oxide before a thermal pretreatment is the same as that of the 200°C thermally treated oxide. The average surface areas (± average error) for 20 minute, 10 minute, and "sealed" 20 minute sulfuric acid anodized aluminum are 18.1±7 m^2/g of oxide, 1.6±0.5 m^2/g of oxide, and 3.4±0.7 m^2/g of oxide, respectively. The average surface areas for 20 minute oxalic acid anodized aluminum, and 20 minute phosphoric acid anodized aluminum are 5.5±3.2 m^2/g of oxide and 20.8±6.3 m^2/g of oxide, respectively. The surface area of the "sealed" anodic oxide(3.3 m^2/g of oxide) is greater than the geometric surface area of a barrier oxide. The geometric surface area of a 1.0 m^2 piece of barrier oxide is 0.0005 m^2/g. The surface area of the "sealed" oxide(3.3 m^2/g of oxide) is greater than the surface area of the 10 minute sulfuric acid anodized aluminum(1.3 m^2/g of oxide) and smaller than the surface area of the 20 minute anodized oxide(18.5 m^2/g of oxide). These results indicate that the "sealed" oxide is not completely sealed or that the hydrated Al_2O_3 is microporous. Emmer, Hajek, and Repa(122) reported that the sealing of sulfuric acid anodized aluminum resulted in a surface of hydrated Al_2O_3 composed of fine, loosely connected platelets and needles. Examining the surface of a "sealed" oxide by SEM, a needle-

like material is observed growing out of the pores as shown in Figure 18. Applying the observation made by Emmer, Hajek, and Repa(122) to the surface area results in this study, it can be concluded that these needles increase the surface area of an otherwise planar oxide.

In Table 8 the oxide thickness, pore diameter, current efficiency, average surface area of the oxide, the geometrically "calculated" surface area of the 20 minute sulfuric acid, oxalic acid, and phosphoric acid anodic aluminum oxides, and the surface areas reported by Yamada et al.(16) are listed. The "calculated" surface areas of the oxides are based on the oxide thickness, the pore diameter, the current efficiency, and the weight of the oxide. The current efficiency is an indirect measure of the porosity of the anodic oxide(136). The coating efficiency is expressed in terms of a coating ratio and is determined gravimetrically. If the columbic efficiency of aluminum conversion to alumina is 100%, then the coating ratio is 1.89. For,

$$2Al^{3+} + 3O^{2-} \longrightarrow Al_2O_3;$$

the coating ratio is calculated as follows:

$$\text{coating ratio} = \frac{\text{weight of oxide formed}}{\text{weight of aluminum consumed}} \qquad [5]$$

$$\frac{102 \text{ grams}}{54 \text{ grams}}$$

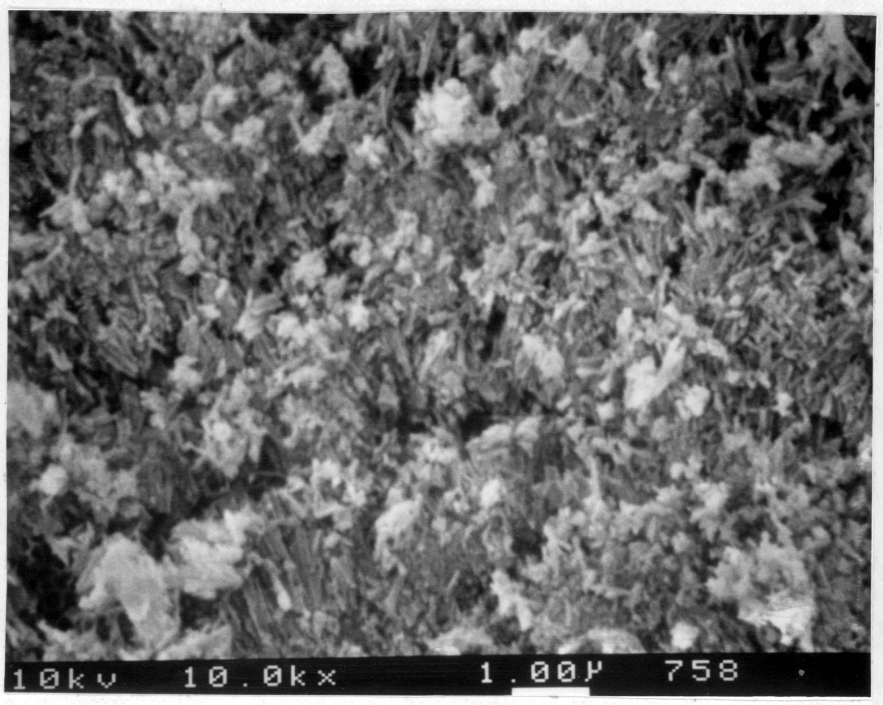

Figure 18. SEM photomicrograph of 20 minute "sealed" 15% sulfuric acid anodic oxide on aluminum.

Table 8

Surface Areas of Anodic Aluminum Oxides

	Oxide thickness (μm)	Pore diameter (Å)	Current efficiency (%)	SA (BET) (m^2/g of oxide)	SA (calc.*) (m^2/g of oxide)	SA (16) (m^2/g of oxide)
15% H_2SO_4	10	100	80	18.1±7.0	16.0	25
3% $H_2C_2O_4$	8	400	70	5.5±3.2	13.8	10
4% H_3PO_4	1	500-1000	40	20.8±6.3	9.7	15

* from geometric dimensions

For two moles of Al^{3+} consumed, one mole of aluminum oxide is formed. Experimental observations(96) indicate that the values measured are always less than 1.89 and decrease as the electrolyte solution temperature and concentration increase. Comparing the measured surface areas based on the oxide weight with the surface areas measured by Yamada et al.(16), it is seen that the order of the surface areas differs slightly. For Yamada et al.(16) the sulfuric acid anodized aluminum has the greatest surface area followed by phosphoric acid anodized aluminum and oxalic acid anodized aluminum. In this study, comparing the "calculated" surface areas to the measured surface areas, some discrepancies are seen. The "calculated" surface areas decrease with increasing pore diameters. The "calculated" surface areas of sulfuric, oxalic, and phosphoric acid anodized aluminum are 16.0 m^2/g of oxide, 13.8 m^2/g of oxide, and 9.7 m^2/g of oxide, respectively. While the corresponding BET "measured" surface areas are 18.1±7 m^2/g of oxide, 5.5±3.2 m^2/g of oxide, and 20.8±6.3 m^2/g of oxide, respectively. Some of the differences between the BET surface areas and "calculated" surface areas are due to experimental errors that are introduced into the surface area measurements, since the lower limit of the measurement is being approached(especially for the phosphoric acid anodic oxides). Water adsorbed on the anodic oxides may

cause differences between the measured and calculated surface areas. Yamada and Itabashi(16) found that after thermal pretreatments at 600°C the surface areas of the oxides increased and the order of the surface areas changed to the order which was expected geometrically (sulfuric >oxalic >phosphoric). According to Yamada, et al. (16), the increase in surface areas and the change in the order of the surface areas were due to the desorption of water from the oxide.

D. RESULTS OF CATALYSIS EXPERIMENTS

1. UNANODIZED ALUMINUM

Unanodized aluminum was studied as a catalyst for the dehydration of isopropanol at temperatures between 150°C and 400°C. The purpose of this study was to determine whether anodization of aluminum is necessary for catalytic activity. Table 9 lists the distribution of products detected over unanodized aluminum samples that were pretreated at 150°C, 175°C, 200°C, 225°C, 250°C, 275°C, 300°C, and 400°C for 2 hours. These results show that unanodized aluminum is not active in the dehydration of isopropanol. After the 400°C thermal pretreatment; however, ≈0.1% activity for isopropanol dehydration is observed.

2. ANODIC OXIDES FORMED IN H_2SO_4

To determine whether the length of the thermal pretreatment had any influence on the dehydration of

Table 9

The Dehydration of Isopropanol over Unanodized Aluminum.

Pretreatment and Reaction Temperature (°C)	Mole Percentage			
	water	propene	acetone	isopropanol
150	<0.01	<0.01	<0.01	100
175	<0.01	<0.01	<0.01	100
200	<0.01	<0.01	<0.01	100
225	<0.01	<0.01	<0.01	100
250	<0.01	<0.01	<0.01	100
275	<0.01	<0.01	<0.01	100
300	<0.01	<0.01	<0.01	100
400	≈0.1	≈0.1	≈0.1	≈99.9

isopropanol, anodic aluminum oxide prepared in 15% H_2SO_4 was studied at temperatures between 150°C and 400°C. The results for dehydration reactions over anodic oxides, not thermally pretreated, thermally pretreated for 2 hours, and thermally pretreated for 13 hours are given in Figure 19. The reaction products, water and propene, were detected using each of the three pretreated catalysts. In Figure 19 the number of mmoles of propene detected/m^2 of oxide is plotted vs. the reaction temperature. For the anodic oxides that were not pretreated, activity was first observed at 250°C where 0.004 mmoles of propene/m^2 of oxide were detected. Total conversion was reached at 300°C(0.13 mmoles of propene/m^2 of oxide). The onset of activity for 2 hour and 13 hour pretreated anodic oxides occurred at 175°C, where 0.004 mmoles of propene/m^2 of oxide were observed. The extent of conversion to propene and water increased with increasing temperature. Total(100%) conversion was reached at 250°C, where 0.13 mmoles of propene/m^2 of oxide were produced. In all cases, equal amounts of water and propene were detected, a result consistent with the stoichiometry of the dehydration reaction.

In an attempt to understand how the thermal pretreatment affected the anodic oxide, transmission infrared spectroscopy was employed to study changes in the

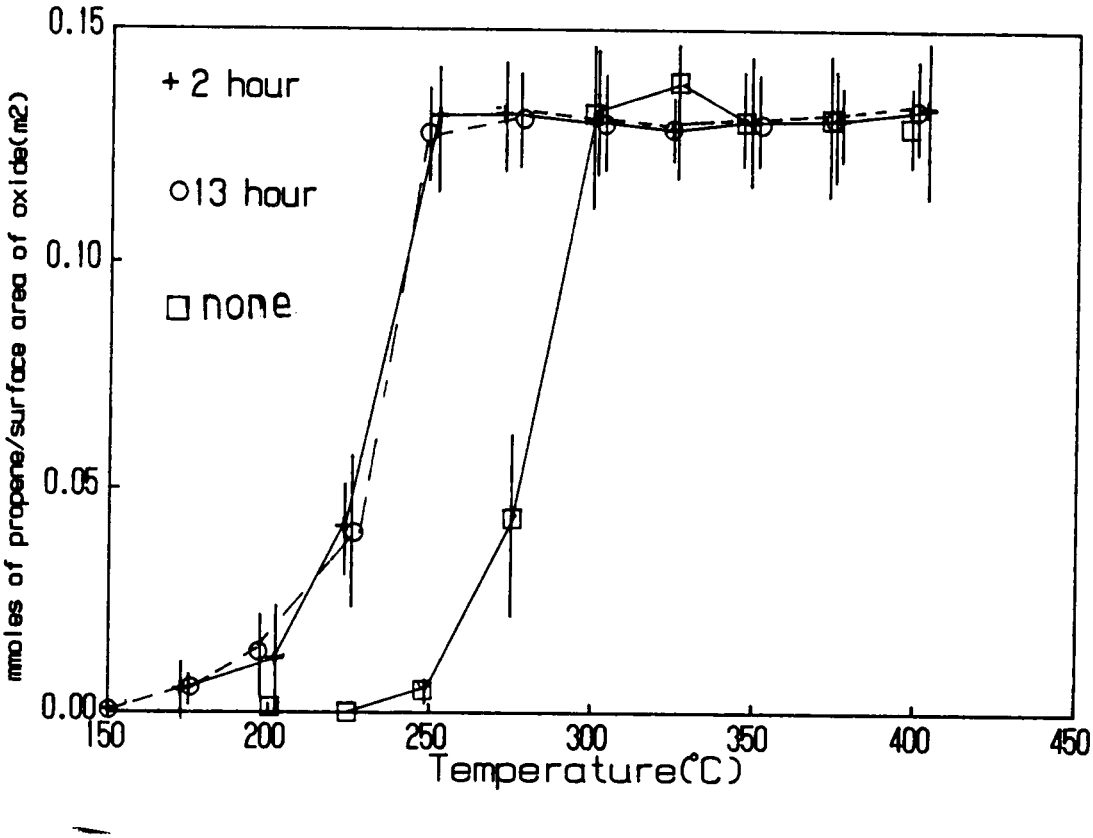

Figure 19. Mmoles of propene/m^2 of oxide observed over non-pretreated, 2 hour, and 13 hour pretreated 15% sulfuric acid anodic oxide on aluminum.

hydroxyl region (3400 cm^{-1}). All the IR spectra obtained by transmission exhibited a wave pattern which is related to the thickness of the windows(137). In Figure 20 is shown an IR spectrum(4800 cm^{-1} - 400 cm^{-1}) of sulfuric acid anodic oxide before it was thermally treated. The O-H stretching vibration of the hydroxyl groups within the anodic oxide occurs at 3400 cm^{-1}, the same frequency observed by Yamada(16). The bands between 1000 cm^{-1} - 400 cm^{-1} are due to the intrinsic vibrations of the aluminum oxide. The band at 1130 cm^{-1} is assigned to the vibration arising from the sulfate species incorporated in the film during anodization(16). In Figure 21 are shown the transmission IR spectra for H_2SO_4 anodic aluminum oxides as a function of pretreatment temperature, where only the region between 4400 cm^{-1} - 2200 cm^{-1} is displayed. The -OH band in Figure 21 looks like a double peak due to birefringence, which is directly related to the thickness of the oxide. The only change in the IR spectra of sulfuric acid anodized aluminum after heating was observed in the hydroxyl region. Before thermal treatment there is a high concentration of hydroxyl groups on the oxide; however, as the temperature increases the concentration of hydroxyl groups decreases. The decrease in hydroxyl group concentration occurs with a shift in band position to a higher frequency. The fact that H_2O is lost at

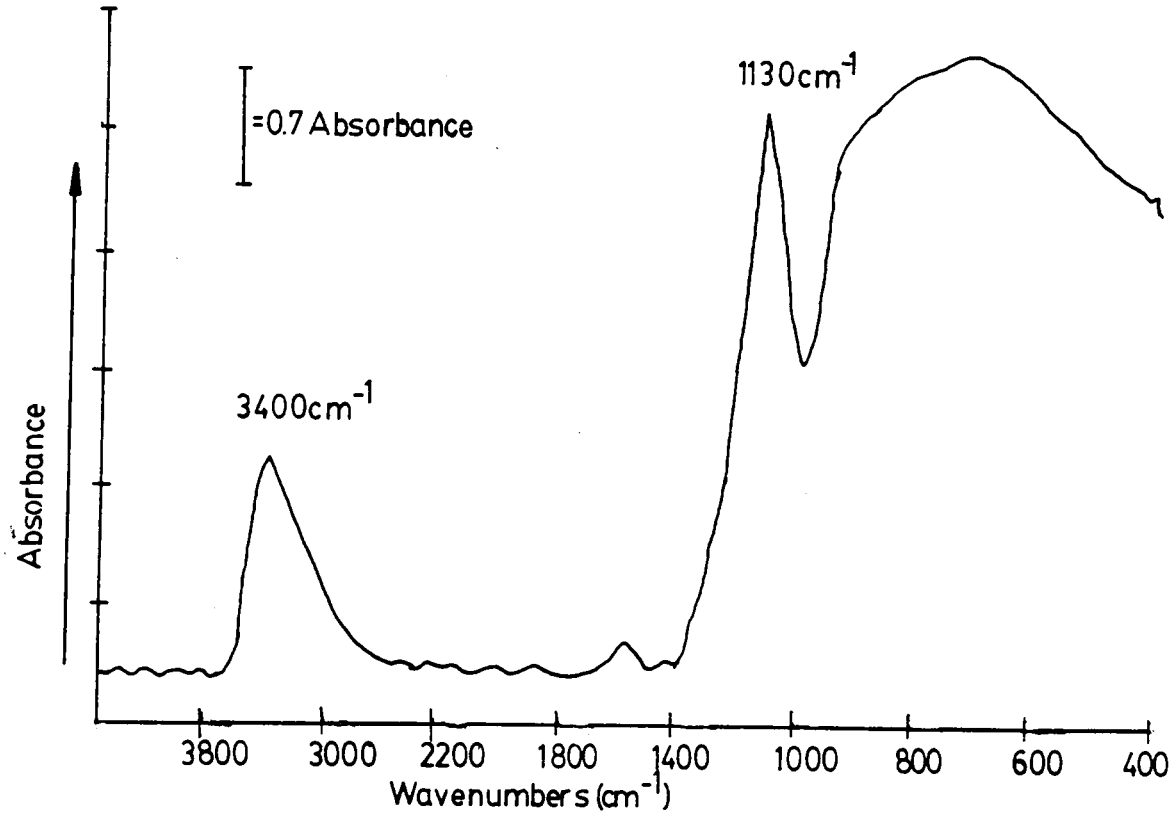

Figure 20. Infrared spectrum of 15% sulfuric acid anodic aluminum oxide before a thermal pretreatment.

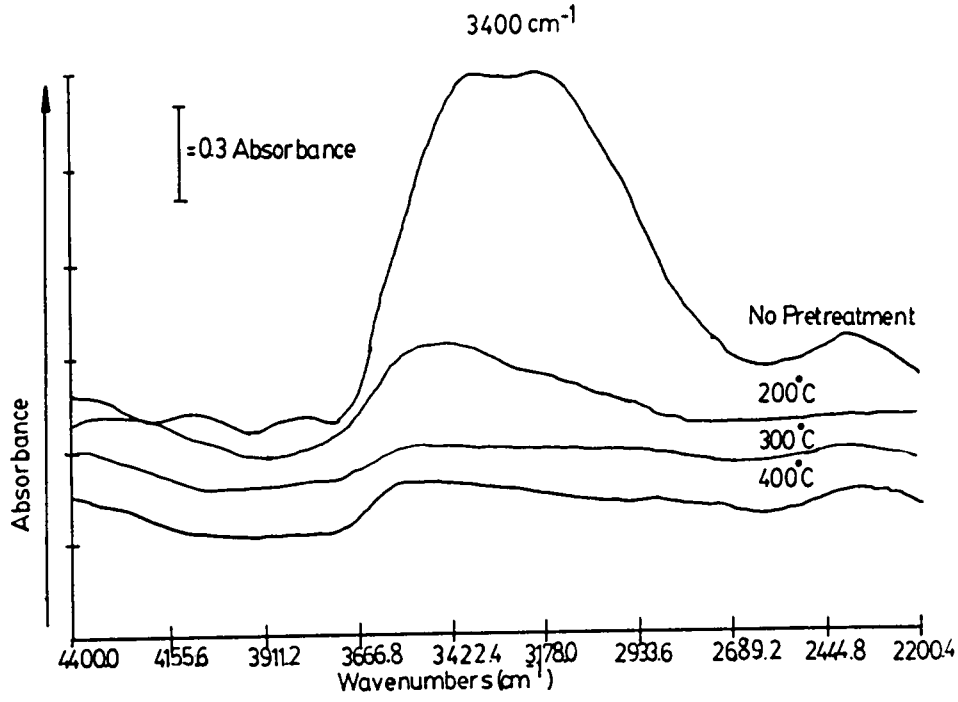

Figure 21. Infrared spectra of hydroxyl region of 15% sulfuric acid anodic aluminum oxide after 2 hour thermal pretreatments at 200°C, 300°C, and 400°C.

lower temperatures shows the -OH groups are less strongly bound than the -OH sites that are left behind. However, the shift in -OH band position to higher frequencies indicates that the -OH groups left behind are less acidic than the -OH site lost. The less strongly bound -OH groups have fewer Al^{3+} ions in their vicinity and are more acidic than the -OH groups which have a greater number of Al^{3+} ions in their vicinity. It has been shown that the dehydrated surface is more active catalytically than the non-pretreated surface. It is therefore concluded that the catalytic activity of H_2SO_4 anodic oxides on aluminum is related to the acidity of the anodic oxide. Recognizing that total isopropanol conversion occurs at 275°C and that complete oxide dehydration is not observed even after treatment at 400°C, suggests the presence of a critical concentration of Brønsted and/or Lewis acid sites.

3. ANODIC OXIDES FORMED IN H_3PO_4

Catalytic reactions over aluminum anodized in 15%(w/w) H_3PO_4 acid yielded results that were unlike the results observed over 15%(w/w) H_2SO_4 anodized aluminum, in that the H_3PO_4 anodic oxides were more active per unit surface area of oxide. The results are shown as a function of temperature in Figure 22. For the anodic oxides that were not thermally pretreated, thermally pretreated 2 hours, and thermally pretreated 13 hours, conversion was first

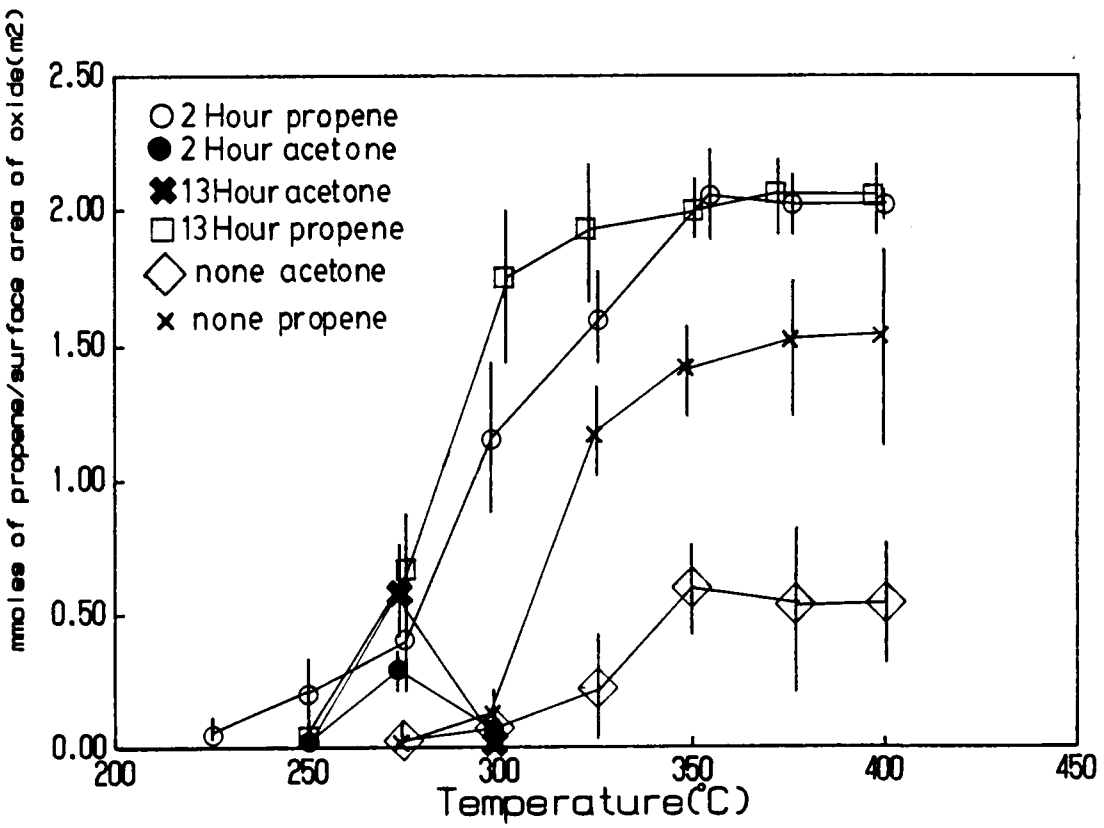

Figure 22. Mmoles of propene and acetone/m^2 of oxide observed over non-pretreated, 2 hour and 13 hour pretreated 15% phosphoric acid anodic aluminum oxide.

observed at 250°C with 0.002, 0.2, and 0.004 mmoles of propene/m^2 of oxide being detected, respectively. In all cases, the extent of conversion increased with increasing reaction temperature. Total conversion (2.0 mmoles of propene/m^2 of oxide) was reached at 350°C for the 2 hour and 13 hour thermally pretreated anodic oxides. Total conversion was reached at 400°C for the non-pretreated anodic oxides where 1.5 mmoles of propene/m^2 of oxide and 0.5 mmoles of acetone/m^2 of oxide were detected.

In Figure 23 is an infrared spectrum for a H_3PO_4 anodic oxide before a pretreatment. An IR absorption band due to the O-H stretching vibration is observed at 3400 cm^{-1}. The peaks due to the intrinsic vibrations of the aluminum oxide are present in the 1000-400 cm^{-1} range. The band at 1150 cm^{-1} is assigned to the vibration from the incorporated phosphate(16). In Figure 24 are shown transmission infrared spectra(4400 - 2200 cm^{-1}) as a function of thermal pretreatment temperature for 4% H_3PO_4 anodic oxides that are 20μm thick. It was necessary to use a 4% instead of a 15% acid solution to obtain windows that were thick enough to detect hydroxide in the IR spectrum. Other than in the -OH region, the IR spectra of the 4% and 15% oxides are the same. The only chemical change in the oxide expected after an anodization in a 4% acid solution compared to an anodization in a 15% acid solution would be in the amount

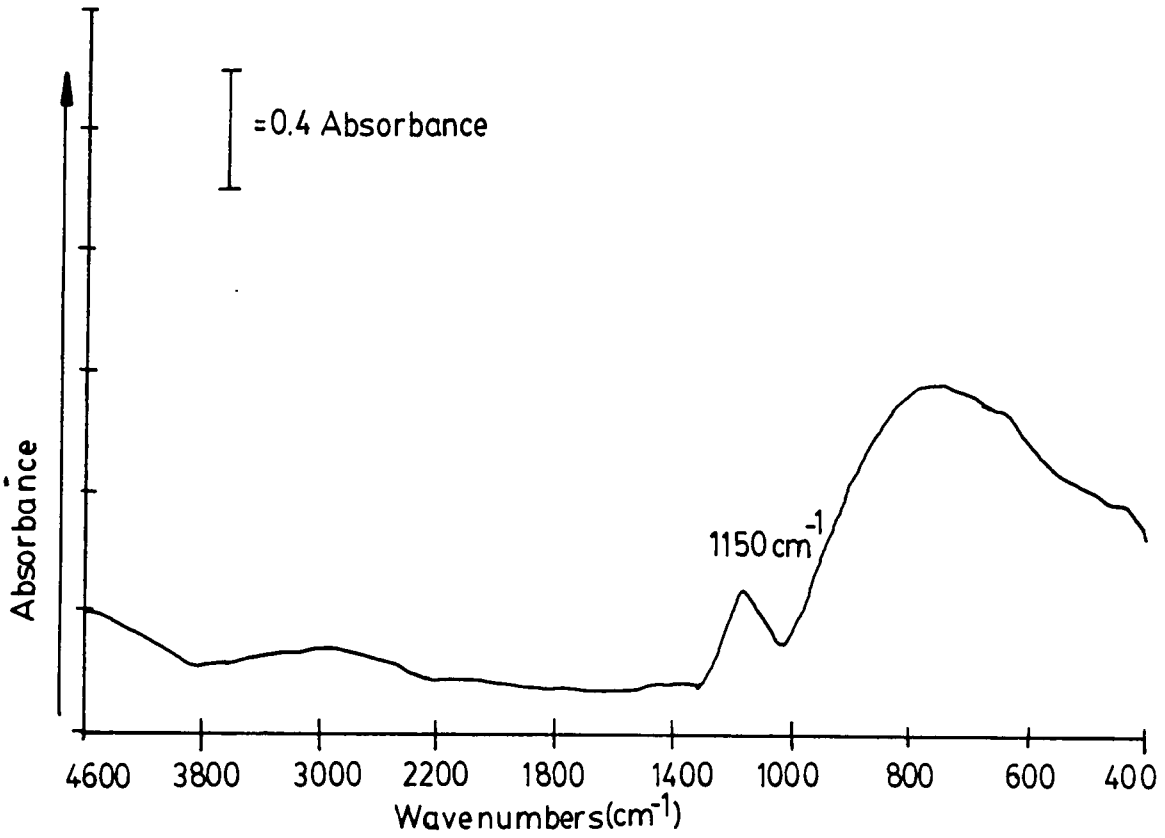

Figure 23. Infrared spectrum of 4% phosphoric acid anodic aluminum oxide before a thermal pretreatment.

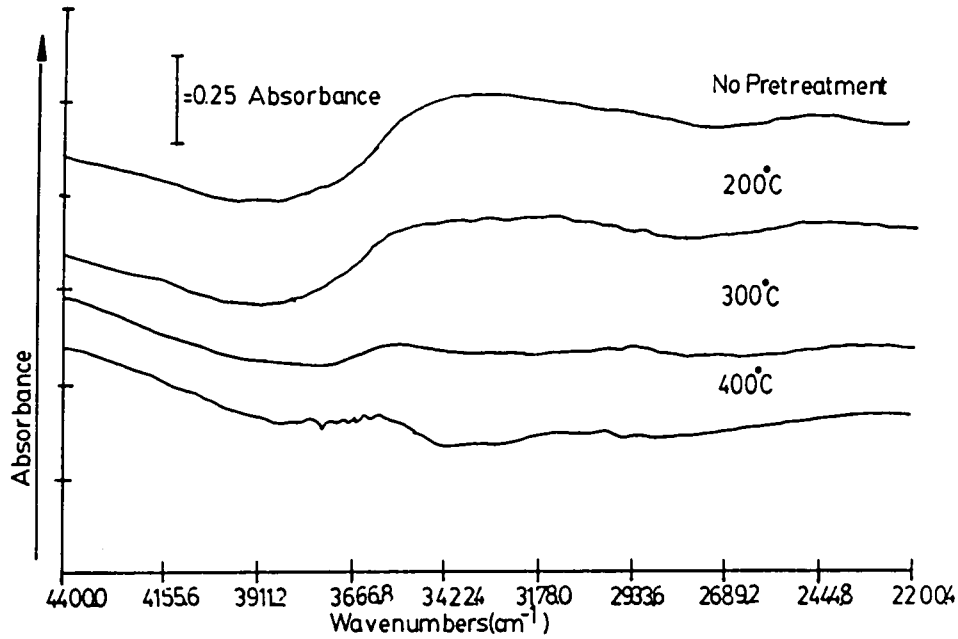

Figure 24. Infrared spectra of hydroxyl region of 4% phosphoric acid anodic aluminum oxides before and after 2 hour thermal pretreatments at 200°C, 300°C, and 400°C.

of phosphate incorporated into the oxide. It was expected that a larger amount of phosphate would be incorporated into the oxide after an anodization in a 15% acid solution than after an anodization in a 4% acid solution. However from the IR spectra equal amounts of phosphate were incorporated into the oxides. Since there are no chemical differences in the 15% and 4% oxides, there is no reason to expect any difference in catalytic activity. The intensity of the -OH band for the 4% phosphoric acid anodic oxide decreases with increasing pretreatment temperature. The activity of the phosphoric acid anodic oxide on aluminum increases slightly after a thermal pretreatment. It is reasoned that the increase in activity is due to the loss of -OH groups.

Acetone was detected as a reaction product under the following conditions: between 325°C and 400°C over H_3PO_4 anodic oxides that were not pretreated, and at 275°C over oxides that were pretreated for 2 and 13 hours. At present there is no experimental result to explain why acetone is not observed over the entire temperature range studied. However acetone formation is believed to be due to the presence of basic sites on anodized aluminum(58).

4. ANODIC OXIDES FORMED IN $H_2C_2O_4$

Catalytic reactions over aluminum anodized in 3% oxalic acid yielded results that were different from the results

observed with H_2SO_4 or H_3PO_4 anodic oxides on aluminum. The oxalic acid oxides were more active per unit surface area of oxide than the H_2SO_4 oxides but less active than H_3PO_4 oxides. The products detected were water, propene, and acetone. Over the non-pretreated oxide, CO_2 was detected (<1%) and is believed to be the result of the decomposition of oxalate incorporated in the oxide matrix.

The conversion results for 3% oxalic acid anodic oxide on aluminum as a function of temperature are summarized in Figure 25 for non-pretreated and 2 hour pretreated oxides. No results are given for the 13 hour pretreated oxides, since they exhibited no catalytic activity.

For $H_2C_2O_4$ anodic aluminum oxides that did not undergo a thermal pretreatment, activity was first observed at 275°C where 0.005 mmoles of propene/m^2 of oxide were measured. Total conversion was reached at 350°C with 0.5 mmoles of propene/m^2 of oxide detected. For $H_2C_2O_4$ (2 hour pretreated) anodic oxide on aluminum, activity was first observed at 250°C, where 0.05 mmoles of propene/m^2 of oxide were measured. Total conversion was reached at 375°C, with the formation of 0.5 mmoles of propene/m^2 of oxide. Acetone was detected at 325°C, 375°C, and 400°C on the non-pretreated oxides and at 250°C, 275°C, 300°C,and 350°C on the 2 hour pretreated oxides.

In Figure 26 is an infrared spectrum (4600 - 400 cm^{-1})

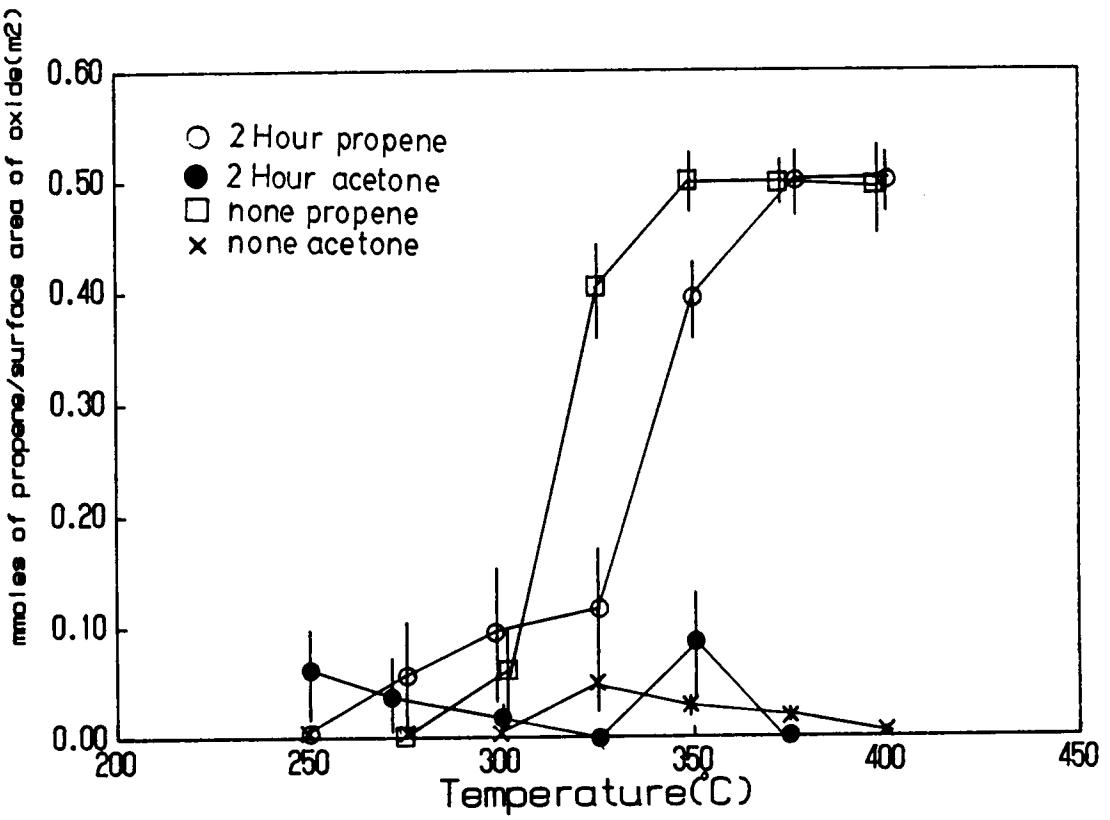

Figure 25. Mmoles of propene and acetone/m^2 of oxide detected over non-pretreated and 2 hour pretreated 3% oxalic acid anodic aluminum oxides.

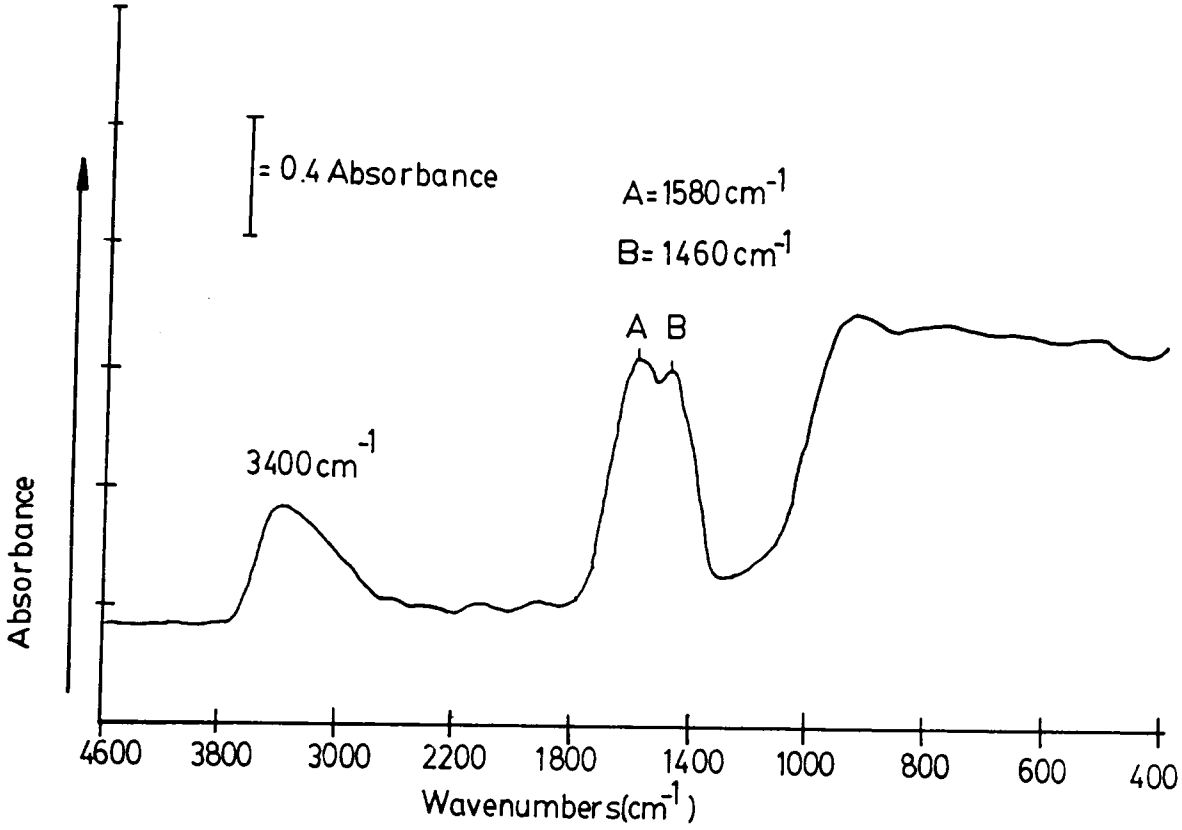

Figure 26. Infrared spectrum of a 3% oxalic acid anodic aluminum oxide before a thermal pretreatment.

of oxalic acid anodic aluminum oxide. The absorption bands due to hydroxyl groups and the aluminum oxide are observed at 3400 cm^{-1} and between 1000-400 cm^{-1}, respectively. The absorption peaks at 1580 cm^{-1} and 1460 cm^{-1} are due to oxalate species incorporated in the oxide during anodization(16). In Figure 27 are shown the IR spectra in the OH stretching region for $H_2C_2O_4$ oxides following treatment at various temperatures. Before pretreatment there was a high concentration of hydroxyl groups on the oxide(3400 cm^{-1}); however, as the temperature was increased a decrease in the concentration of hydroxyl groups occurred. All hydroxyl groups were removed during a 2 hour thermal treatment at 300°C. The infrared spectra confirmed that the thermal pretreatment dehydrates the bulk of the oxide.

Acetone formation occurred on non-pretreated $H_2C_2O_4$ oxides at temperatures higher than on the pretreated $H_2C_2O_4$ oxides. From the results obtained thus far, it is difficult to explain this observation. However, acetone formation is thought to be related to the basicity of anodized aluminum(58), possibly an O^{2-} or $C_2O_4^{2-}$ site.

These results demonstrate that anodization of aluminum creates a catalytically active surface. The increase in catalytic activity compared to unanodized aluminum may be due to the creation of acidic and basic sites during the

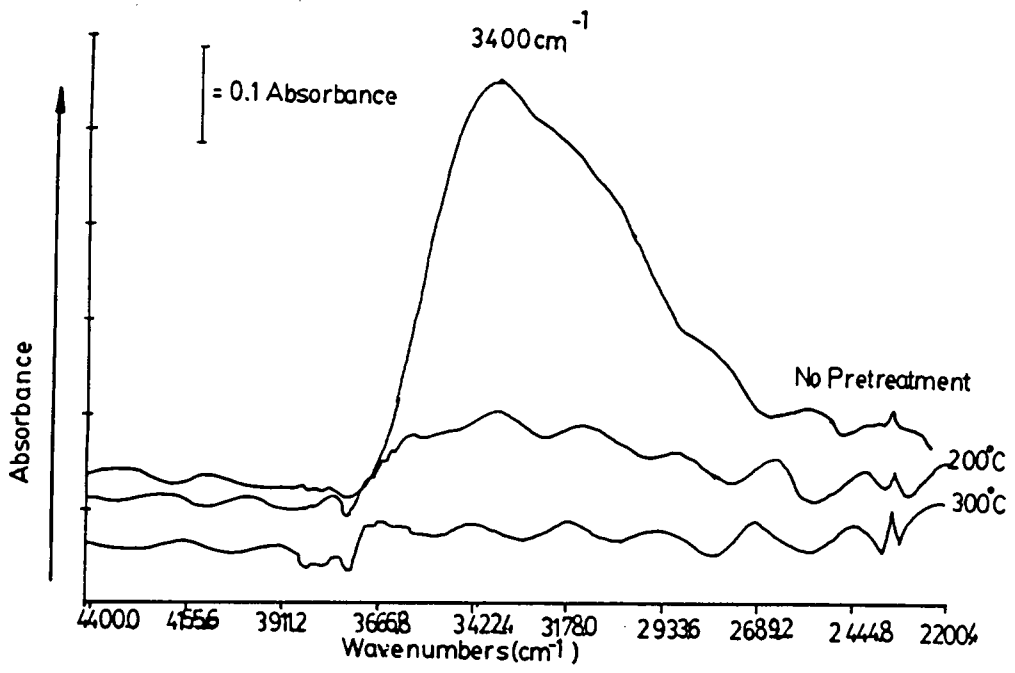

Figure 27. Infrared spectra of hydroxyl region of non-pretreated, 200°C and 300°C thermally pretreated 3% oxalic acid anodic aluminum oxides.

anodization or to the increase in the surface area.

5. γ-Al_2O_3

γ-Al_2O_3 was studied as a catalyst in the dehydration of isopropanol. In Figure 28 are the results for isopropanol dehydration over γ-Al_2O_3 that was pretreated 2 hours at the reaction temperature. Activity was first observed at 175°C (0.001 mmoles of propene/m^2 of oxide) and total conversion occurred at 200°C(0.03 mmoles of propene/m^2 of oxide). In Table 10 is a summary of the mmoles of propene/m^2 of oxide detected at 100% conversion for each catalyst. The activity per unit surface area of oxide followed the trend: phosphoric> oxalic > sulfuric > γ-Al_2O_3.

Hönicke(13) studied the catalytic activity of anodized aluminum in the dehydration of isopropanol over sulfuric acid anodized aluminum and γ-Al_2O_3, the results of which are summarized in Figure 29. He found that the reaction rate based on surface area of the anodized aluminum(Al + oxide) for the dehydration of isopropanol over sulfuric acid anodized aluminum was approximately 30 times greater than over γ-Al_2O_3. The results in this study, show a 4 times greater activity for sulfuric acid anodized aluminum and a 70 times greater activity for phosphoric acid anodized aluminum based on the surface area of the oxide compared to γ-Al_2O_3. There is only one obvious experimental difference in the studies that may account for

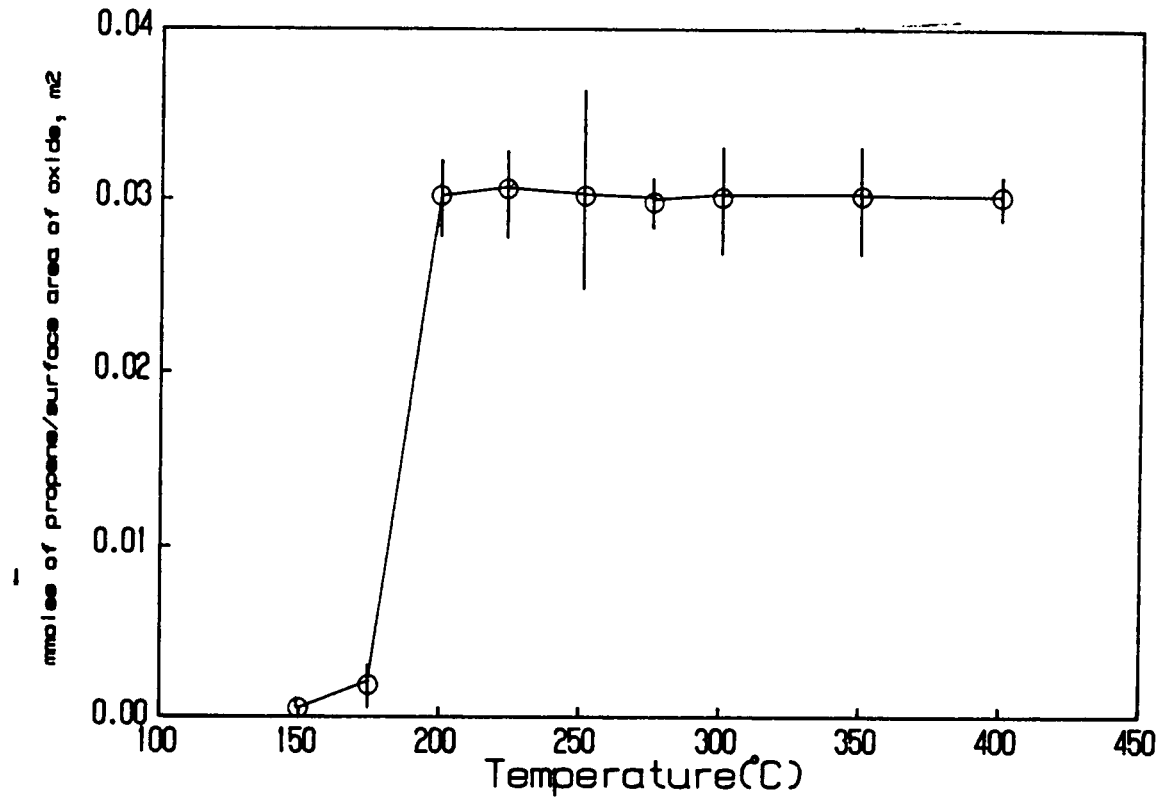

Figure 28. Mmoles of propene/m^2 of oxide detected over 2 hour pretreated γ-Al_2O_3.

Table 10

Summary of Catalytic Results

Surface	propene/surface area of oxide(mmoles/m^2)
sulfuric acid anodized aluminum	0.13
oxalic acid anodized aluminum	0.50
phosphoric acid anodized aluminum	2.00
γ-Al_2O_3	0.03

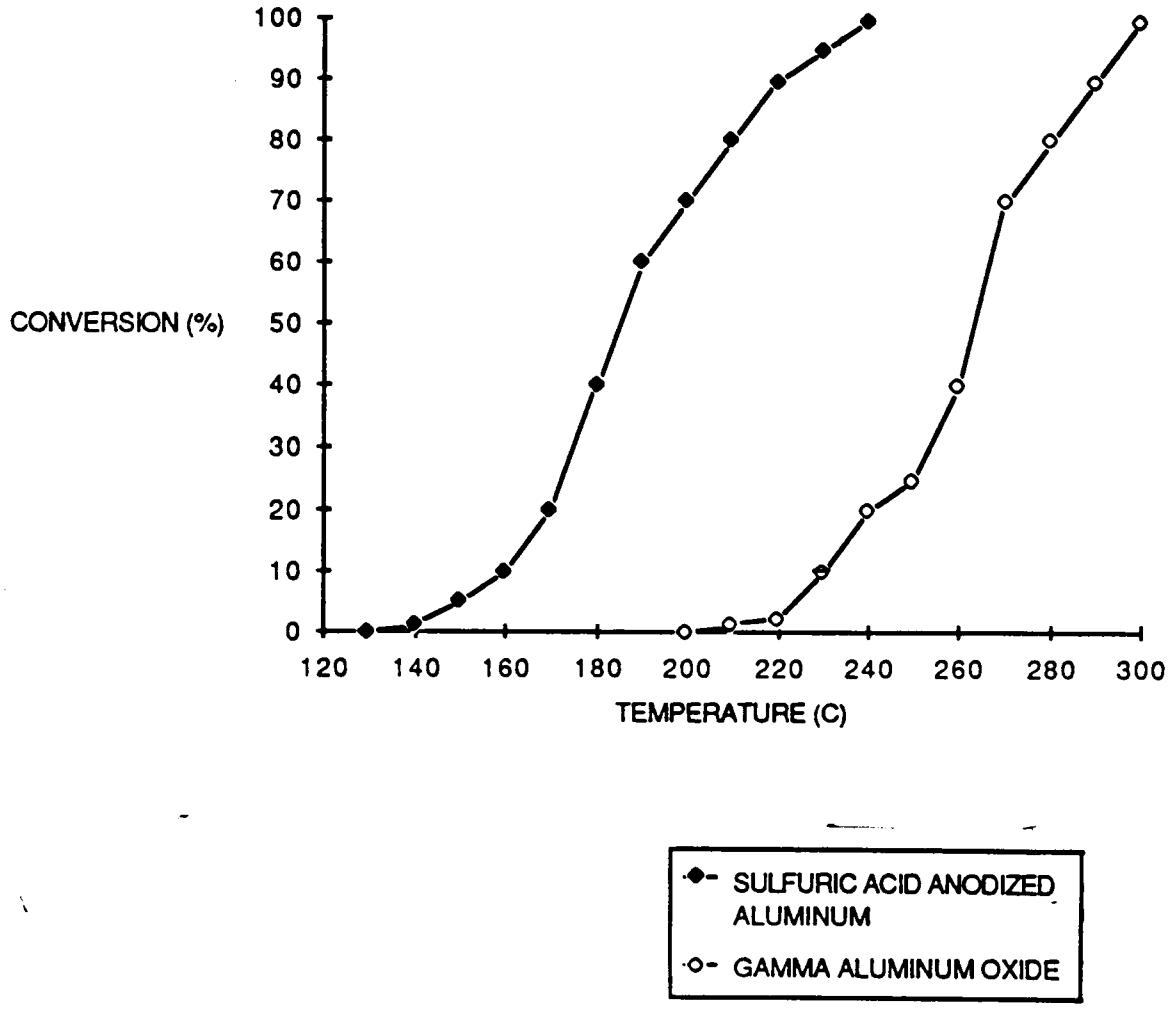

Figure 29. Summary of Hönicke's(13) results of the dehydration of isopropanol over γ-Al_2O_3 and sulfuric acid anodic aluminum oxide.

some of the differences observed. Hönicke carried out a 400-500°C thermal post-treatment after anodization in order to obtain complete conversion to γ-Al_2O_3. In this study the oxides were thermally pretreated at the reaction temperature (200°C-400°C).

E. EFFECTS OF PORE LENGTH

Once it was shown that anodic oxides were catalytically active and that activity depended on the anodizing electrolyte, it was of interest to determine whether the length of the pores had any effect on activity. Three catalysts were compared: 20 minute, 10 minute, and "sealed" 20 minute sulfuric acid anodic aluminum oxides. The oxide produced after a 20 minute anodization was 10±1 μm thick, the oxide produced after a 10 minute anodization was 4±1 μm thick. The sealing process presumably plugs the pores of the oxide with $Al(OH)_3$, so that no pores are available. However, as discussed earlier, even though the pores are closed the surface area of the "sealed" oxide is greater than expected for a barrier oxide.

As shown in Figure 30, it is found that the 10 minute anodized aluminum is more active/unit surface area of oxide than the 20 minute sulfuric acid anodized aluminum. It is possible that the 10 minute anodized aluminum has a greater number of acid sites/unit surface area of oxide than the 20 minute anodized aluminum. Therefore, the greater activity

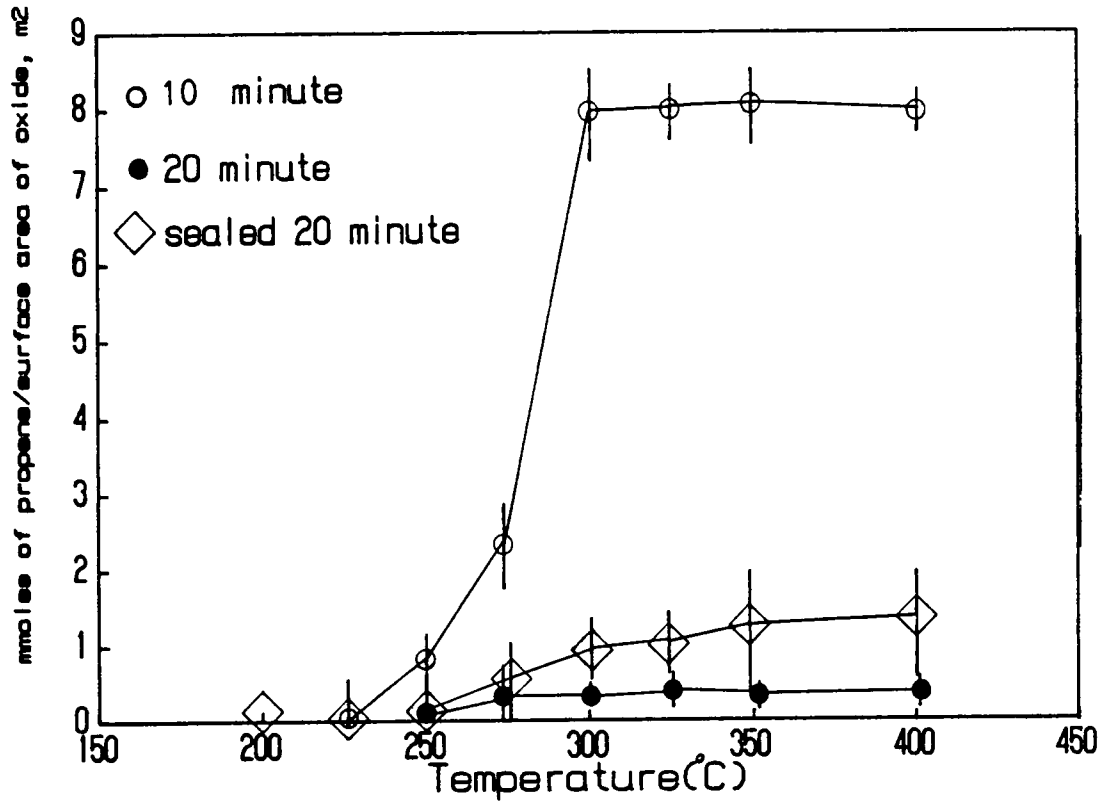

Figure 30. Mmoles of propene/surface area of oxide detected over 10 minute, 20 minute, and 20 minute "sealed" sulfuric acid anodic aluminum oxides.

of the 10 minute anodic oxide may be related to the greater acidity of the 10 minute anodic oxide/unit surface area. The greater acidity/surface area of the 10 minute anodic oxide may be due to the formation of the acid sites early in the anodization, once the initial acid sites have been formed, increasing the length of the anodization has no effect on the total number of sites. Therefore, the same total number of acid sites are present on the 10 minute and 20 minute anodic oxides. The smaller surface area material would therefore have a greater number of acid sites/unit surface area of oxide than the larger surface area material.

F. LONG-TERM REACTIONS

In order to investigate duration of the catalytic activity, sulfuric acid anodic aluminum oxide was used at 300°C for 73 hours in the dehydration of isopropanol. The results are shown in Figure 31, where the percent conversion to propene is plotted versus time. The catalyst pretreated for 2 hours at 300°C is active up to 73 hours and 18 minutes and 99% of the isopropanol is converted to propene. The fluctuations observed in the activity of the oxides are within the experimental error(±10%) of the measurement and temperature control. From these results, it is clear that there is no degradation in the activity of the sulfuric acid anodic oxides on aluminum with extended

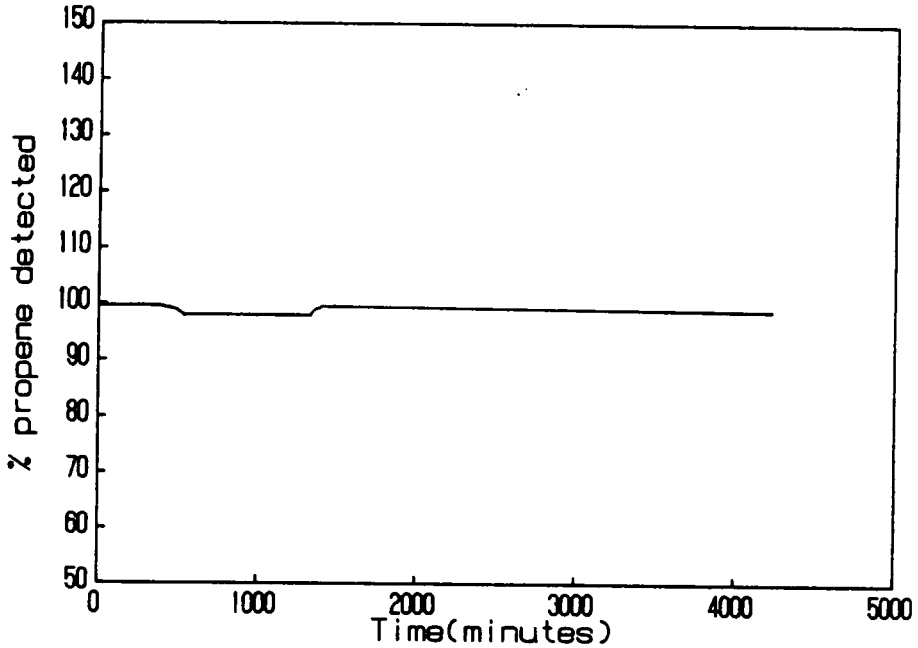

Figure 31. Percent conversion of isopropanol to propene as a function of time at 300°C over sulfuric acid anodic aluminum oxide.

use.

G. ACIDITY OF OXIDES

The dehydration of the oxide, resulting from thermal pretreatments, activates the oxide for catalysis. Since the dehydration of alcohols is an acid catalyzed reaction(19), it is critical to determine experimentally the acidic nature of the oxide after various thermal treatments. The acidity of anodic oxides was studied by the adsorption of indicators, and the adsorption of gaseous bases. The adsorption of ammonia and pyridine was studied by IR spectroscopy and temperature programmed desorption mass spectrometry(TPD-MS).

The adsorption of ammonia is used as a measure of weak acid sites($pK_a \approx 5$) and the adsorption of pyridine as a measure of strong acid sites($pK_a \approx 9$). However, there is a distribution of acid strengths measured by both ammonia and pyridine adsorption. The thermal desorption of ammonia and pyridine further delineates the strengths of acid sites. Thus, when discussing ammonia adsorption it is possible to have both strong and weak acid sites, which are weaker than the sites detected by pyridine adsorption. Likewise, it is possible to have strong and weak acid sites detected by pyridine adsorption, both of which are stronger than the sites detected by ammonia adsorption.

1. γ-Al_2O_3

The adsorption of ammonia on 200°C, 300°C, and 400°C thermally pretreated γ-Al_2O_3 was studied by transmission IR spectroscopy. The IR spectra for ammonia adsorbed at room temperature on γ-Al_2O_3 pretreated at 200°C, 300°C, and 400°C are shown in Figure 32. The band at 1655 cm^{-1} is due to adsorption on Lewis acid sites, the band at 1460 cm^{-1} results from adsorption on Brønsted acid sites, and the band at 1505 cm^{-1} indicated the formation of NH_2^- on the oxide. The IR band assignments were based on previous work by Peri(84) and Mapes et al.(79). Ammonia adsorbs to Lewis acid sites with a $pK_a \leq 5$. The shoulder on the low wavenumber side of the 1655 cm^{-1} band increases with increasing pretreatment temperature, indicating an increase in the concentration of weak Lewis acid sites. The low wavenumber band is assigned to a weak acid site based on equation 6, which is derived from Hooke's law.

$$\nu = \frac{1}{2\pi c}\left[\frac{f}{\frac{m_x m_y}{m_x + m_y}}\right]^{\frac{1}{2}} \qquad [6]$$

ν = frequency (sec^{-1})

c = velocity of light(cm/sec)

f = force constant of bond(dynes/cm)

m_x and m_y = mass(g) of atom x and atom y, respectively.

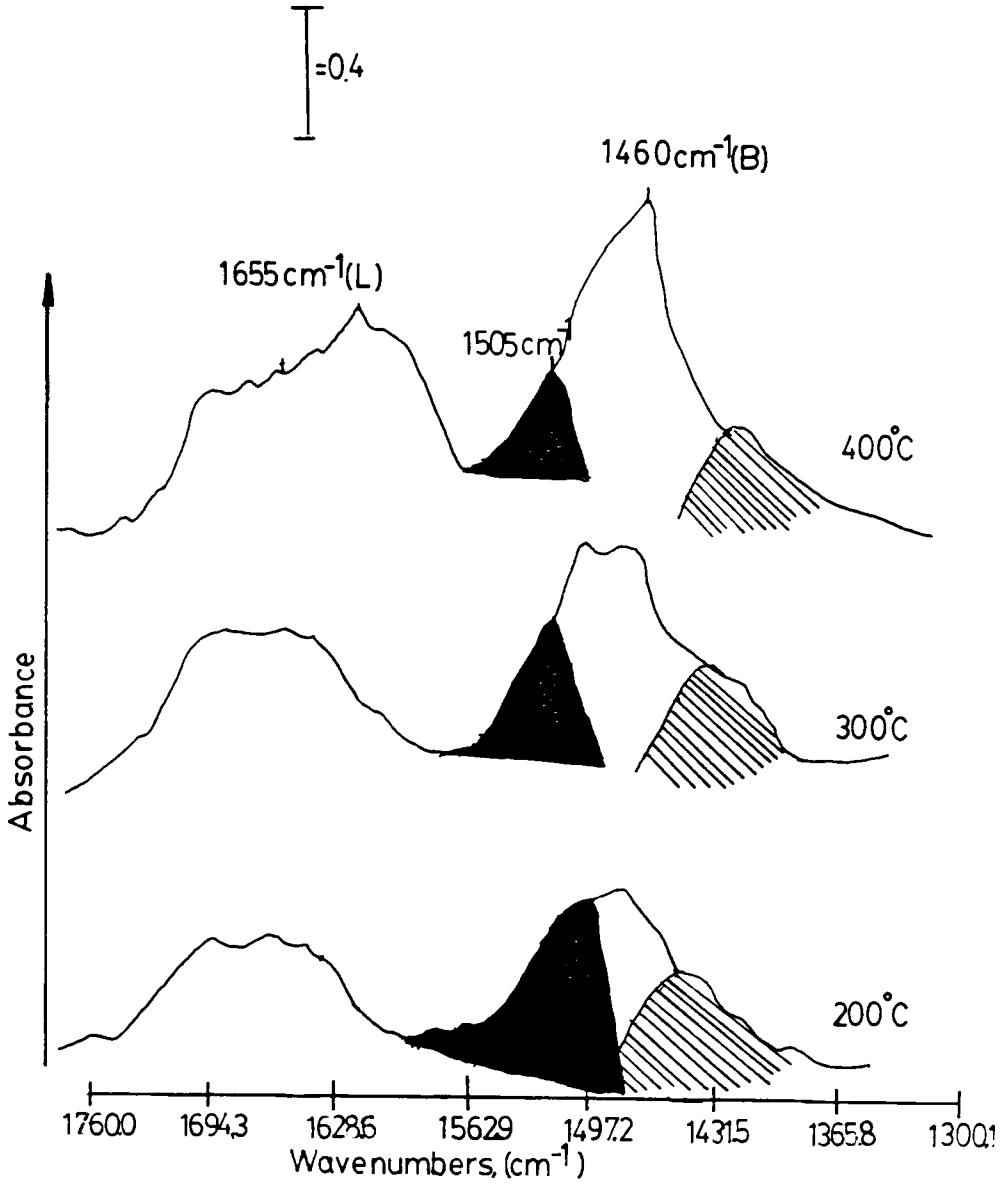

Figure 32. Infrared spectrum of ammonia adsorbed on γ-Al_2O_3.

Equation 6 states the relationship between frequency of oscillation, atomic masses, and the force constant of the vibration. When a molecule is adsorbed to a weak acid site the bond between the acid site and the adsorbed molecule is weak and the force constant, f is small compared to adsorption on a strong acid site. The IR absorption band for the molecule adsorbed to the weak site appears at a lower wavenumber in the IR spectrum than for the molecule adsorbed to a strong site.

Peri(84) studied the adsorption of ammonia on alumina calcined in oxygen at 800°C and found no evidence for Brønsted acid sites. He suggested that at temperatures ≈400°C there was the possibility of OH^- and H^+ migration, the driving force of this migration was the minimization of surface defects(basic sites). Applying Peri's(84) observations to this study, as γ-Al_2O_3 is heated the oxide is dehydrated. After the 200°C pretreatment there are strong Brønsted acid sites(OH^- sites with many adjacent O^{2-} sites) and weak Brønsted acid sites (OH^- sites with few adjacent O^{2-} sites). After the 300°C pretreatment the concentration of weak Brønsted acid sites decreases or the weak -OH sites are lost.

The areas under the respective IR absorption bands due to ammonia adsorption are plotted versus the pretreatment temperature in Figure 33. The changes in band area

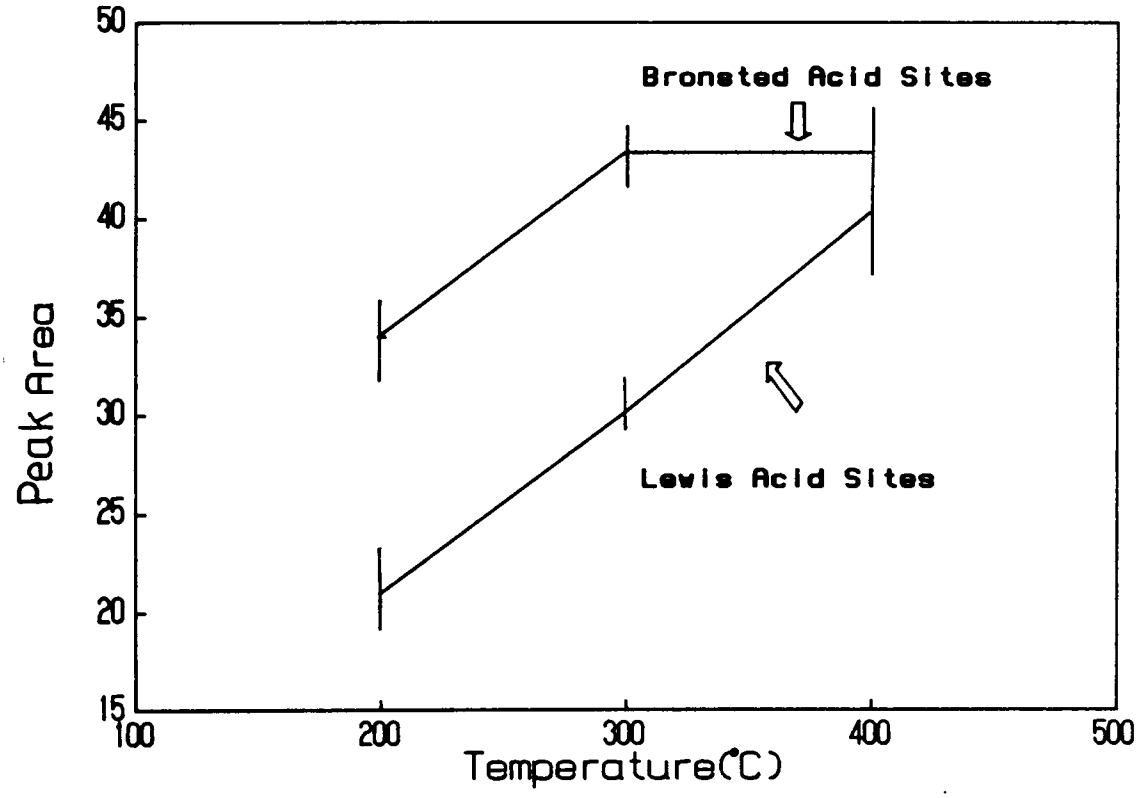

Figure 33. Peak area of IR absorption bands due to ammonia adsorbed on γ-Al_2O_3.

indicate that Lewis acidity increases for pretreatments between 200°C and 400°C. Brønsted acidity increases when comparing the 200°C and 300°C pretreatment, but equal amounts of Brønsted acidity are noted for the 300°C and 400°C pretreated γ-Al_2O_3. As the oxide is dehydrated, a greater number of Lewis acid sites(coordinatively unsaturated Al^{3+}) occurs on the oxide. The invariant Brønsted peak area for the 300°C and 400°C pretreated oxides is attributed to the decrease in both NH_2^- formation and weak Brønsted acid sites and the increase in strong Brønsted acid sites. As shown in Figure 32, the IR band at 1460 cm^{-1} is due primarily to the adsorption of ammonia on the Brønsted acid site. However, there are two shoulders on the 1460 cm^{-1} IR band, one at 1515 cm^{-1} due to NH_2^- formation on Al^{3+} sites (after reacting catalytically with an adjacent O^{2-} group) and a low wavenumber shoulder due to the adsorption of ammonia on weak Brønsted acid sites. With increasing pretreatment temperature there is a decrease in NH_2^- formation. Peri(84) showed that after high pretreatment temperatures resulting in low hydroxyl densities, NH_2^- groups are formed due to dissociative chemisorption on acid-base pair sites(Al^{3+},O^{2-}). In this study there is a decrease in NH_2^- formation with increasing pretreatment temperature corresponding to the increase in strong Brønsted acid sites and decrease in weak Brønsted

acid sites. These results indicate the weak -OH sites are needed for NH_2^- formation. A weakly acidic OH^- site corresponds to an OH^- site that has few adjacent O^{2-} vacancies(84). As the surface is dehydrated the number of O^{2-} vacancies adjacent to the remaining OH^- sites increases and the OH^- sites become more acidic. The reason Brønsted acidity is observed in this study and not in the case of Peri(84) is likely due to the pretreatment procedure employed. In this study γ-Al_2O_3 was thermally treated at 200°C, 300°C, or 400°C leaving hydroxyl groups capable of acting as Brønsted acid sites. Peri(84) calcined alumina at 800°C, completely dehydrating the oxide leaving no hydroxyl groups to act as Brønsted acid sites.

2. ANODIC OXIDES FORMED IN SULFURIC ACID

a. INDICATOR METHOD

The acidity of pretreated sulfuric acid anodized aluminum samples was measured using the series of pH indicators is listed in Table 7. The adsorbed indicator results are given in Figure 34. After a 200°C pretreatment the surface is basic with a pH between 6.8 and 7.6; however, after a 2 hour pretreatment at 300°C, 400°C, or 500°C the surface becomes more acidic having a pH between 4.6 and 5.4.

b. PYRIDINE ADSORPTION

The adsorption of pyridine on sulfuric acid anodized

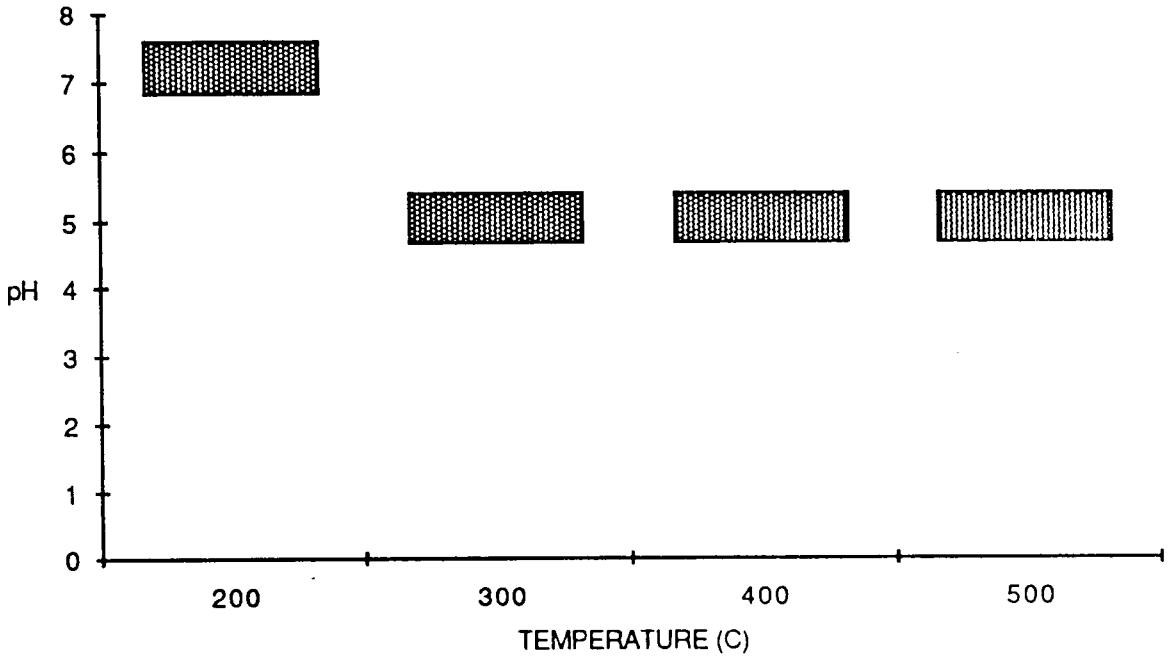

Figure 34. pH ranges observed on 200°C, 300°C, 400°C, and 500°C pretreated 15% sulfuric acid anodic aluminum oxides.

aluminum was studied as a function of pretreatment temperature. The IR spectra(1610 cm^{-1}-1340 cm^{-1}) in Figure 35 are spectra of pyridine adsorbed on thermally pretreated oxides and of pyridine adsorbed on 400°C pretreated oxides after thermal desorption treatments at 150°C and 200°C. The band located at 1528 cm^{-1} is due to the adsorption of pyridine on Brønsted acid sites and the band at 1445 cm^{-1} arises from the adsorption of pyridine on Lewis acid sites(28). The position of the 1445 cm^{-1} band increases in wavenumber with increasing pretreatment temperature, indicating that the Lewis acid sites increase in strength. As -OH sites are lost there is a change in the number of O^{2-} sites surrounding the Al^{3+} site. Initially there may have been only a few O^{2-} sites near the Al^{3+} site. As the oxide is dehydrated there is an increase in the number of O^{2-} sites near the Al^{3+} sites, causing the Al^{3+} site to increase in strength.

The peak area results for the adsorption of pyridine at room temperature on pretreated samples are shown in Figure 36. The amount of pyridine adsorbed increases with increasing pretreatment temperature; therefore, the concentration of strong($pK_a \leq 9$) Lewis acid sites increases with increasing pretreatment temperature. There is a small amount of Brønsted acidity after the 200°C pretreatment; however, after the 300°C and 400°C pretreatment there is no

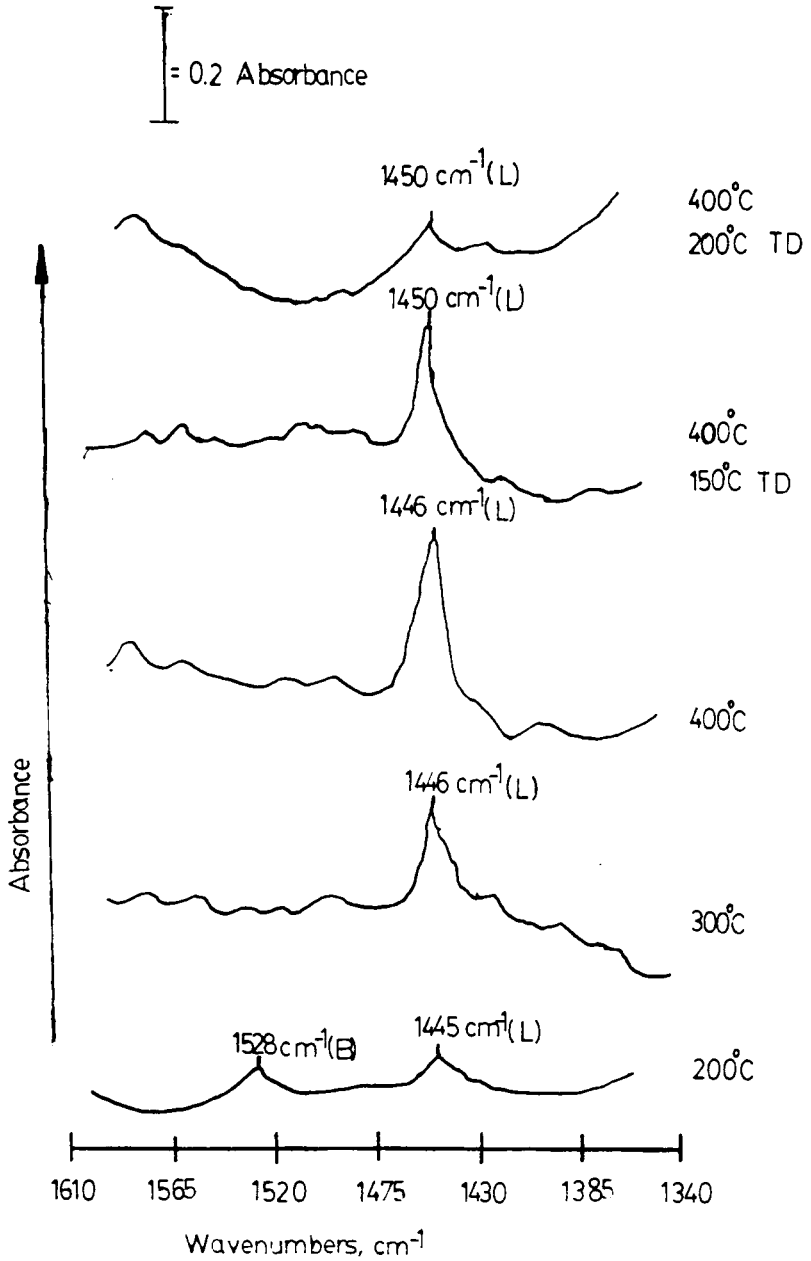

Figure 35. Infrared spectra of pyridine adsorbed on sulfuric acid anodic aluminum oxides. TD = Thermal Desorption

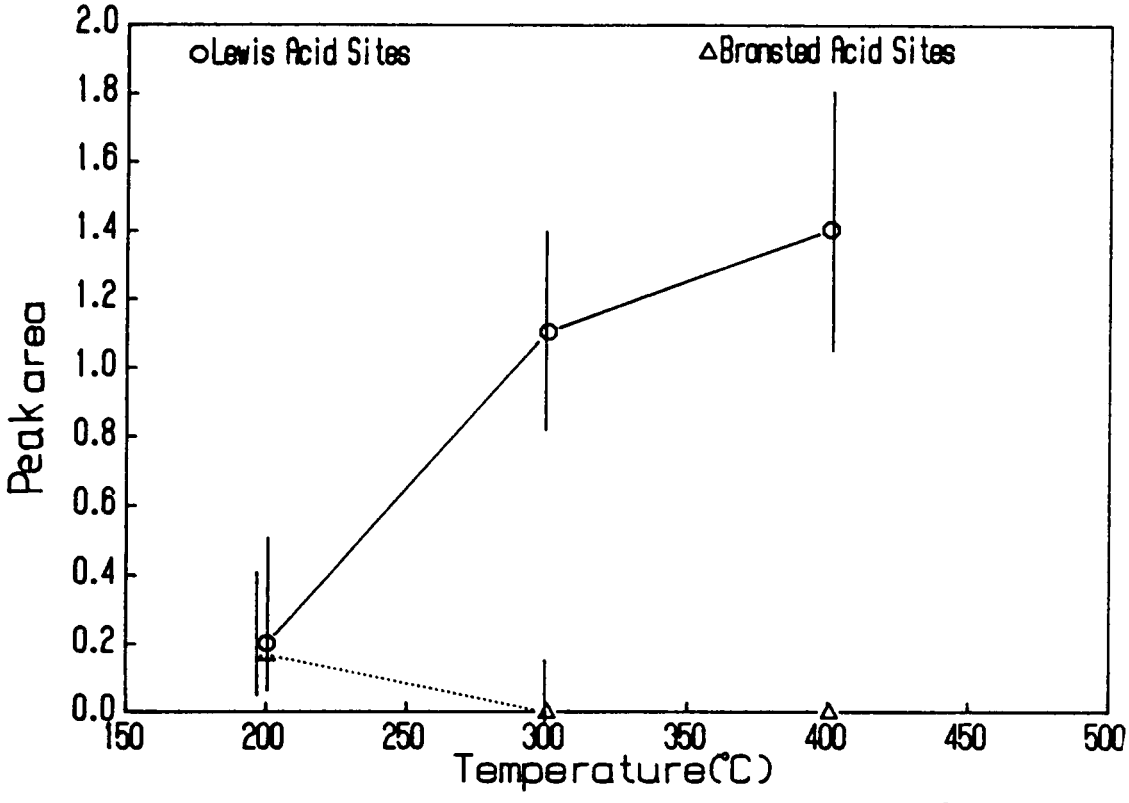

Figure 36. Peak area results for pyridine adsorbed on 15% sulfuric acid anodic aluminum oxides.

detectable Brønsted acidity. Even though the extinction coefficients were not measured in this study a number of authors have reported the ratio of the extinction coefficients for the IR bands at 1450 cm^{-1} and 1540 cm^{-1} is close to 1, as shown below:

$$\frac{\epsilon(1450\ cm^{-1})}{\epsilon(1540\ cm^{-1})}$$

0.9±0.1 (138)
1.08±0.09(139)
1.0 ±0.03(86)

Therefore, the sensitivity of the area measurements of the two IR bands is about equal.

The strength of the acid site on which pyridine is adsorbed can be correlated with the temperature at which pyridine is desorbed. The spectra of pyridine adsorbed on 400°C pretreated sulfuric acid anodized aluminum, and after thermal desorption of pyridine at 150°C and 200°C are also shown in Figure 35. In these spectra the intensity of the band around 1445 cm^{-1} decreases as the temperature is increased. A shift in IR band position from 1446±0.5 cm^{-1} to 1450±0.5 cm^{-1} is detected after the 150°C and 200°C thermal desorption treatment. This shift to higher wavenumber suggests an increase in the strength of the acid sites. Similar thermal desorption results were observed for

the 300°C pretreated oxides. The shifts in band position indicate that the weakly adsorbed pyridine is lost after the 150°C thermal desorption leaving only strongly adsorbed pyridine.

The peak area results corresponding to thermal desorption of pyridine from 200°C, 300°C, and 400°C pretreated oxides are shown in Figure 37. All adsorbed pyridine is removed from the 200°C pretreated oxides after the 150°C thermal treatment, indicating that pyridine was weakly adsorbed on strong Lewis and Brønsted acid sites. The 400°C pretreated oxides retain a larger concentration of pyridine at higher temperatures than the 200°C and 300°C pretreated oxides, confirming that the acid sites on the 400°C pretreated oxides are the strongest.

Adsorption of pyridine on Lewis acid sites is observed on sulfuric acid anodic aluminum oxide; however, few Brønsted acid sites are detected. The number and strength of the Lewis acid centers increase with increasing pretreatment temperature. These IR results indicate that in the case of sulfuric acid anodic oxide on aluminum the increase in acidity observed by the indicator method is due to an increase in the number of Lewis acid sites.

c. AMMONIA ADSORPTION

To understand the strength of the Brønsted and Lewis acid sites on sulfuric acid anodized aluminum more

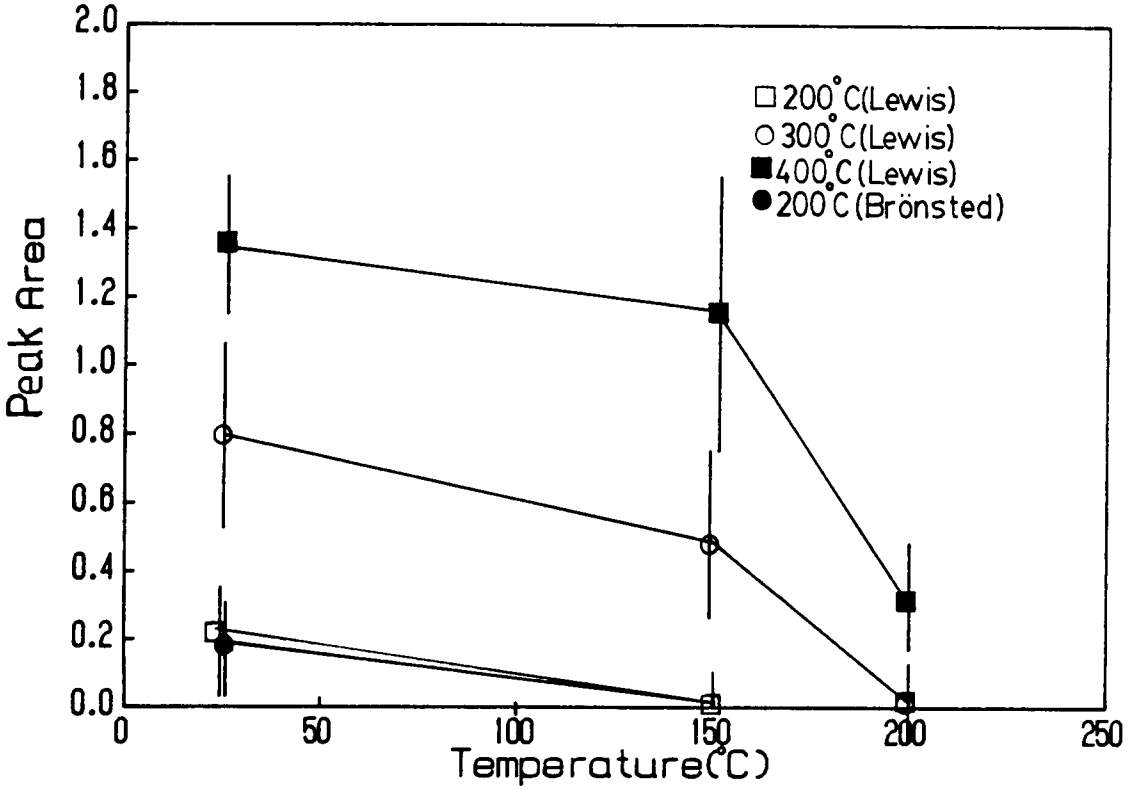

Figure 37. Peak area results for the desorption of pyridine from 15% sulfuric acid anodic aluminum oxides.

completely, ammonia adsorption was studied. The IR spectra(1710 cm^{-1}-1400 cm^{-1}) in Figure 38 are spectra of ammonia adsorbed on a thermally pretreated sample. For the IR band near 1600 cm^{-1} there is an increase in the intensity of a low wavenumber(1607 cm^{-1}) peak, indicating an increase in the concentration of weak Lewis acid sites that are measurable by ammonia adsorption. The intensity of the IR band at 1620 cm^{-1} increased with increasing pretreatment temperature indicating an increase in the concentration of strong Lewis acid sites, that are measurable by ammonia adsorption. There is a decrease in the area of the shoulder at 1495 cm^{-1} with increasing pretreatment temperature which is attributed to a decrease in NH_2^- formation (a decrease in weak OH^- sites). The IR band at 1445 cm^{-1}, due to the adsorption of ammonia on Brønsted acid sites increases with increasing pretreatment temperature. Figure 39 is a graph of the area results for the adsorption of ammonia on sulfuric acid anodic oxides on aluminum at room temperature. From the plot it is clear that the 200°C pretreated oxides exhibit less Lewis acidity than the 300°C or 400°C pretreated oxides. The ammonia adsorption results show Brønsted acidity on sulfuric acid anodized aluminum. The 200°C,300°C, and 400°C pretreated oxides adsorb equal amounts of ammonia on the Brønsted acid sites(this also includes NH_2^- formation).

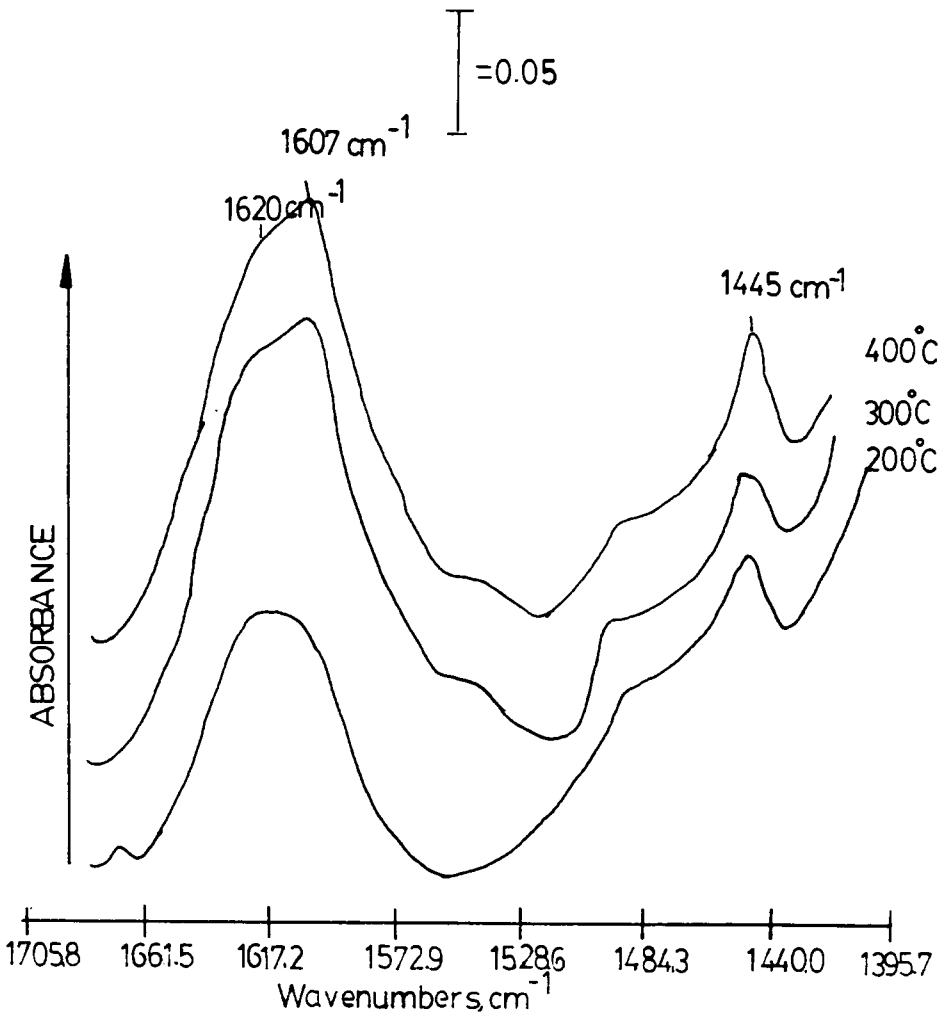

Figure 38. Infrared spectra of ammonia adsorbed on 15% sulfuric acid anodic aluminum oxides.

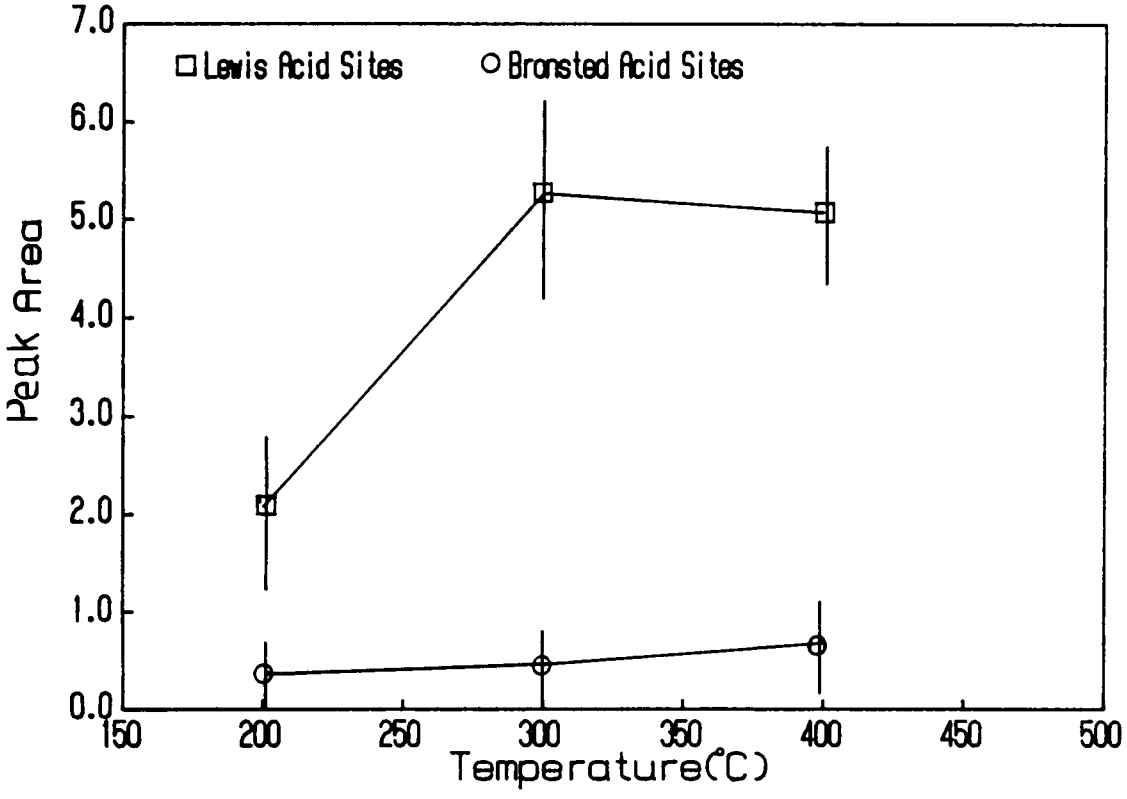

Figure 39. Peak areas of IR absorption bands resulting from the adsorption of ammonia on 15% sulfuric acid anodic aluminum oxides.

The IR peak areas following thermal desorption for 200°C, 300°C, and 400°C pretreated oxides are graphed in Figure 40. The 200°C, 300°C, and 400°C pretreated oxides lose little ammonia from Lewis acid sites as result of the 150°C and 200°C thermal desorption treatments; therefore, ammonia is strongly adsorbed to the Lewis acid sites. After the thermal desorption at 150°C from the pretreated oxides, some ammonia is lost from the Brønsted acid sites but each oxide still possesses about equal amounts of Brønsted acidity. As shown in Figure 40, after the 200°C thermal desorption treatment little detectable ammonia remains on the Brønsted sites of the 200°C, 300°C and 400°C pretreated oxides. The thermal desorption results indicate that the Brønsted acid sites on the 200°C, 300°C and 400°C pretreated oxides are the same strength. As the oxide is dehydrated the concentration of weak -OH sites(sites with few adjacent O^{2-}sites) is expected to decrease and the concentration of strong -OH sites(sites with many adjacent O^{2-} sites) is expected to increase. However, from the pyridine results a decrease in the concentration of strong Brønsted sites was seen with increasing pretreatment temperature. There is a constant concentration of weak acid sites(ammonia adsorption). After the 200°C pretreatment, there are very strong and very weak Brønsted acid sites.

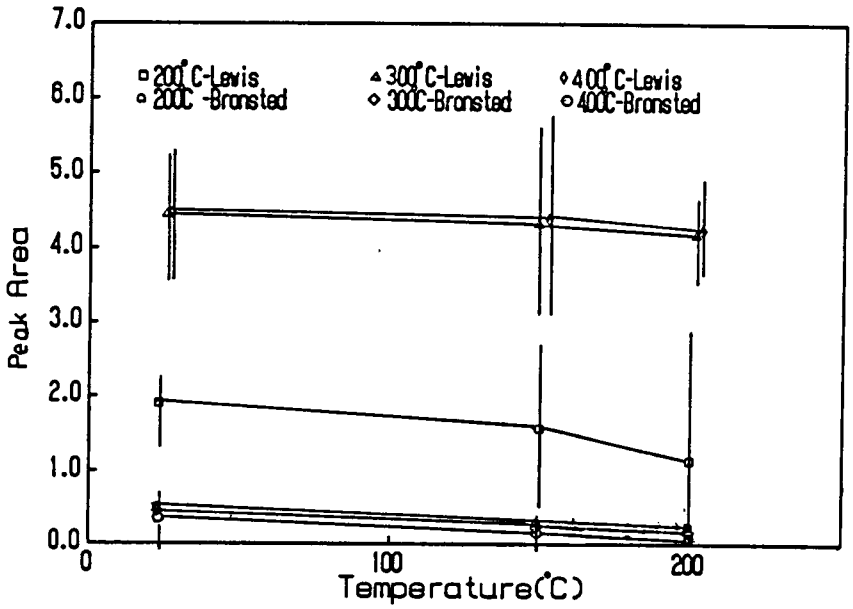

Figure 40. Peak areas of IR absorption bands following the desorption of ammonia from 15% sulfuric acid anodic aluminum oxides.

The very strong Brønsted acid sites are the sites that have many adjacent O^{2-} sites and the weak Brønsted acid sites are the OH sites with no adjacent O^{2-} sites. After pretreatments at 300°C and 400°C there is the possibility of loss of weak -OH sites(further dehydration) and of hydroxyl group or H^+ migration(84), the OH^- site that was originally a strong acid site may migrate to a point where there are fewer adjacent O^{2-} sites, becoming a weaker acid site. Therefore, the concentration of strong -OH sites decreases and the concentration of weak acid sites remains constant. The driving force for the hydroxyl group or H^+ migration is surface defect minimization.

3. ANODIC OXIDES FORMED IN PHOSPHORIC ACID

a. pH INDICATORS

In Figure 41, the pH range of pretreated phosphoric acid anodic oxides on aluminum is shown. Comparing these results with those for sulfuric acid anodic oxide on aluminum, it is noted that both surfaces become more acidic with increasing pretreatment temperature. Since this method is based on observed color changes, it is only possible to report changes in acidity on similarly colored surfaces. The phosphoric acid anodic aluminum oxide has a slight blue color and the oxide of sulfuric acid anodized aluminum is colorless, thus it is difficult to compare the acidity of the oxides.

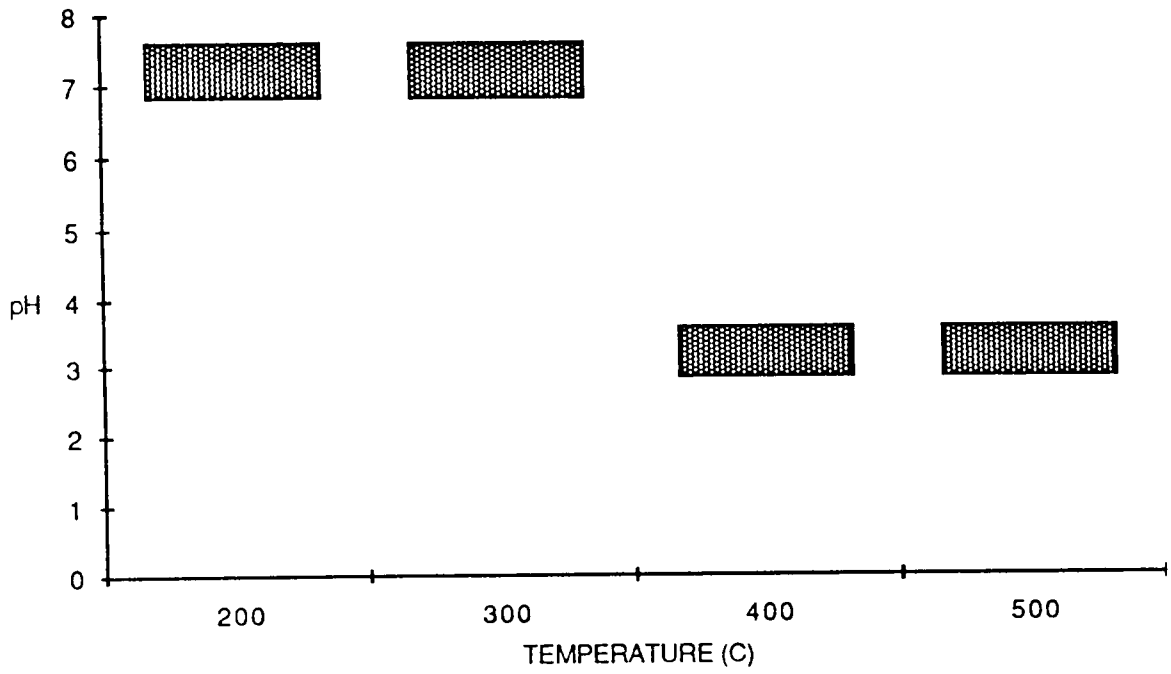

Figure 41. pH range of thermally pretreated 15% phosphoric acid anodic aluminum oxides.

b. PYRIDINE ADSORPTION

The IR spectra of pyridine adsorbed on thermally pretreated phosphoric acid anodic oxide on aluminum and of the 400°C pretreated oxide after a thermal desorption treatment are given in Figure 42. The IR band position attributed to adsorption on Lewis acid sites shifts to higher wavenumber with increasing pretreatment temperature. The band shift indicates that the Lewis acid sites become stronger with increasing pretreatment temperature. Shown in Figure 43 is a graph of the area of the IR bands due to adsorption of pyridine on Lewis and Brønsted acid sites versus the pretreatment temperature. The concentration of Lewis sites on 200°C, 300°C, and 400°C pretreated oxides is equivalent. The amount of Brønsted acidity decreases with increasing pretreatment temperature. There are no bands attributable to Brønsted acid sites after the pretreatment at 400°C.

The IR spectrum of pyridine adsorbed on phosphoric acid anodized aluminum after a 150°C thermal desorption treatment is in Figure 42. Accompanying the loss of pyridine after thermal treatment at 150°C is an increase in the band position from 1449±0.5 cm^{-1} to 1451±0.5 cm^{-1} as the more weakly adsorbed pyridine is desorbed from strong Lewis sites. The same shift in band position is also observed for 200°C and 300°C pretreated oxides. No shifts

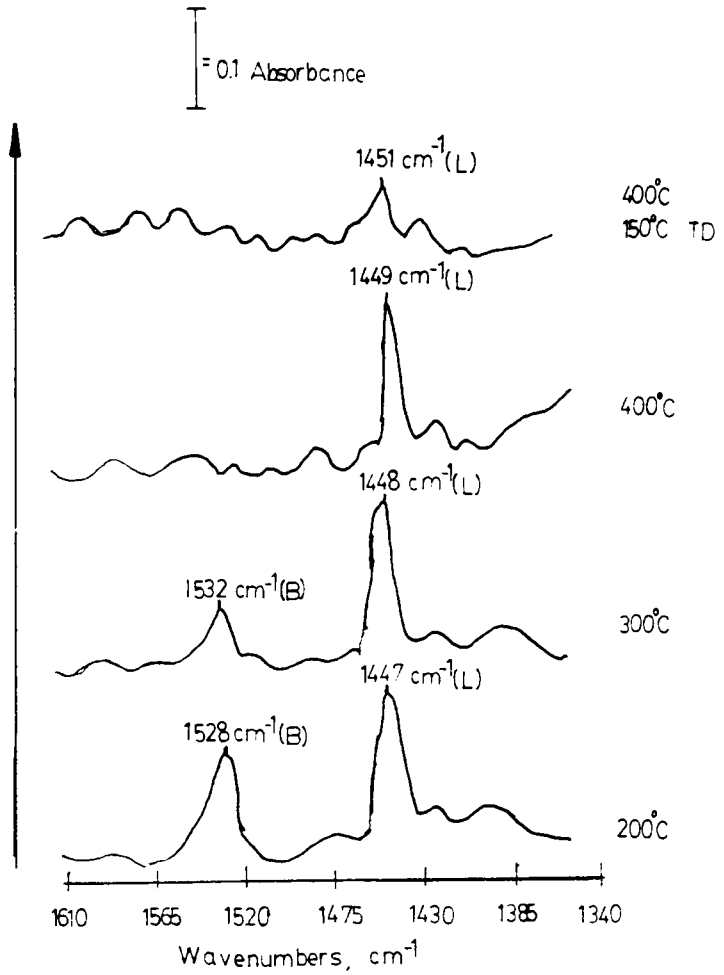

Figure 42. Infrared spectra of pyridine adsorbed on thermally pretreated 4% phosphoric acid anodic aluminum oxides.

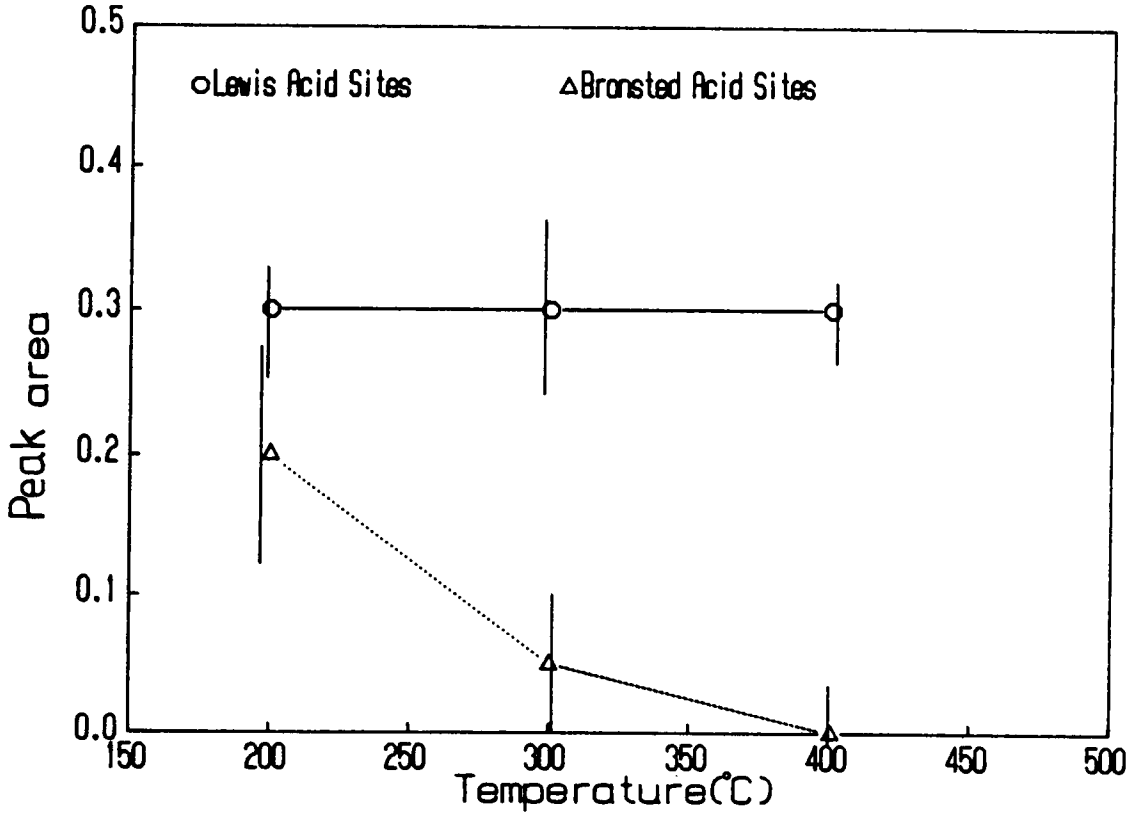

Figure 43. Peak area results for the adsorption of pyridine on thermally pretreated 4% phosphoric acid anodic aluminum oxides.

were observed in the band position as pyridine was desorbed from the Brønsted acid sites.

Figure 44 is a graph of the areas of the IR bands due to the adsorption of pyridine on Lewis and Brønsted acid sites before and after thermal desorption treatments at 150°C and 200°C. The amount of pyridine adsorbed on Lewis acid sites decreases after the 150°C thermal desorption treatment on all the oxides; however, there is some pyridine that remains adsorbed after the 200°C thermal desorption treatment. This result indicates a wide distribution of Lewis acid site strengths since a difference in the temperature at which pyridine desorbs indicates a difference in acid strength. Pyridine is lost from the Brønsted acid sites of the 200°C pretreated oxide after the 150°C thermal desorption treatment. Pyridine remains adsorbed on the Brønsted acid sites on both the 200°C and 300°C pretreated oxides, even after the 200°C thermal desorption treatment. These thermal desorption results indicate a wide distribution of Brønsted acid site strengths on the 4% phosphoric acid anodic aluminum oxide.

From the pyridine adsorption studies on phosphoric acid anodized aluminum, assuming a $\epsilon(1450\ cm^{-1})/\epsilon(1540\ cm^{-1})$ ratio=1, the predominant acid site is the Lewis acid site and the concentration of Lewis acid sites remains constant

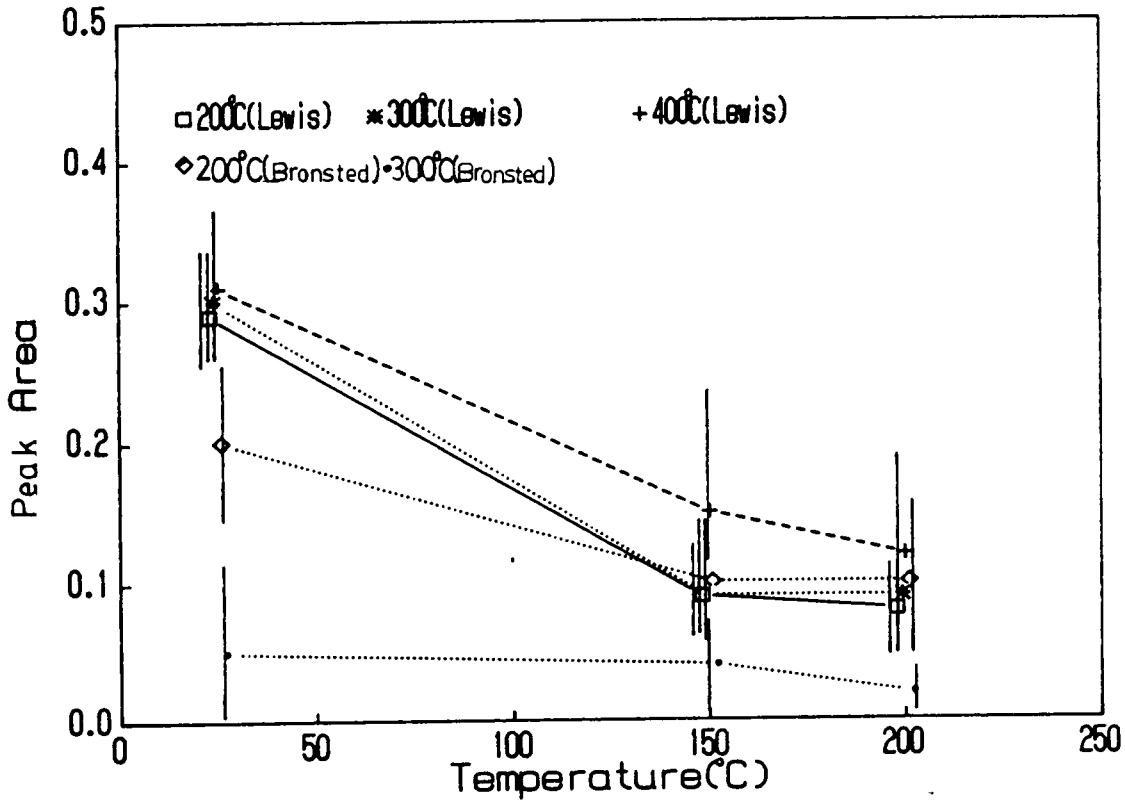

Figure 44. Peak area results for pyridine desorbed from 4% phosphoric acid anodic aluminum oxides.

strength increases. The concentration of the Brønsted acid sites decreases with increasing pretreatment temperature.

c. AMMONIA ADSORPTION

In Figure 45 are the IR spectra (1650 cm^{-1}-1340 cm^{-1}) of ammonia adsorbed on phosphoric acid anodic oxide on aluminum pretreated at 200°C, 300°C, and 400°C. The positions at which the bands due to Brønsted acidity appear are constant for 200°C, 300°C, and 400°C pretreated oxides. However, after the 400°C pretreatment there is a band at 1495 cm^{-1} due to the formation of NH_2^- on the oxide. After a 300°C and 400°C pretreatment the band due to adsorption on Lewis acid sites is broader than after a 200°C pretreatment. After the 200°C pretreatment the band due to Lewis site adsorption appears at 1620 cm^{-1}; however, after the 300°C pretreatments a low wavenumber shoulder appears at 1607 cm^{-1}. After the 400°C pretreatment the "shoulder" at 1607 cm^{-1} is the dominant feature. The appearance of the shoulder is due to an increase in the concentration of weak Lewis acid sites with increasing pretreatment temperature as measured by ammonia adsorption. The band area results for room temperature adsorption of ammonia are graphed in Figure 46. As a result of the 300°C pretreatment the Lewis acidity increased while the 400°C pretreatment resulted in no change in Lewis acidity(measured by the area of the band

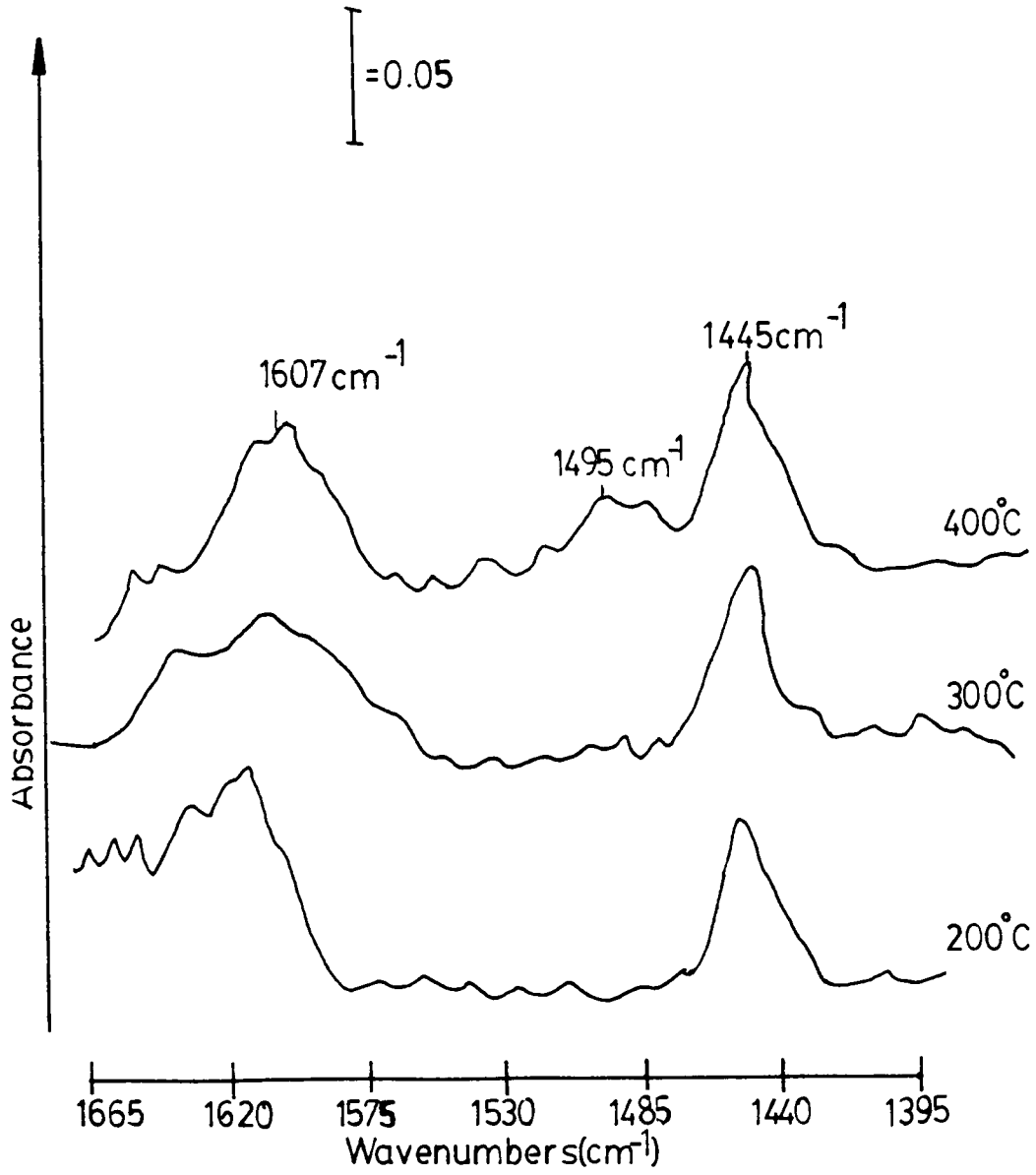

Figure 45. Infrared spectra of ammonia adsorbed on 4% phosphoric acid anodic aluminum oxides.

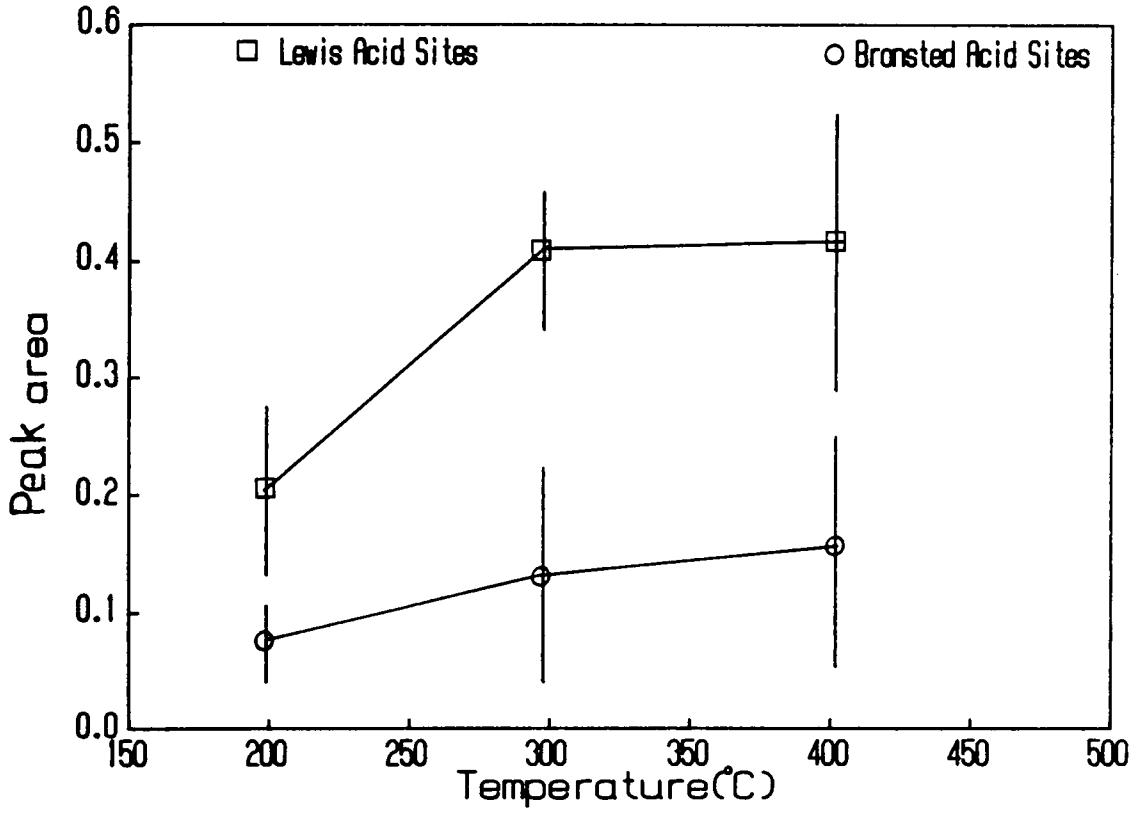

Figure 46. Peak areas of infrared bands resulting from the adsorption of ammonia on 4% phosphoric acid anodic oxides on aluminum.

at 1620 cm^{-1}), but a decrease in strong Lewis acid sites and an increase in weak Lewis acid sites, measurable by ammonia adsorption.

There is a loss of ammonia from the Lewis acid sites on the 200°C, 300°C, and 400°C pretreated oxides as a result of the 150°C and 200°C thermal desorption as shown in Figure 47. However, all ammonia is not desorbed indicating a wide range of Lewis acid site strengths on the oxides.

The quantity of ammonia adsorbed on Brønsted acid sites is equivalent at each pretreatment temperature. For the 200°C, 300°C, and 400°C pretreated samples, ammonia adsorbed to the Brønsted acid sites is retained after the 150°C and 200°C thermal desorption treatment. Therefore, the Brønsted acid sites are the strongest Brønsted acid sites, measurable by ammonia adsorption; however, in the case of the 400°C pretreated oxides the Brønsted acid sites are not strong enough to adsorb pyridine. Therefore, the Brønsted acid sites are strong enough to strongly adsorb ammonia, however the strength decreases with increasing pretreatment temperature.

The band position for ammonia adsorbed on Lewis acid sites after the 400°C pretreatment is equal for phosphoric and sulfuric acid anodized aluminum oxides(1607 cm^{-1}). However, for γ-Al_2O_3 the band that appears at 1655 cm^{-1} is very broad, indicating the Lewis acid sites are of a wide

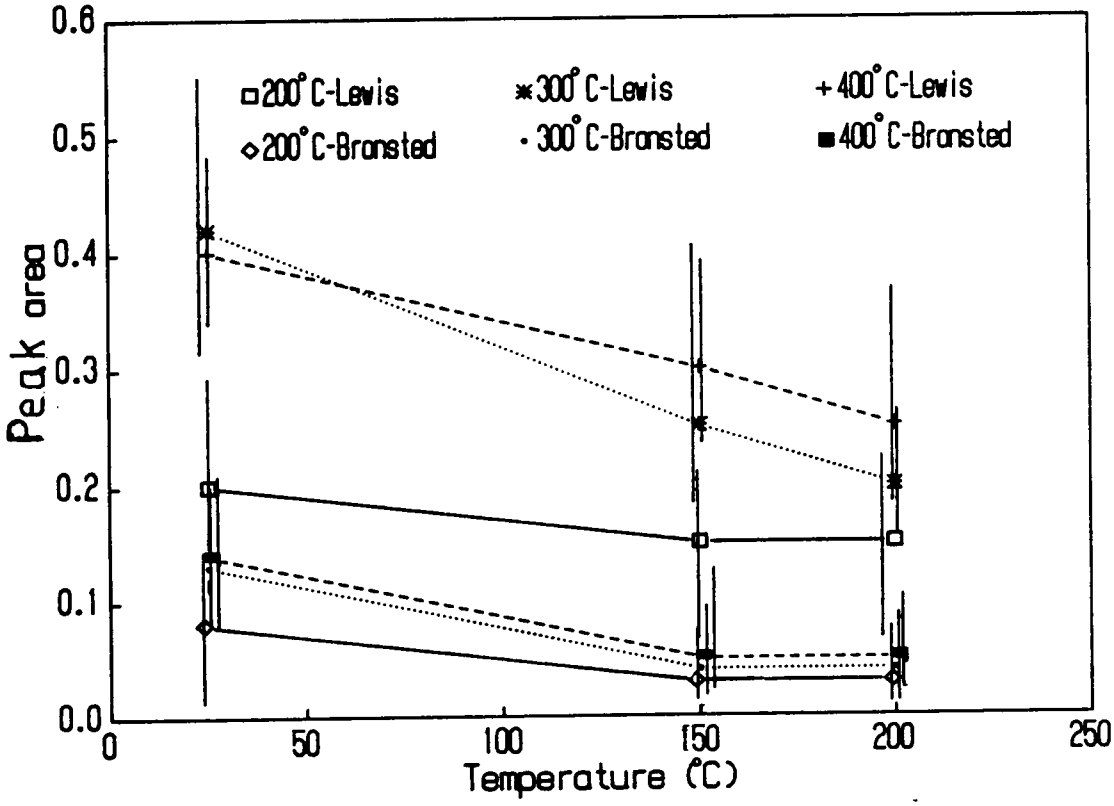

Figure 47. Peak areas of infrared bands due to the desorption of ammonia from 4% phosphoric acid anodic aluminum oxides.

distribution of strengths, some stronger and some of equal strength to the sites on the anodic oxides. For anodic oxides the Brønsted acid band appears at 1445 cm^{-1} and for γ-Al_2O_3 the band appears at 1460 cm^{-1}, a result which suggests that the Brønsted acid sites are stronger on γ-Al_2O_3 than on the anodic oxides. The stronger acid sites on the γ-Al_2O_3 may be due to the fact that SO_4^{2-} and PO_4^{3-} are incorporated into the anodic oxides which through interactions with the Al^{3+} or OH^- sites result in acid sites that are not as strong as sites in γ-Al_2O_3. One might envision the interaction of the electrolyte anion with the aluminum or -OH site as shown below.

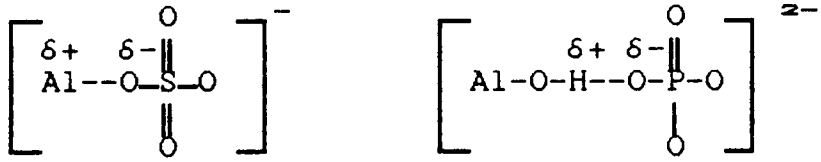

When comparing ammonia and pyridine adsorption on both sulfuric and phosphoric acid anodic aluminum oxides it should be noted that the SO_4^{2-} oxide compared to PO_4^{3-} oxide has a tendency for 10 times greater adsorption of ammonia, while the pyridine adsorption is about the same. One possible explanation of this result may be that the SO_4^{2-} and PO_4^{3-} oxides have equal amounts of strong acid sites while the SO_4^{2-} oxides have a larger number of weak acid sites than the PO_4^{3-} oxide.

4. ANODIC OXIDES FORMED IN OXALIC ACID

The results for the adsorption of pH indicators on thermally pretreated oxalic acid anodic oxides on aluminum are shown in Figure 48. After a 200°C, 300°C, and 400°C 2 hour thermal pretreatment the pH of the oxides is between 6.9 and 7.7. After a 500°C pretreatment the surface becomes more acidic with a pH between 4.6 and 5.4. It is difficult to compare these results with the previous results using indicators on phosphoric and sulfuric acid anodized aluminum since the oxide formed in oxalic acid is yellow.

The adsorption of ammonia and pyridine on oxalic acid anodized aluminum was not studied by IR, because the bands due to adsorption of ammonia and pyridine appear in the same region as the bands due to the oxalate incorporated into the oxide during the anodization.

5. SUMMARY OF AMMONIA AND PYRIDINE ADSORPTION RESULTS

A small amount of strong Brønsted acidity was detected on the phosphoric and sulfuric acid anodized aluminum. The Brønsted acidity decreased with increasing pretreatment temperature and the activity of the oxide increased with increasing pretreatment temperature. The amount of Lewis acid sites on the sulfuric acid anodic oxides increased with increasing pretreatment temperature as the oxide became increasingly active as a catalyst. If one uses the

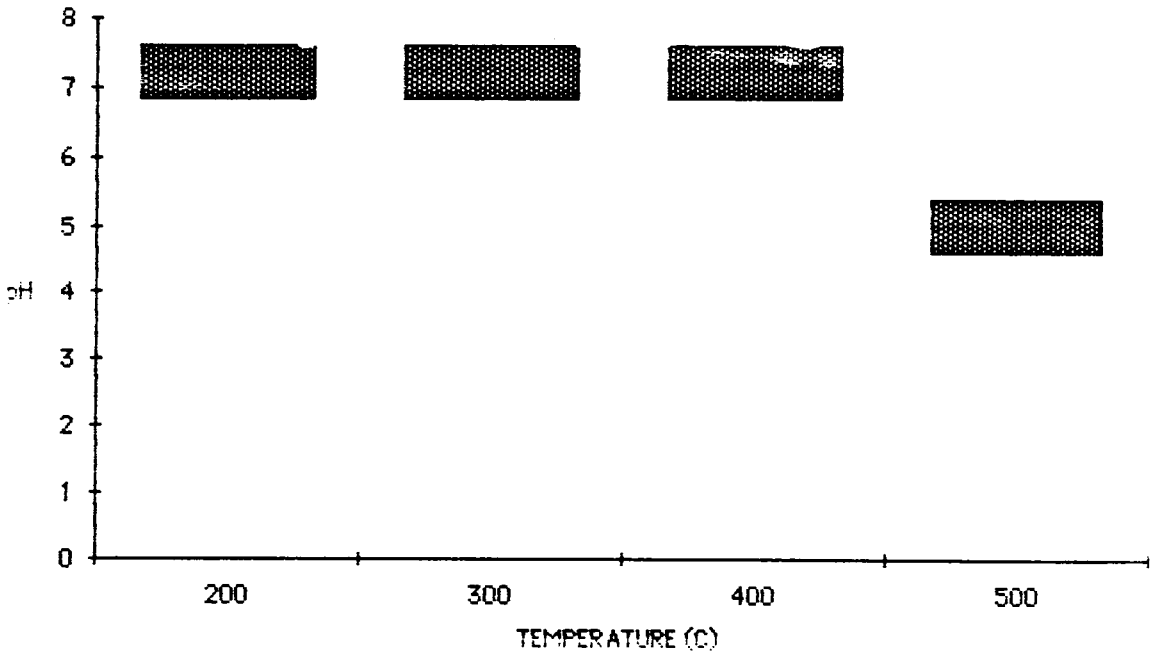

Figure 48. pH range determined by adsorption of indicators on thermally pretreated 3% oxalic acid anodic aluminum oxides.

acidity measurements as the only means of interpreting the catalytic results, one might believe that the Lewis acid site is the major acid site in the dehydration of the isopropanol. However, there have been reports in the literature of poisoning studies(67) in which the dehydration of alcohol over γ-Al_2O_3 is believed to occur over the Brønsted acid sites even though no Brønsted acid sites were detected. Knözinger and Ratnasamy(67) believed that only a small(undetectable) concentration of Brønsted acid sites was necessary to dehydrate the alcohol. If Knözinger and Ratnasamy's conclusion is true, in spite of the acidity results(this study) it is possible that the alcohol is dehydrated over the Brønsted acid site, since there are no reasons that γ-Al_2O_3 and anodized aluminum oxides should not behave in a catalytically similar manner.

At this point it is appropriate to summarize the possible structures and strengths of the Lewis and Brønsted acid sites. This discussion will begin with the Brønsted acid sites. Peri(66) and Knözinger and Ratnasamy(67) proposed the following Brønsted acid sites for aluminas.

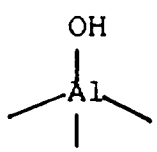

1a

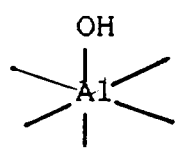

1b

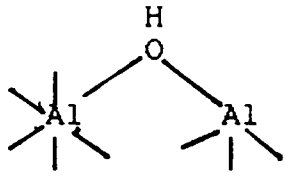

2a

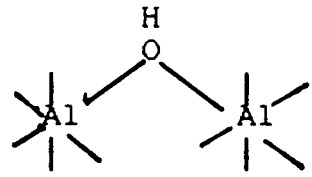

2b

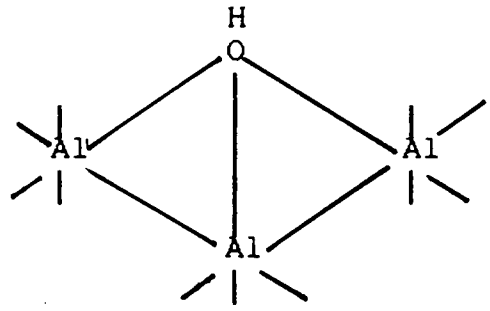

3

The least acidic acid sites are 1a and b and the most acidic site is 3. In addition to the possible sites due to the alumina structure in anodic oxides, there is also the possibility of the electrolyte anions acting as Brønsted acid sites, as shown below.

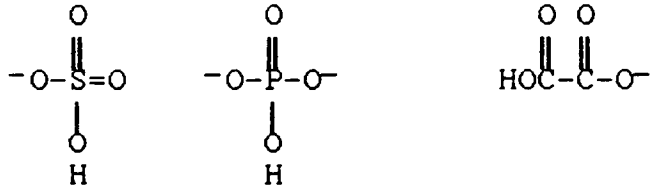

A comparison of the strengths of the Brønsted acid sites associated with the electrolyte anion to the strength of the Brønsted acid sites associated with the alumina, based

on the pK_a's of the acids indicates that the acid sites of the electrolyte anion are stronger than any of the acid sites of the alumina. If there were a large enough concentration of Brønsted acid sites to be detectable by ammonia and pyridine adsorption one might envision the electrolyte site and the alumina site (3) as being the sites detected by pyridine adsorption, the electrolyte site as the strong acid site and the alumina site as the weak acid site. Sites(1) and (2) would be detected by ammonia adsorption with (1) as the weak Brønsted acid site and (2) as the strong Brønsted acid site. In addition to the acid sites discussed, there is also the possibility that the anion acts to weaken the alumina acid sites as shown below by a weak association between the OH of the oxide and the O^- of the anion.

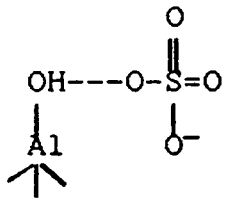

The acidity measurements have shown very little Brønsted acidity, however a wide distribution of Lewis acidity has been shown to exist.

The Lewis acid sites are structurally very similar to the Brønsted acid sites, instead of the OH site there is an

anion vacancy as shown below.

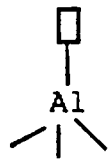

1a

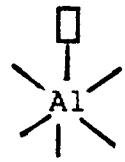

1b

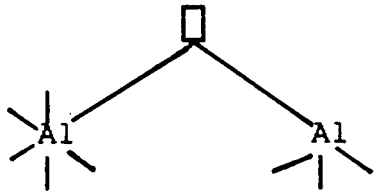

2a

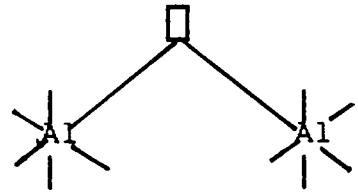

2b

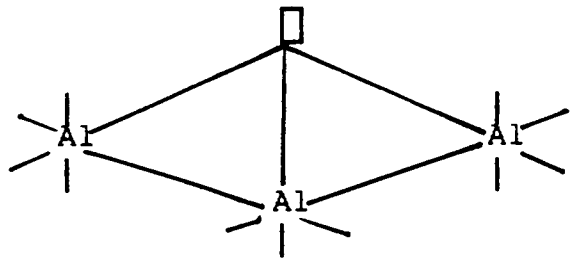

3a

The Lewis acid sites depicted in 1a and 1b are the weakest, because only one Al^{3+} ion is contributing to the strength of the site, this site is the least electropositive. The Lewis acid site illustrated in 3a is the strongest, because three Al^{3+} sites are contributing to the strength of the acid site. The only effect the electrolyte anion might have on the Lewis acid site would be an association with the coordinatively unsaturated Al^{3+}, resulting in a weakening of the Lewis acid site as shown on the next page

(even though sulfate was used in all these examples, phosphate or oxalate can also be used). The weakening results from SO_4^{2-}, being electronegative, contributing charge to the Lewis acid site, causing the Al^{3+} site to be less electropositive(or more electronegative).

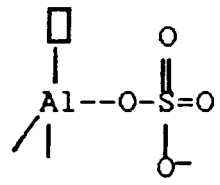

1c

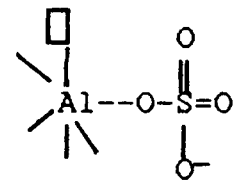

1d

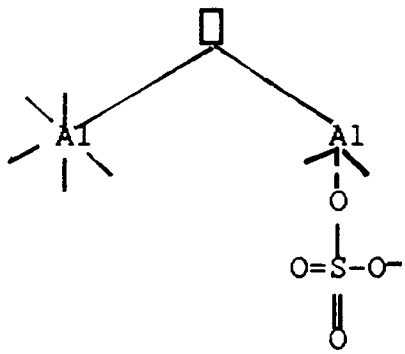

2c

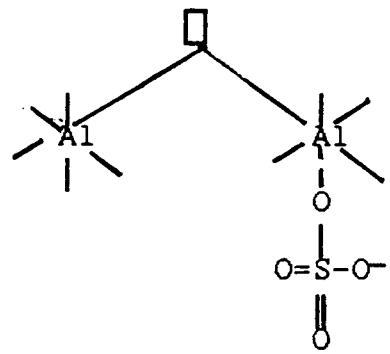

2d

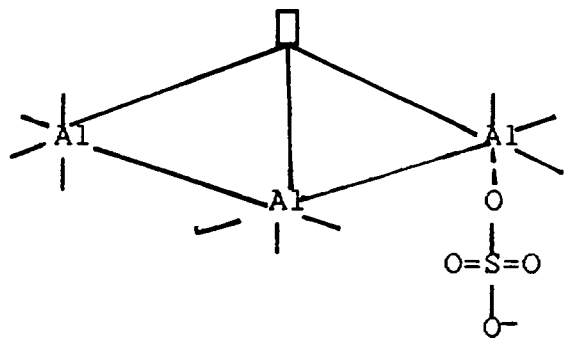

3b

Considering all the possible Lewis acid sites discussed the strength might be enivisioned as follows:3a > 3b > 2a > 2b

> 2c > 2d > 1a > 1b > 1c > 1d. The acid sites that are not associated with the anion are still stronger than the sites that are associated with the anion because the Al^{3+} is more electropositive. Therefore, the strongest Lewis acid site detected by pyridine adsorption is 3a and the weakest site is 2a or 2b. While the strongest Lewis acid site detected by ammonia adsorption is 2c and /or 2d and the weakest acid site is 1c and/or 1d.

For both Brønsted and Lewis acid sites on anodic oxides there are any number of sites that can be pictured as the acid sites, the acid sites discussed here are some of the more obvious. The breakdown of acid strengths and assignments as weak and strong sites are relative and are only meant to show how they might exist. However, it is known from the results in this study that there are wide distributions of acid strengths on the anodic oxides.

6. EFFECT OF BROMINE ETCH ON ACTIVITY OF OXIDES

The goal of the infrared studies was to measure the acidity of anodic oxides that were pretreated in the same manner as the catalysts used in this study. However, in order to carry out the IR studies it was necessary to obtain a transparent oxide window by dissolving aluminum in a bromine/methanol solution. In order to determine if the

bromine etch had any effect on the catalytic properties of the oxide, a bromine etched sulfuric acid anodized aluminum catalyst was used after a 2 hour pretreatment at 300°C in the dehydration of isopropanol. The result of this experiment showed that the catalytic activity of the oxide was unchanged after the bromine etch, 0.14 mmoles of propene/m^2 of oxide was detected as a reaction product. Bromine etched phosphoric acid anodized aluminum was not studied as a catalyst; however, there is no reason to believe that it would behave differently.

H. THERMAL DESORPTION STUDIES

To further understand the acidity of anodic oxides on aluminum, the adsorption of pyridine was studied by temperature programmed thermal desorption-mass spectrometry(TPD-MS). Thermal desorption was used by a number of authors(89-95) to measure the acidity of catalytic materials. The adsorption of amines typically yields two desorption peaks, a low temperature peak(α) associated with desorption from Brønsted acid sites and a high temperature peak(β) attributed to desorption from Lewis acid sites(95). The thermal desorption of pyridine from sulfuric, oxalic, and phosphoric acid anodic aluminum oxides and non-anodized aluminum was studied. Not only is it possible to measure the acidity of an oxide by TPD-MS, but it may also be possible to determine how the adsorbate

interacts with the catalyst by examining the mass spectra of the desorption products. In the cases of amine desorption, the decomposition of amines has been reported(93) as occurring by the following mechanisms:

1) Disproportionation

$$2RNH_2 \rightleftharpoons R_2NH + NH_3,$$

$$2R_2NH \rightleftharpoons R_3N + RNH_2.$$

2) Deamination

$$RCH_2CH_2NH_2 \rightarrow RCH{=}CH_2 + NH_3.$$

The mass spectrum of pure pyridine was compared with the mass spectra measured at the TPD peak maximum for pyridine desorbed from the oxides. Table 11 lists the percent relative abundances of the peaks between m/z 17 and m/z 80 relative to m/z 52 as the base peak for pure pyridine and the ions assigned to these peaks. A bar graph used to compare the m/z 17-80 peaks for pure pyridine with the peaks in the mass spectra of pyridine desorbed from 300°C thermally treated sulfuric acid anodized aluminum is presented in Figure 49. The mass spectra of desorbed pyridine in Figure 49 were measured at 95°C(α) and 200°C(β). In all the studies of pyridine desorption no mass spectral evidence for the decomposition of pyridine was found. Comparing the mass spectrum of pyridine with those for pyridine desorbed from the oxides, the major m/z peaks are the same and any differences in the mass spectra

Table 11

Pure Pyridine

m/z	%RI	ion
17	3.0	NH_3^+, OH^+
18	5.1	H_2O^+
25	3.5	C_2H^+
26	17.5	$C_2H_2^+$, CN^+
27	8.1	$C_2H_3^+$
28	31.1	N_2^+, $C_2H_4^+$, CO^+
37	8.0	C_3H^+
38	11.6	$C_3H_2^+$
39	21.2	$C_3H_3^+$
40	7.3	$C_3H_4^+$
50	40.9	$C_4H_2^+$
51	51.6	$C_4H_3^+$
52	100	$C_4H_4^+$
53	10.1	$C_3H_3N^+$
78	11.8	$C_5H_4N^+$
79	81.8	$C_5H_5N^+$
80	4.9	$C_5H_6N^+$, $^{13}CC_4H_5N^+$

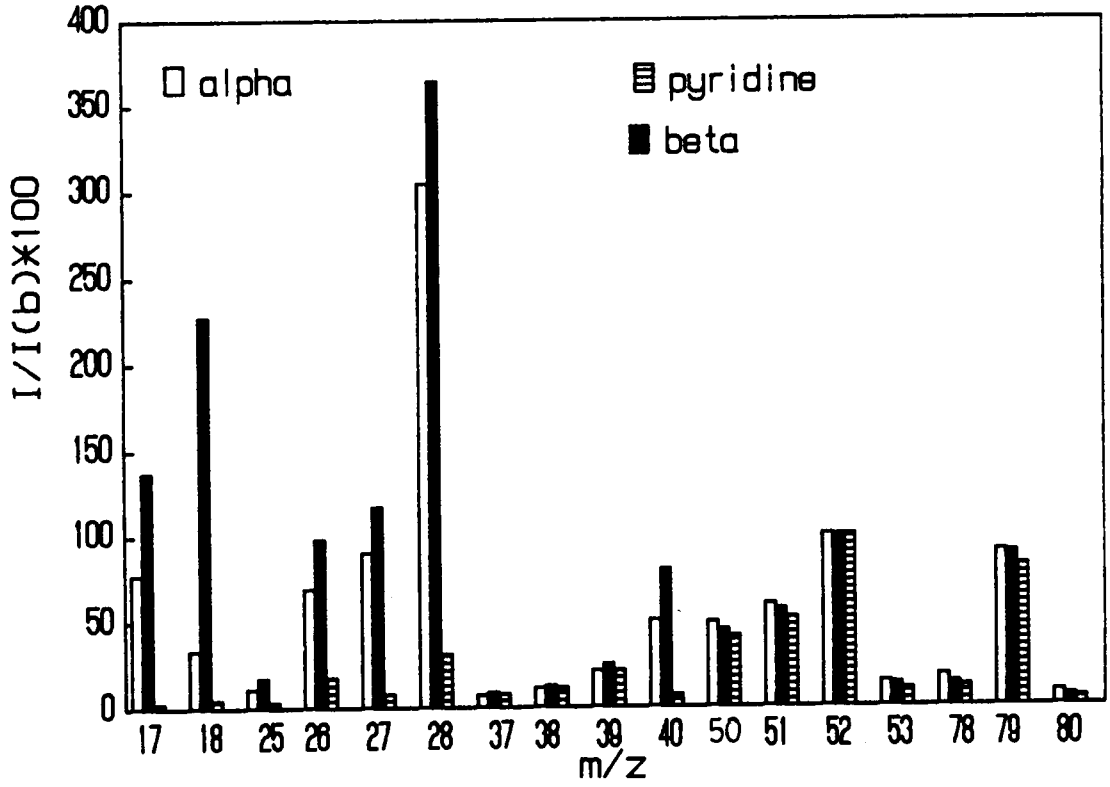

I/I(b)* 100 = Relative abundance of m/z(b).

b= base peak

Figure 49. Mass spectra, m/z 17-80 for pure pyridine and pyridine desorbed from α and β sites on 300°C thermally pretreated 15% sulfuric acid anodic oxide on aluminum.

are due to the desorption of water from the oxide and CO from the filament heater.

1. ANODIC OXIDES FORMED IN SULFURIC ACID

TPD-MS profiles are shown in Figure 50 for desorption of pyridine from sulfuric acid anodic oxides on aluminum that had been pretreated 2 hours at 200°C, 300°C, or 400°C. All TPD-MS spectra discussed in the following sections were measured for m/z 79($C_5H_5N^+$). The m/z 79 peak was selected as the peak to be used in the TPD studies, since it is one of the most intense peaks in the mass spectrum of pyridine. Two peaks are resolvable in Figure 50, labeled α and β. These two peaks are the result of desorption of pyridine from two types of acid sites. Pyridine on the α site desorbs between 50°C and 100°C with a peak maximum at 95°C. The broad β peak is observed between 150°C and 400°C. The β peak is believed to be due to the presence of a wide distribution of Lewis acid site strengths and/or diffusion of pyridine from the pores(89). It was not possible to separate the contribution to the β peak from either the Lewis acid sites or the diffusion of pyridine from the pores. The broadness of the β peak makes it impossible to assign a peak maximum. The α peak is not due to physically adsorbed pyridine, since the position and width of the peak change with the pretreatment and the type of oxide. The α peak is thought to be due to desorption from Brønsted acid

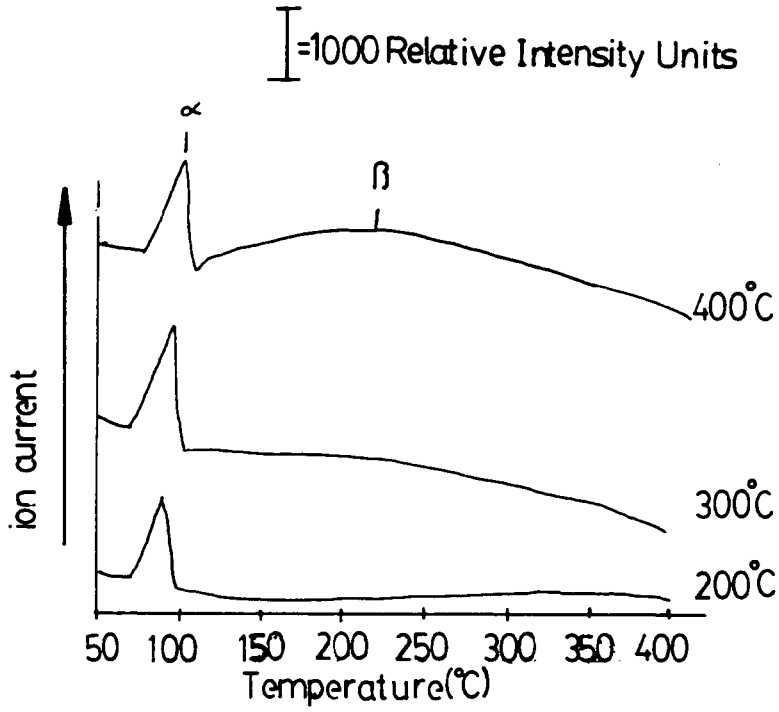

Figure 50. TPD-MS profiles (m/z 79) of pyridine desorbed from 15% sulfuric acid anodic oxides on aluminum.

sites(89). After a 400°C pretreatment 1.0 mmoles of pyridine/m^2 of oxide desorbs which is approximately equal to one monolayer of pyridine(0.8 mmoles of pyridine/m^2 of oxide). Monolayer coverage was calculated based on the molecular area of pyridine(24$Å^2$) and the surface area of the oxide available for adsorption of pyridine. The mmoles of pyridine desorbed per square meter of oxide from the α and β sites on sulfuric acid anodized aluminum are graphed in Figure 51 versus the pretreatment temperature. Comparing the 200°C, 300°C, and 400°C pretreatment results there is little(±0.01 mmoles/m^2) change in the amount of pyridine desorbed from the α acid sites, indicating the concentration of Brønsted acid sites is equal. The increase in the amount of β-type pyridine desorbed from the 400°C pretreated oxide shows a greater concentration of Lewis acid sites. Comparing these results with the IR results for pyridine adsorption in Figure 36, a decrease in Brønsted acidity was seen. The slight inconsistencies between the IR results and the TPD-MS results could be due to a number of reasons such as experimental error(±10%), the desorption temperature was not high enough to completely desorb all the pyridine from the oxide, the α peak may not be entirely due to Brønsted acid sites or the porosity of the oxides may complicate the interpretation of the results(the definition of the α and β sites may not be

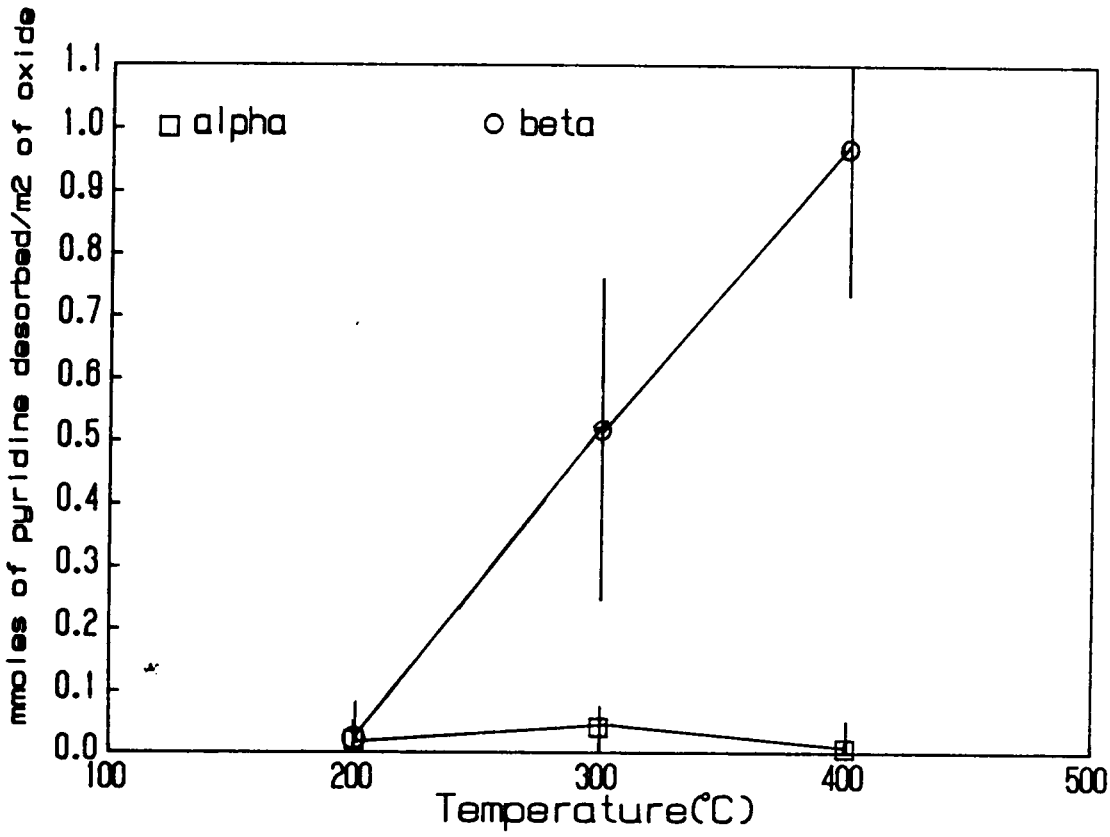

Figure 51. Mmoles of pyridine desorbed/m^2 of oxide from 15% sulfuric acid anodic oxides on aluminum.

as straight forward as thought).

2. ANODIC OXIDES FORMED IN OXALIC ACID

TPD-MS profiles of pyridine desorbed from 200°C, 300°C, and 400°C thermally pretreated oxalic acid anodic aluminum oxide are shown in Figure 52. After the 200°C pretreatment, one broad peak is observed between 50°C and 350°C which is most likely due to desorption of pyridine from a composition of α and β sites. After a 300°C pretreatment three peaks,labeled α, β_1, and β_2 are recorded. The α peak is completely resolvable and occurs between 50°C and 100°C, with a peak maximum at 70°C, β_1 is observed between 100°C and 250°C, and β_2 is recorded between 250°C and 400°C. After the 400°C pretreatment only two peaks are observed. The α peak occurs between 50°C and 100°C with a maximum at 70°C and the β peak was observed between 100°C and 400°C. The β peaks are too broad to accurately determine the peak maxima. The α peaks are thought to be the result of the desorption of pyridine from Brønsted acid sites. The β peaks are believed to be the result of the desorption of pyridine from Lewis acid sites having a wide distribution of strengths.

The mmoles of pyridine detected per square meter of oxide due to desorption of pyridine from the α and β acid sites are graphed versus the pretreatment temperature in Figure 53. One monolayer of pyridine is equivalent to 0.9

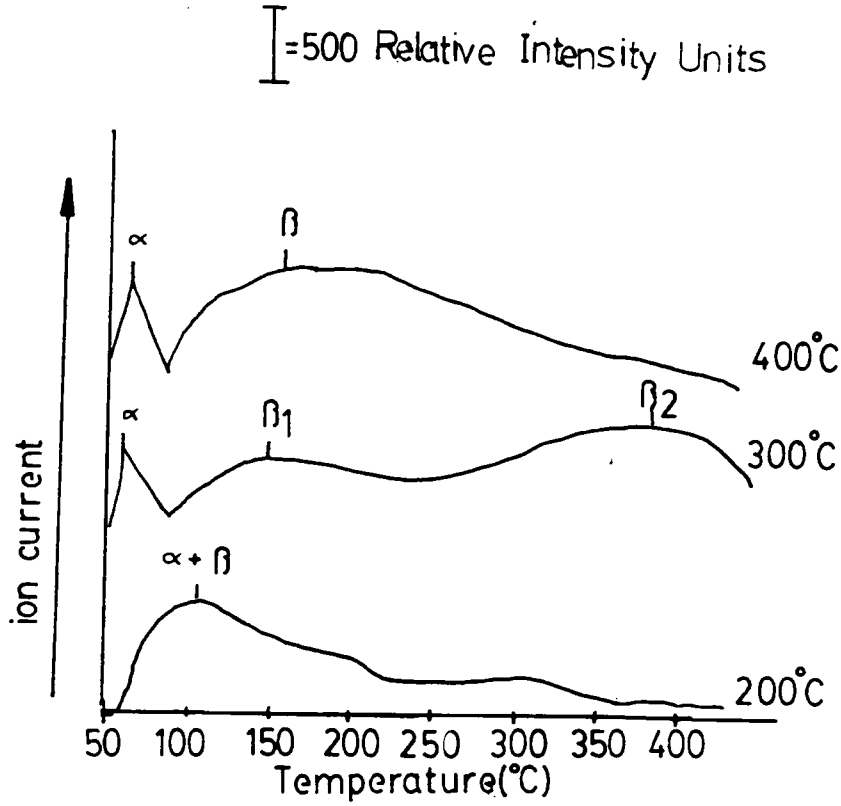

Figure 52. TPD-MS profiles (m/z 79) of pyridine desorbed from 3% oxalic acid anodic oxides on aluminum.

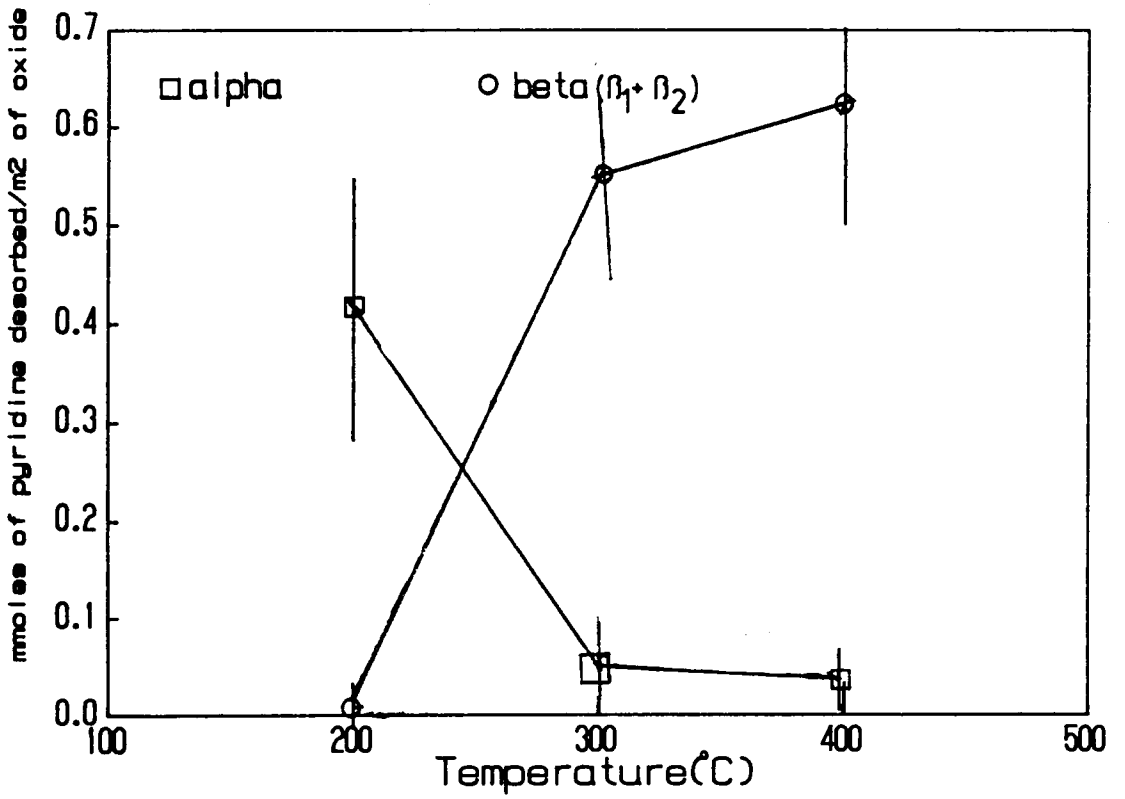

Figure 53. Mmoles of pyridine desorbed/m^2 of oxide from 3% oxalic acid anodic oxides on aluminum.

mmoles/m^2 of oxide(based on the size of the pyridine molecule and the surface area of the oxide available for the adsorption of pyridine). Since 0.6 mmoles of pyridine/m^2 of oxide desorbs from the oxide, it appears that one monolayer of pyridine is adsorbed in this experiment. Since the β_1 and β_2 peaks are not resolvable the total area of both peaks was used as a measure of pyridine desorbed from the Lewis acid sites. The amount of pyridine desorbed from α sites(Brønsted acid sites) decreases between the 200°C and 300°C thermal pretreatments. For the purpose of graphing the TPD peak observed for the 200°C pretreated oxide is assumed to be due to α site desorption, even though it may be due to desorption from both α and β sites. The concentration of pyridine desorbed from the β(Lewis) acid sites increases between the 200°C and 300°C thermal pretreatments. Therefore, from the TPD-MS results the concentration of Brønsted acid sites decrease and the concentration of Lewis acid sites increase with increasing pretreatment temperature.

3. ANODIC OXIDES FORMED IN PHOSPHORIC ACID

In Figure 54 are the TPD profiles for pyridine desorbed from phosphoric acid anodic aluminum oxides that were first thermally pretreated at 200°C, 300°C, and 400°C. The broad peak, α, occurs between 50° and 210°C in the case of the

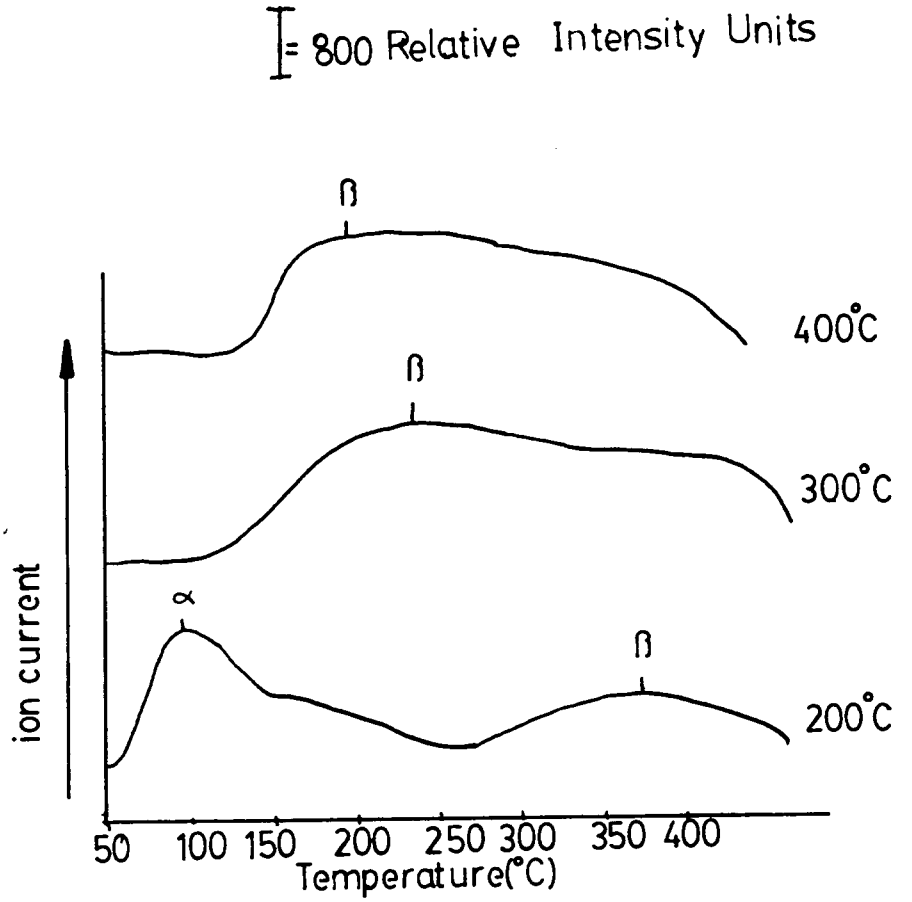

Figure 54. TPD-MS profiles (m/z 79) of pyridine desorbed from 4% phosphoric acid anodic oxides on aluminum.

200°C pretreated oxides due to the desorption of pyridine from Brønsted acid sites. The β peak is a broad peak due to desorption from Lewis acid sites with a wide distribution of strengths. For the 300°C and 400°C pretreated oxides the β peak is the only desorption peak detected and in both cases it occurs between 150°C and 400°C. The concentration results are summarized in Figure 55, where the mmoles of pyridine desorbed/m^2 of oxide from the α and β sites are plotted as a function of pretreatment temperature. The concentration of Brønsted acid sites decreases between the 200°C and 300°C pretreatment, while the concentration of Lewis acid sites increases. After the 400°C pretreatment the amount of pyridine desorbed(0.6 mmoles/m^2 of oxide, based on the area of the pyridine molecule and the surface area of the oxide available for adsorption of pyridine) is approximately equal to one monolayer of pyridine(0.8 mmoles/m^2 of oxide). The concentrations of Lewis acid sites are equal for the 300°C and 400°C pretreated oxides.

4. UNANODIZED ALUMINUM

Since unanodized aluminum has been shown to be inactive in the dehydration of isopropanol, it was necessary to compare the acidity of anodized aluminum with the acidity of unanodized aluminum. The desorption of pyridine from the unanodized aluminum yields two TPD peaks as shown in Figure 56. The first peak is due to the desorption of

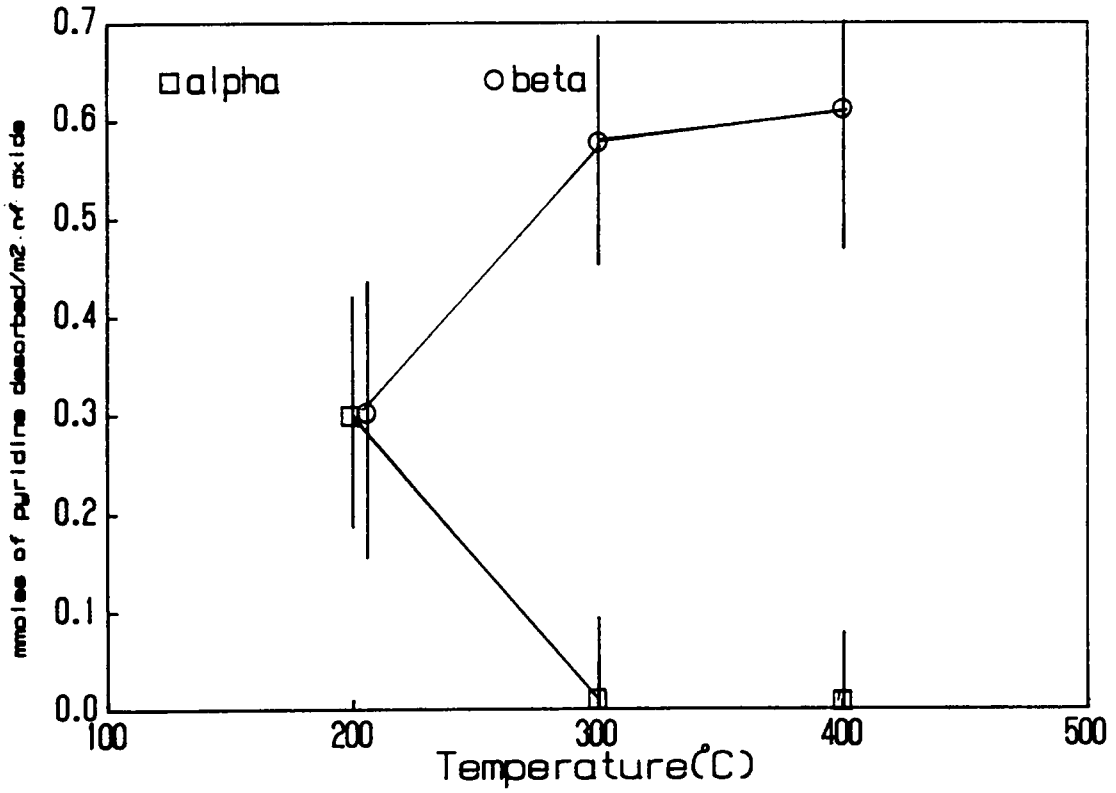

Figure 55. Mmoles of pyridine desorbed/m^2 of oxide from thermally pretreated 4% phosphoric acid anodic oxides on aluminum.

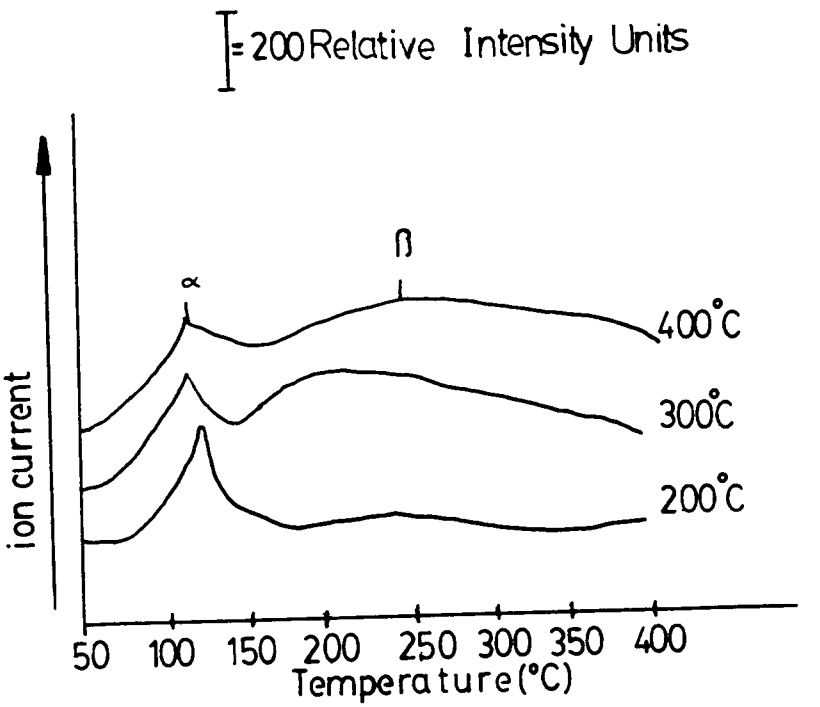

Figure 56. TPD-MS profiles (m/z 79) of pyridine desorbed from unanodized aluminum.

pyridine from Brønsted(α) acid sites and the second peak is due to the desorption of pyridine from Lewis acid, β sites. The peak due to α site desorption occurs between 80°C and 150°C. The β peak occurs between 150°C and 400°C. Plotted in Figure 57 are the mmoles of pyridine/m^2 of oxide for unanodized aluminum versus the thermal pretreatment temperature. The 200°C pretreated aluminum has a high concentration of Brønsted acid sites and few Lewis acid sites. The number of Brønsted acid sites decreases after the 300°C and 400°C pretreatments and the number of Lewis acid sites increases. The maximum of the α peaks shifts from 110±2°C to 100±2°C after the 300°C pretreatment, indicating a decrease in the strength of the Brønsted acid sites. The β peaks are too broad to determine the peak maxima accurately.

The mmoles of pyridine desorbed from the pretreated oxides before and after adjusting for the surface areas are summarized in Table 12. The amount of pyridine desorbed from the oxides before a correction for surface area is based on the amount desorbed from a 1 cm^2 sample. The unanodized aluminum surface area was based on a geometric calculation of the area of the 1 cm^2 piece of aluminum. The concentration of α and β sites/m^2 of oxide for unanodized aluminum is greater than for the anodized aluminum, after being corrected for the surface areas. However, the

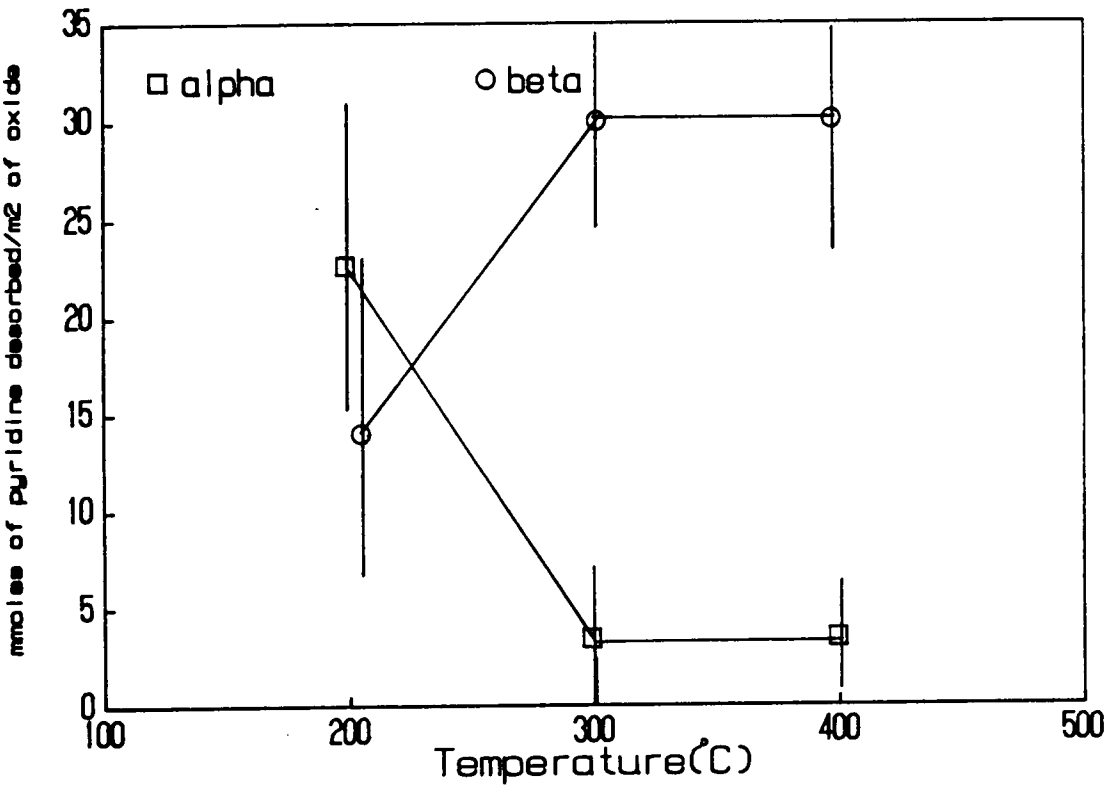

Figure 57. Mmoles of pyridine desorbed/m^2 of oxide from thermally pretreated unanodized aluminum.

Table 12

Summary of TPD-MS results

Anodization	Pretreatment Temperature(°C)	α mmoles/m^2 (oxide)	β	α mmoles/cm^2 of sample	β
H_2SO_4	200	0.01	0.5	0.07	3.1
"	300	0.01	0.5	0.07	3.1
"	400	0.01	1.0	0.07	6.2
H_3PO_4	200	0.35*	0.35	2.4	2.4
"	300	<0.05	0.6	<0.05	4.1
"	400	<0.05	0.65	<0.05	4.4
$H_2C_2O_4$	200	0.4	<0.05	0.07	<0.05
"	300	0.2	0.05	0.4	0.1
"	400	0.05	0.65	0.1	1.2
unanodized	200	23	14	0.003	0.002
"	300	3	30	0.0007	0.005
"	400	3	30	0.0007	0.005

* combination of α and β sites

measurement of the total amount of pyridine(before a surface area correction) desorbing from the acid sites on the unanodized aluminum is beyond the detection limits of this technique (0.1 mmoles), therefore these amounts reported are questionable and may be meaningless.

I. COMPARISON OF TDP-MS, IR, AND CATALYTIC RESULTS

A comparison of the IR results with the TPD results for pyridine interaction with sulfuric and phosphoric acid anodized aluminum shows the trends observed in the acidity measurements agree. In Table 13 the ratio of pyridine adsorbed or desorbed from Lewis/Brønsted acid sites as measured by IR and TPD-MS, respectively are summarized. It is impossible to compare directly the TPD-MS and IR data since the IR data is a tabulation of peak areas and not amounts, the extinction coefficients for pyridine adsorbed on anodized aluminum are not known. However, it is possible to compare the ratios of Lewis/Brønsted acid sites. Table 13 also summarizes the amount of propene detected over the oxides at each reaction temperature. For the IR results for pyridine adsorption on sulfuric acid anodic oxides on aluminum, the Lewis/Brønsted acidity ratio increased between 200°C and 400°C. For the TPD-MS results the β/α ratio of acid sites increased between 300°C and 400°C. The trend of an increasing Lewis/Brønsted acidity ratio occurred in both the TPD-MS and IR results; however the

Table 13

Summary of Pyridine Adsorption/Desorption Results Measured by IR and TPD-MS

Anodization	Pretreatment Temperature(°C) (2 hours)	TPD-MS β/α	IR L/B	Catalytic mmoles of propene/m^2 of oxide
sulfuric	200	50	1	0.01
sulfuric	300	50	80	0.13
sulfuric	400	100	120	0.13
phosphoric	200	1	1.5	<0.01
phosphoric	300	12	6	1.0
phosphoric	400	13	30	2.0
oxalic	200	0.13	**	<0.01
oxalic	300	0.25	**	0.1
oxalic	400	0.3	**	0.5

L = Lewis acid sites

B = Brønsted acid sites

** = not measured

ratios varied. The variation in the acidity ratios may be due to a number of factors. First, in the IR study it was assumed that the ratio of the L/B extinction coefficients was 1.0(86,138,139), if for any reason this was not a correct assumption the L/B ratio(IR results) could be affected. Second, in the TPD-MS study the definition of the α peak as due to the desorption of pyridine from the Brønsted acid sites and β peak as due to the desorption of pyridine from the Lewis acid sites may not be as clear cut as thought. It is possible that pyridine from Brønsted acid sites, ie strong acid sites, is still desorbing under the β peak. Third, it is possible in order to completely desorb the pyridine from the oxide, the upper thermal desorption temperature in the TPD-MS study must go above 400°C, therefore the amount of pyridine desorbed from the Lewis acid sites may be lower than the amount actually adsorbed.

The catalytic activity increased between the 200°C and 300°C pretreatment. The increase in catalytic activity of the oxide corresponds to the increase in the L/B ratio with increasing pretreatment temperature.

For phosphoric acid anodized aluminum the IR and TPD-MS results showed that the ratio of Lewis/Brønsted acid sites increased between the 200°C and 400°C pretreatments. When comparing the IR results with the TPD-MS results for

the anodic oxides it was found that the same trends in acidity with pretreatment temperature were observed; however, again there were differences in the absolute ratios. These differences in ratios are thought to be due to factors similar to those discussed for sulfuric acid anodic aluminum oxides. Comparing the catalytic results with the acidity measurements, it was noted that the activity of phosphoric acid anodized aluminum increased between 200°C and 400°C as the L/B ratio increased. These acidity and catalytic results can be interpreted in a couple of ways: the Lewis acid site is the only site available for isopropanol dehydration, since the concentration of Lewis acid sites increases and Brønsted acid sites decreases or catalytic activity is favored by a very small concentration(undetectable) of Brønsted acid sites. From these results it is impossible to determine which one or if both mechanisms are correct; however, based on Knözinger and Ratnasamy's(67) results, the Brønsted acid sites are the important sites in the dehydration of the isopropanol.

For oxalic acid anodized aluminum the activity in the dehydration of isopropanol increased between 200°C and 400°C while the β/α ratio increased. These results suggest that the major acid site is the Lewis acid site; however, the small concentration of Brønsted acid sites may be all

that is necessary for the dehydration of the alcohol.

The concentration of Lewis/Brønsted acidity(Table 13) follows the trend : sulfuric > oxalic ≈ phosphoric acid anodized aluminum and the catalytic activity follows the trend : phosphoric > oxalic > sulfuric. The comparison of the acidity and catalytic results indicates that the Lewis acidity of the oxide does not contribute to the increased activity of phosphoric acid anodized aluminum compared to the sulfuric and oxalic acid anodized aluminum. The trend of the catalytic activity of the oxides follows the diameter of the oxide pores; that is, phosphoric > oxalic > sulfuric. In addition to the pore diameter, oxide thickness may also contribute to determining the catalytic activity of the oxide. The phosphoric acid anodized aluminum is the thinnest of the oxides, while the oxalic and sulfuric acid anodized aluminum are of equal thickness. The thinner oxide however may have a concentration of Brønsted acid sites that is closest to the threshold concentration of Brønsted acidity necessary for optimum catalytic activity. Therefore, the thinner oxide may be more active simply because it has an optimum number of Brønsted acid sites.

J. MECHANISMS FOR THE DECOMPOSITION OF ISOPROPANOL

The decomposition of alcohol over γ-Al_2O_3 has been studied and a number of mechanisms have been proposed both

for the dehydration and dehydrogenation of alcohols. Even though it has been shown in this work that the measured acidity of the oxides may not account for the increased activity of the anodized aluminum as a catalyst, the nature of the acid sites on which the alcohol adsorbs is still important in determining the mechanisms by which the alcohol is dehydrated. The generally accepted mechanism for the dehydration of alcohols is the mechanism proposed by Knözinger(19), involving both an acidic and basic site, shown in Mechanism I. The alcohol is thought to be adsorbed via two hydrogen-bonds between a hydroxyl proton of the alcohol and an oxygen ion of the surface and between hydroxyl protons of surface hydroxyl groups and free electron pairs of the hydroxyl of the alcohol. The formation of both hydrogen bonds results in the cleavage of the C-O bond, the C-H bond, and a hydride transfer resulting in the formation of a C-C double bond and H_2O.

In this study, it was found that there is a point where the surface is sufficiently dehydrated to become catalytically active, possibly the oxide has been dehydrated to the point where just enough hydroxyl groups remain. If Knözinger's(19) mechanism(I) is applicable then dehydration of the oxide results in the exposure of O^{2-} sites which in combination with remaining OH^- sites results in the catalyst being effective for the dehydration of

MECHANISM I

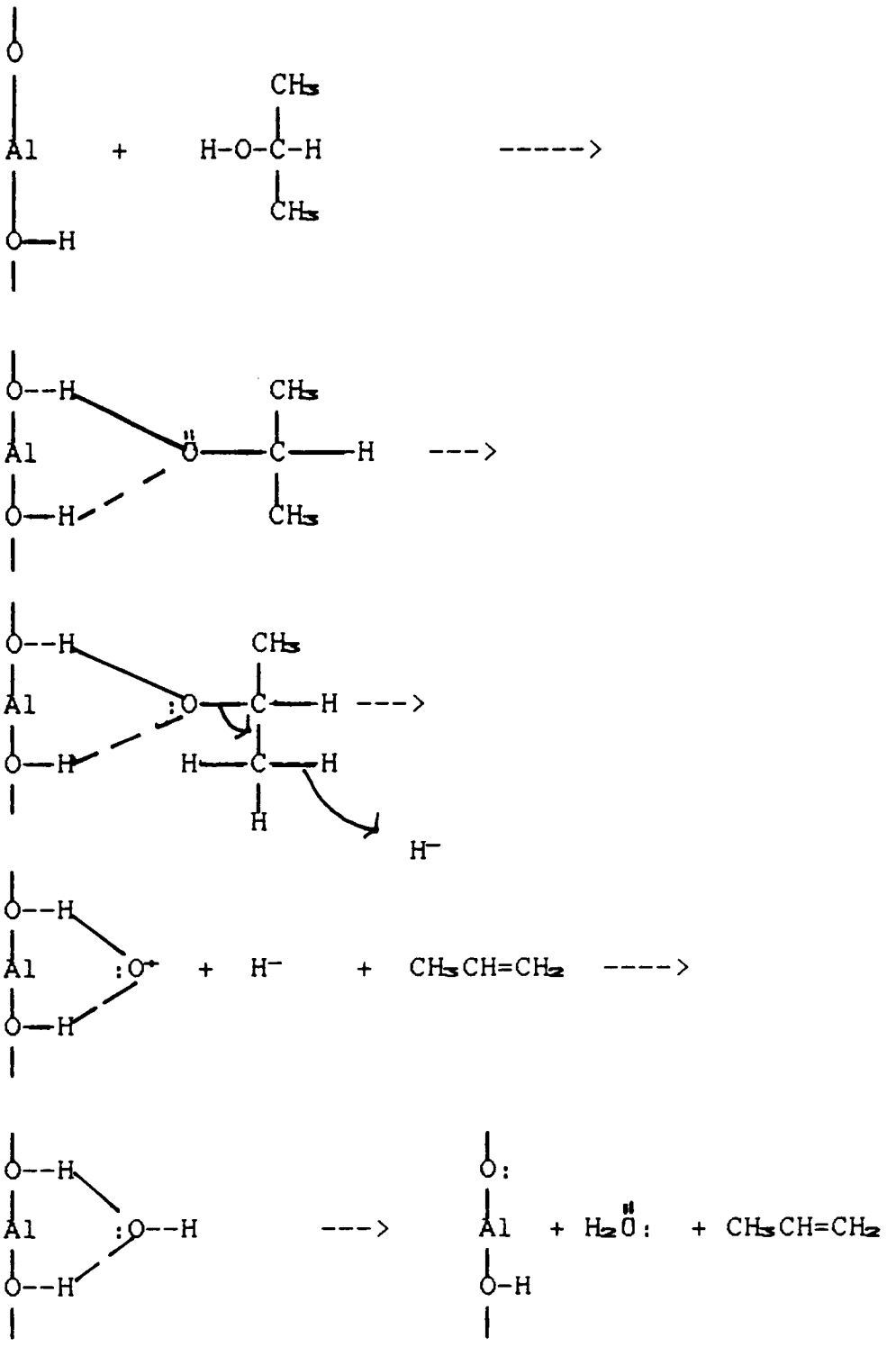

* all Al^{3+} species are octahedral.

isopropanol. This could be the case for the anodic oxides since there are hydroxyl groups present and detectable by IR. However, the adsorption of ammonia and pyridine indicates that the major acid sites on the oxides are (coordinatively unsaturated Al^{3+}) Lewis acid sites. Even when Brønsted acid sites are detected, it was shown that as the pretreatment temperature increases the concentration of Brønsted acid sites decreases. The activity of the oxide increased as the concentration of Brønsted sites decreased. Thus, it is reasonable that the mechanism for the dehydration of isopropanol involves a small concentration of Brønsted acid sites and the amount of Brønsted acid sites must be at a certain threshold level before they become active. It is also possible that the Brønsted acid sites are P-OH, S-OH, or C-OH sites instead of Al-OH sites, similar to the structure below. It was not possible to differentiate between AlOH, POH, SOH, or COH sites by the adsorption of ammonia or pyridine, since they would all occur in the same general region of the IR spectrum.

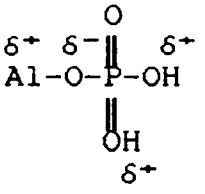

Studies of the dehydrogenation of alcohols using various dehydrogenation catalysts including hydroxyapatite

$Ca_{10}(PO_4)_6(OH)_2$(59,60), and alumina doped with Cu^{2+} (63) have been published. In each of these cases the basicity of the catalyst was directly related to the dehydrogenation activity of the catalyst. Kibby and Hall(60) studied $Ca_{10}(PO_4)_6(OH)_2$ as a catalyst in the dehydrogenation and dehydration of t-butanol. In the study(60) it was found that acids poisoned the dehydrogenation of t-butanol and bases poisoned the dehydration of t-butanol. It was concluded that the acid and base sites for the dehydrogenation and dehydration cannot be the same for both reactions. Kibby and Hall(60) suggested possible choices for the acidic and basic sites in the dehydrogenation over hydroxyapatite catalysts including the catalyst cations or the protons of HPO_4^{2-} groups for the acidic sites and the OH^- groups or the PO_4^{3-} groups for the basic sites. While PO_4^{3-} ions increase acetone formation, there have been reports of SO_4^{2-} ions inhibiting acetone formation(60). In this study on anodized aluminum, acetone was observed over phosphoric and oxalic acid anodized aluminum while no acetone was detected over sulfuric acid anodized aluminum. This suggests that the electrolyte incorporated into the anodized aluminum is related to the formation of acetone. If this is the case, the acid site could then be HPO_4^{2-} or $HC_2O_4^-$, and the basic site could be PO_4^{3-} or $C_2O_4^{2-}$ groups, as shown in Mechanism II. Cleavage of the alcohol must

MECHANISM II

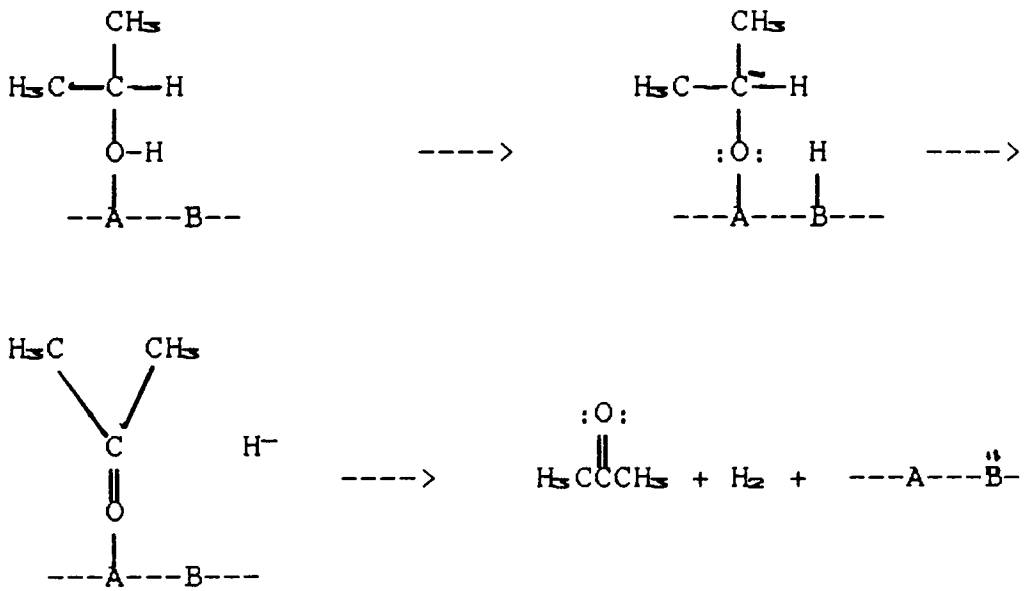

A = HPO_4^{2-} or $HC_2O_4^-$

B = PO_4^{3-} or $C_2O_4^{2-}$

first occur to form the alkoxide. The cleavage is thought to be heterolytic, leaving a net negative charge on the α-carbon, the α-hydrogen is then abstracted, with the PO_4^{3-} acting as a hydrogen ion acceptor(60).

K. X-RAY PHOTOELECTRON SPECTROSCOPY

XPS was employed to characterize the oxides and to determine how the incorporated electrolyte was affected by the use of the oxide as a catalyst. No changes in binding energies, peak shapes or peak intensities were observed for the Al 2p and O 1s photopeaks after each reaction. Hydrocarbon was present in all samples and decreased on the surface of the oxide after use as a catalyst.

1. H_2SO_4 ANODIZED ALUMINUM

The XPS results for H_2SO_4 anodized aluminum non-pretreated, pretreated for 2 hours, and pretreated for 13 hours are shown in Table 14. The binding energies and atomic ratios determined from the S 2p, O 1s, and Al 2p photopeaks are listed for anodic oxides used in catalytic reactions, for an untreated anodic oxide, for an aluminum sulfate standard, and γ-Al_2O_3. The atomic ratio for sulfur/aluminum remains constant 0.06 ± 0.005 indicating there is no migration or loss of SO_4^{2-}. The binding energies of the S 2p photopeaks are constant (169.7±0.1 eV) indicating that the chemical oxidation state of sulfur on the surface of the anodic oxides is unchanged by the

Table 14

XPS Results

15% H_2SO_4 Anodic Oxides on Aluminum

Pretreatment: 0 hours

Pretreatment and Reaction Temperature(°C)	Binding Energy(eV) (±0.1eV) Al 2p	O 1s	S 2p	Atomic Ratios O/Al (±0.1)	S/Al (±0.005)
250	74.8	531.9	169.7	1.6	0.06
275	74.7	531.9	169.7	1.7	0.06
300	74.7	531.9	169.7	1.7	0.06
325	74.8	531.9	169.7	1.7	0.06
350	74.8	532.0	169.6	1.6	0.06

Pretreatment: 2hours

Pretreatment and Reaction Temperature(°C)	Binding Energy(eV) (±0.1eV) Al 2p	O 1s	S 2p	Atomic Ratios O/Al (±0.1)	S/Al (±0.005)
175	74.8	531.9	169.7	1.6	0.06
200	74.8	531.9	169.7	1.6	0.06
225	74.7	531.9	169.6	1.6	0.06
250	74.7	532.0	169.7	1.7	0.06
275	74.7	532.0	169.6	1.7	0.06
300	74.8	531.9	169.6	1.7	0.06

Pretreatment: 13 hours

Pretreatment and Reaction Temperature(°C)	Binding Energy(eV) (±0.1eV) Al 2p	O 1s	S 2p	Atomic Ratios O/Al (±0.1)	S/Al (±0.005)
150	74.7	531.9	169.7	1.7	0.06
175	74.7	531.9	169.7	1.6	0.06
200	74.7	531.9	169.6	1.7	0.06
225	74.8	532.0	169.7	1.6	0.06
275	74.7	531.9	169.6	1.7	0.06
300	74.7	531.9	169.6	1.7	0.06
$Al_2(SO_4)_3 \cdot 8H_2O$	75.9	533.0	170.1	6.3	1.5
Anodized Aluminum	74.7	531.9	169.6	1.7	0.06
γ-Al_2O_3	73.5	530.5	---	1.5	---

pretreatment and reaction conditions. The S 2p binding energy for an aluminum sulfate standard, 170.1 eV, is slightly higher than the binding energy for sulfate in anodized aluminum. The reason for this difference in binding energy is related to the chemical environment of the sulfate. The differences in binding energies indicate there is greater electron density around the sulfur in the anodized aluminum than in the $Al_2(SO_4)_3 \cdot 8H_2O$. The atomic ratio of S/Al for the aluminum sulfate standard is 1.5 as expected stoichiometrically. The O/Al atomic ratio for the aluminum sulfate standard($Al_2(SO_4)_3 \cdot 8H_2O$), 6.3, is lower than the expected value, 10. This is due to the loss of some of the water of hydration in the vacuum chamber(10^{-8} torr) thus decreasing the O/Al atomic ratio.

The binding energies of the Al 2p(74.7±0.1eV) and O 1s (531.9±0.1 eV) photopeaks remained constant for samples prepared under the reaction conditions used in this study. The O/Al atomic ratios also remained constant at 1.7±0.1. The O/Al atomic ratio is not what is expected stoichiometrically for pure Al_2O_3(1.5). The O 1s photopeak is also broader(FWHM=2.8 eV) than for γ-Al_2O_3(FWHM=2.1 eV).The increased oxygen content and broadened photopeak are due to the presence of a second type of oxygen. The second oxygen is probably not hydroxide for two reasons. First, there is no change in the O 1s peak shape,

intensity, or FWHM after the oxides have been heated as shown in Figure 58. If the second oxygen were due to hydroxide the O/Al atomic ratio would decrease and the O 1s FWHM would decrease as the oxide was dehydrated. Second, there is no IR evidence for hydroxide in the bulk of the thermally pretreated oxides, therefore surface hydroxide is not expected. The excess oxygen is most likely due to the anodizing electrolyte SO_4^{2-} incorporated into the oxide. Since there is a 0.06 S/Al atomic ratio there should be a 0.24 O/Al atomic ratio that is due to the oxygen of the sulfate. If the contribution to the O/Al atomic ratio due to the oxygen of the sulfate is subtracted from the total O/Al atomic ratio, it becomes 1.46±0.1 which is what was predicted stoichiometrically for the pure Al_2O_3. The O 1s photopeaks were not curve-fit because of the highly symmetric peaks observed, making the curve-fit highly subjective. Not only was there no evidence for sulfate loss or migration on the surface of the oxides, but with the help of IR spectroscopy there was no evidence for loss or migration of sulfate in the bulk of the oxide.

2. H_3PO_4 ANODIZED ALUMINUM

The P 2p, O 1s, and Al 2p photopeaks of the anodic oxides (Table 15) are compared with those of $AlPO_4$. The P 2p photopeaks for the anodic oxides and $AlPO_4$ have approximately equal binding energies(±0.1 eV). Therefore

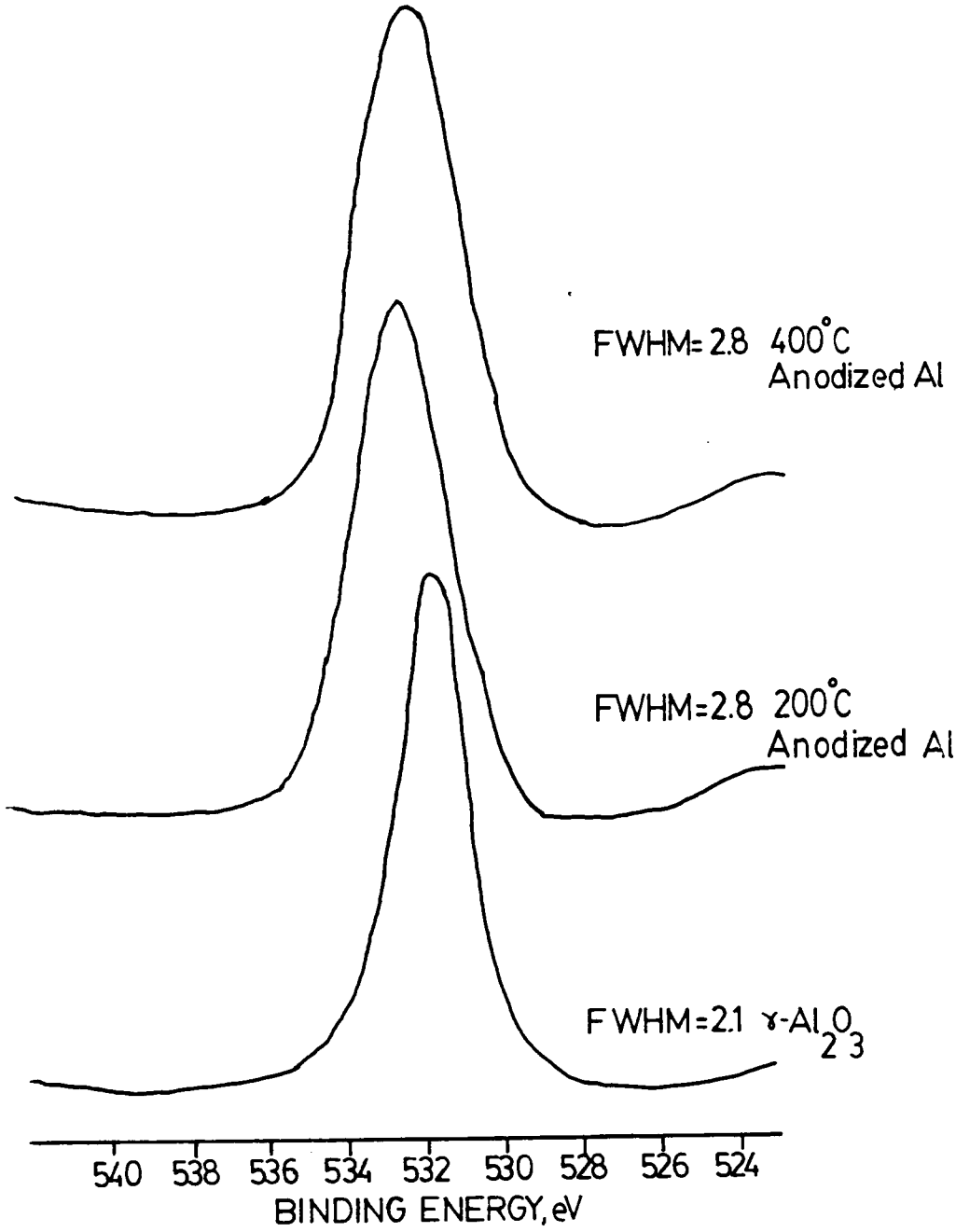

Figure 58. O 1s photopeaks for 20 minute 15% sulfuric acid anodic aluminum oxides before and after use as a catalyst.

Table 15

XPS Results

15% H_3PO_4 Anodic Oxides on Aluminum

Pretreatment: 0 hours

Pretreatment and Reaction Temperature (°C)	Binding Energy, eV (±0.1 eV) Al 2p	O 1s	P 2p	Atomic Ratios O/Al	P/Al
275	74.8	531.9	134.5	1.8	0.06
300	74.7	531.9	134.6	1.7	0.06
325	74.7	531.8	134.6	1.7	0.06
350	74.8	531.9	134.5	1.8	0.06
375	74.8	531.8	134.6	1.7	0.06
400	74.7	531.8	134.5	1.8	0.06

Pretreatment: 2 hours

Pretreatment and Reaction Temperature (°C)	Binding Energy, eV (±0.1 eV) Al 2p	O 1s	P 2p	Atomic Ratios O/Al	P/Al
200	74.8	531.9	134.5	1.8	0.07
225	74.7	531.8	134.5	1.7	0.06
275	74.7	531.8	134.5	1.8	0.07
300	74.7	531.8	134.5	1.7	0.06
350	74.7	531.8	134.5	1.7	0.06

Pretreatment: 13 hours

Pretreatment and Reaction Temperature (°C)	Binding Energy, eV (±0.1 eV) Al 2p	O 1s	P 2p	Atomic Ratios O/Al	P/Al
200	74.7	531.8	134.5	1.7	0.06
225	74.7	531.8	134.5	1.7	0.06
275	74.7	531.8	134.5	1.7	0.06
300	74.7	531.8	134.5	1.7	0.06
350	74.8	531.8	134.5	1.8	0.07
$AlPO_4$	75.9	533.0	134.7	4.1	1.0
Anodized Aluminum	74.7	531.8	134.5	1.7	0.06

the anodic oxides have phosphate incorporated into the oxides. The phosphate may be any of the following species, since it is not possible to differentiate among them by XPS: PO_4^{3-}, HPO_4^{2-}, $H_2PO_4^-$ or H_3PO_4. The phosphorus/aluminum atomic ratio(Table 14) does not change after use as a catalyst (0.06±0.01), indicating there is no migration or loss of PO_4^{3-} on the surface of the oxide. IR spectroscopy also shows no evidence of loss or migration of phosphate in the bulk of the oxide. The Al 2p and O 1s photopeaks behave as they did for the sulfuric acid anodized aluminum. The binding energies and O/Al atomic ratios for phosphoric acid anodized aluminum are nearly identical to the binding energies and atomic ratios for sulfuric acid anodized aluminum. The increased O/Al atomic ratio is attributed to the presence of two types of oxygen, the oxygen of phosphate and the oxygen of Al_2O_3.

3. $H_2C_2O_4$ ANODIZED ALUMINUM

The XPS results for oxalic acid anodized aluminum non-pretreated, pretreated for 2 hours, and pretreated for 13 hours are summarized in Table 16. The total carbon atomic ratio decreases after anodized aluminum was used as a catalyst. This is caused by a loss of hydrocarbon from the surface of the oxide. Hydrocarbon content also decreased on the surface of H_2SO_4 and H_3PO_4 anodic oxides following use as a catalyst.

Table 16

3% $H_2C_2O_4$ Anodic Oxides on Aluminum

Pretreatment: 0 hours

Pretreatment and Reaction Temperature(°C)	C 1s Binding Energies(eV) Oxalate (±0.1 eV)	Hydrocarbon (±0.1 eV)	Carbide (±0.3 eV)
250	288.8(0.06)	285.0(0.16)	280.1(0.07)
275	288.8(0.06)	285.0(0.16)	280.1(0.06)
300	288.8(0.05)	285.0(0.18)	279.7(0.06)
325	288.7(0.05)	285.0(0.17)	280.1(0.06)
375	288.8(0.05)	285.0(0.20)	279.7(0.06)
400	288.8(0.06)	285.0(0.20)	279.8(0.06)

Pretreatment: 2 hours

Pretreatment and Reaction Temperature(°C)	C 1s Binding Energies(eV) Oxalate (±0.1 eV)	Hydrocarbon (±0.1 eV)	Carbide (±0.3 eV)
250	288.8(0.06)	285.0(0.17)	---
275	288.9(0.05)	285.0(0.16)	280.2(0.05)
300	288.9(0.06)	285.0(0.15)	280.1(0.06)
325	288.9(0.05)	285.0(0.15)	280.2(0.03)
375	288.9(0.05)	285.0(0.18)	280.1(0.04)

Pretreatment: 13 hours

Pretreatment and Reaction Temperature(°C)	C 1s Binding Energies(eV) Oxalate (±0.1 eV)	Hydrocarbon (±0.1 eV)	Carbide (±0.3 eV)
250	288.8(0.05)	285.0(0.18)	280.1(0.03)
325	288.8(0.05)	285.0(0.16)	280.1(0.05)
$Na_2C_2O_4$	288.8	285.0	
Anodized Aluminum	288.8(0.06)	285.0(0.33)	----
HfC			281.0(ref.140)
TiC			281.7(ref.140)
WC			282.9(ref.140)
AlC_3			280.0

() = C/Al atomic ratio

In Figure 59, C 1s spectra for $H_2C_2O_4$ anodized aluminum are compared (top to bottom) for an unused catalyst, a non-pretreated catalyst used at 300°C, a 2 hour pretreated catalyst used at 300°C, and a 13 hour pretreated catalyst used at 250°C. The peak at 288.8±0.1 eV has been assigned to oxalate, by comparing this C 1s binding energy to that in $Na_2C_2O_4$. Sodium oxalate has a C 1s binding energy of 288.3 eV which is 0.5 eV lower than measured for oxalate (288.8±0.1 eV) in anodic oxides, since the oxalate in the oxide is in a more electropositive environment. The peak occurring at 285.0 eV corresponds to hydrocarbon.

For oxalic acid anodized aluminum used as a catalyst, a peak appears between 279.7 and 280.2 eV in the region where carbides occur(140), it is not possible for this peak to be assigned to any species besides a carbide. This peak does not appear for H_2SO_4 and H_3PO_4 anodic oxides. The binding energy of the oxalate carbon remains constant at 288.8±0.1 eV under all reaction conditions. The amount of oxalate on the surface of the anodic oxides remains constant both before and after use as a catalyst. There is no IR evidence for the loss or migration of oxalate in the bulk of the oxide. The observation that the oxalate content remains constant both before and after use as a catalyst contradicts the earlier conclusion that CO_2 detected upon heating of the oxalic acid anodized aluminum was due to

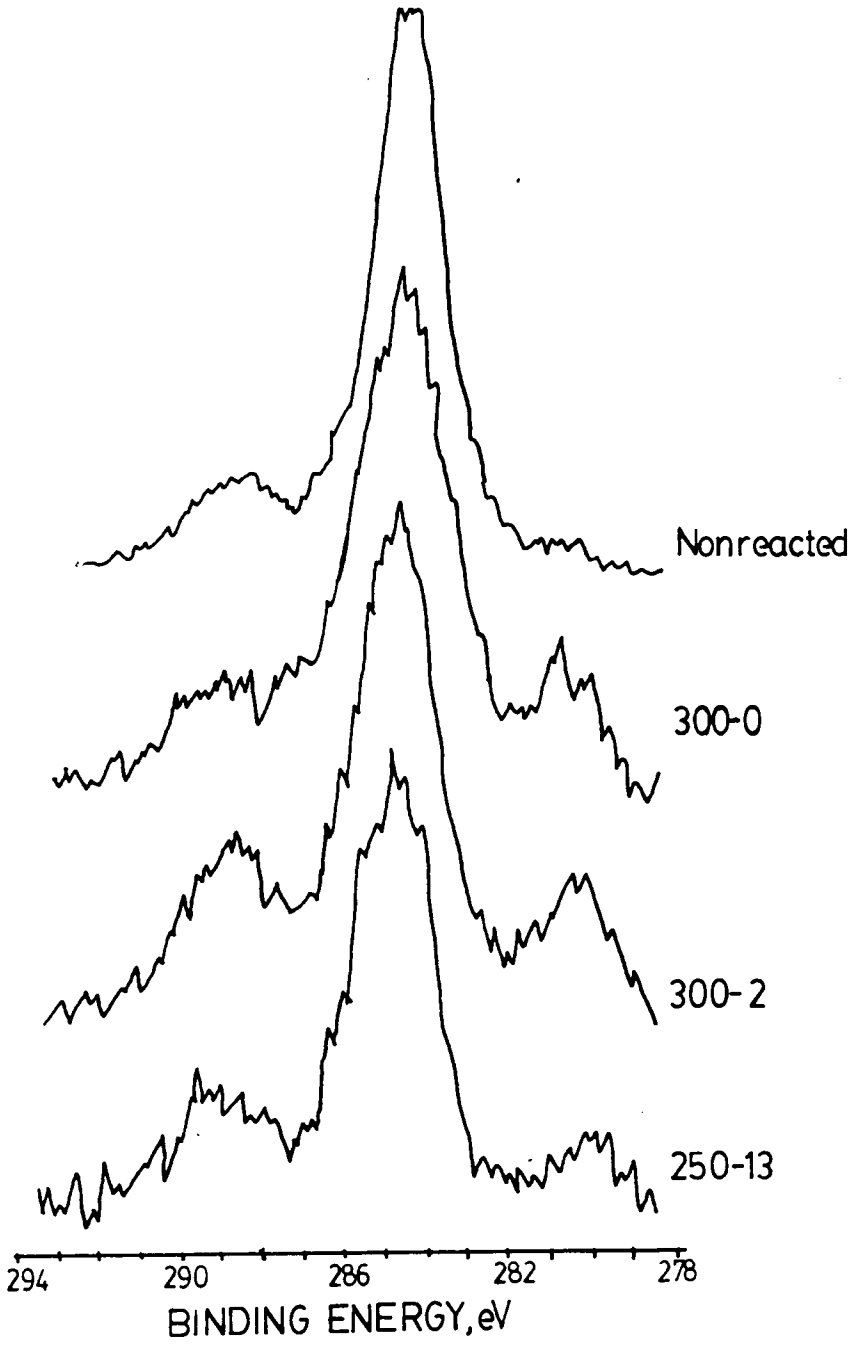

Figure 59. C 1s XPS spectra of 3% oxalic acid anodic aluminum oxides comparing (top to bottom) an unused catalyst, a non-pretreated catalyst used at 300°C, a 2 hour pretreated catalyst used at 300°C, and a 13 hour pretreated catalyst used at 250°C.

decomposition of the oxalate. However, the CO_2 detected by GC was <1%, a loss of this magnitude is below the detection limit of XPS or IR.

The activity of the 2 hour pretreated and non-pretreated oxides is not affected by carbide formation. However, the 13 hour pretreated oxides are not active as catalysts. It is doubtful that the lack of activity of the 13 hour pretreated oxides is due to carbide formation since all the oxalic oxides(active or not active) have equal amounts of carbide on their surfaces. Carbide formation is probably the result of alcohol decomposition on the surface of the oxalic acid anodized aluminum via some reaction not identified in this study. It is not possible to write a thermodynamically reasonable reaction for the formation of the carbide on the oxide, however there is the XPS evidence for the carbide formation. There is no other evidence that might be helpful in the identification of this peak. The O 1s and Al 2p photopeak binding energies and intensities are shown in Table 17. The O/Al ratio is higher than expected(1.6±0.1) for pure Al_2O_3 (1.5). The high O/Al atomic ratio is due to the contribution of the oxygen of oxalate. If the expected contribution due to the oxygen of oxalate is subtracted from the total O/Al atomic ratio the atomic ratio becomes 1.5.

Table 17

3% Oxalic Acid Anodic Oxides on Aluminum

Pretreatment: 0 hours

Pretreatment and Reaction Temperature (°C)	Binding Energy (eV) (±0.1) Al 2p	O 1s	Atomic Ratio O/Al	C/Al
250	74.8	531.8	1.6	0.06
275	74.7	531.8	1.7	0.06
300	74.8	531.8	1.6	0.05
325	74.8	531.9	1.6	0.05
375	74.7	531.8	1.6	0.05
400	74.7	531.8	1.6	0.06

Pretreatment: 2 hours

Pretreatment and Reaction Temperature (°C)	Binding Energy (eV) (±0.1) Al 2p	O 1s	Atomic Ratio O/Al	C/Al
250	74.8	531.8	1.7	0.06
275	74.8	531.7	1.6	0.05
300	74.7	531.8	1.6	0.06
325	74.8	531.9	1.6	0.05
375	74.9	531.8	1.6	0.05

Pretreatment: 13 hours

Pretreatment and Reaction Temperature (°C)	Binding Energy (eV) (±0.1) Al 2p	O 1s	Atomic Ratio O/Al	C/Al
250	74.8	531.8	1.6	0.05
325	74.8	531.7	1.6	0.05
Anodized Aluminum	74.8	531.8	1.6	0.06

Chapter 5

SUMMARY AND CONCLUSIONS

The catalytic activity of anodized aluminum was studied for the dehydration of isopropanol. The adsorption of ammonia and pyridine on anodic oxides was studied by IR spectroscopy and TPD-MS. The adsorption of gaseous bases made it possible to characterize the acidic sites, created by the dehydroxylation of the oxide. It was demonstrated that the activity of the oxides per unit surface area of oxide varied as follows: phosphoric > oxalic > sulfuric acid anodized aluminum > γ-Al_2O_3.

There is no XPS or IR evidence for the loss or migration of the incorporated electrolytes sulfate; phosphate, or oxalate, after use as a catalyst.

From the IR results it was shown that the oxides were dehydrated as a result of the thermal pretreatments.

The acidity measurements demonstrated that the acidity of the oxides increased with increasing pretreatment temperature. The adsorption and desorption of gaseous bases indicate that the largest concentration of acid sites on the anodic oxides was due to the presence of Lewis acid sites. However, it is believed based on the precedent in the earlier studies, that the site that the dehydration of

isopropanol most likely occurs over is the Brønsted acid site. Only a small threshold concentration of Brønsted acid sites is believed to be necessary. The Brønsted acid site may be AlOH, POH, SOH, or COH, it was not possible to define the Brønsted acid site.

REFERENCES

1. Cocke,D.L.,E.D. Johnson and R.P. Merrill, Catal. Rev.-Sci. Eng., 1984, **26**, 163.

2. Ihm, S. and E. Ruckenstein, Ind. Eng. Chem. Prod. Res. Dev., 1978, **17**, 110.

3. Rai, K.N. and E. Ruckenstein, J. Catal., 1975, **40**, 117.

4. Ihm, S.K. and E. Ruckenstein, J. Colloid Interface Sci., 1977, **61** (1), 146.

5. Chu, Y.F. and E. Ruckenstein, J. Catal., 1976, **41**, 373.

6. Chu, Y.F. and E. Ruckenstein, J. Catal., 1978, **55**, 281.

7. Ruckenstein, E. and M.L. Malhotra, J. Catal., 1976, **41**, 303.

8. Chu, Y.F. and E. Ruckenstein, J. Catal., 1976, **41**, 384.

9. Chen, J.J. and E. Ruckenstein, J. Catal., 1981, **69**, 254.

10. Ruckenstein, E. and D.B. Dadybujor, J. Catal., 1977, **48**, 73.

11. Skoulikidis, T.N., Ind. Eng. Chem. Prod. Res. Dev., 1979, **18**, 238.

12. Hönicke, D., Appl. Catal., 1983, **5**, 179.

13. Hönicke, D., Appl. Catal., 1983, **5**, 199.

14. Hönicke, D., J. Catal., 1987, **105**, 10.

15. Hönicke, D., J. Catal., 1987, **105**, 19.

16. Yamada, M. and K. Itabashi, Proceedings of the

Eighth International Congress on Catalysis, 1984, IV, 835.

17. Miller, D.G. and M. Moskovits, Proceedings of the Tenth Canadian Symposium on Catalysis, 1986, 16.
18. Moskovits, M., Canadian Patent for Heterogeneous Catalysis, Can. CA., 1,137,962,21 Dec.1982.
19. Knözinger, H., Angew. Chem. Internat. Edit, 1968, **7**, 791.
20. Whitmore, F.C., J. Amer. Chem. Soc., 1932, **54**, 3274.
21. Brey, W. S. and K. A. Krieger, J. Amer. Chem. Soc., 1949, **71**, 3637.
22. Bremner, J.G.M., J. Amer. Chem. Soc., 1948, **70**, 1222.
23. Ross, R.A. and D.E.R. Bennett, J. Catal., 1967, **8**, 289.
24. Winfield, M.E. in Catalysis, P.H. Emmett; Ed., Reinhold, New York, 1960, Vol. VII, p. 93.
25. Pines, H. and W.O. Haag, J. Amer. Chem. Soc., 1961, **83**, 2847.
26. Munro, L.A. and W.R. Horn, Canad. J. Res., 1935, **12**, 707.
27. Eucken, A. and E. Wicke, Naturwissenschaften, 1944, **32**, 161.

28. Parry, E.P., J. Catal., 1963, **2**, 371.

29. Knözinger, H. and H. Spannheimer, Ber. Bunsenges. Physik. Chem., 1966, **70**, 575.

30. Eucken, A. Naturwissenschaften, 1947, **34**, 374.

31. Wicke, E., Z. Elektrochem. Angew. physik. Chem., 1948, **52**, 86.

32. Senderens, J.B., Bull. Soc. Chem. France, 1907, **4**, 692.

33. Ipatieff, V. N. : Catalytic Reactions at High Pressures and Temperatures, Macmillan Co., New York, 1936.

34. Topchieva, K.V. K. Yun-Pin, and I.V. Smirnova, Advances Catalysis Related Subjects, 1957, **9**, 799.

35. Greenler, R. G., J. Chem. Phys., 1962, **37**, 2094.

36. Treibmann, D. and A. Simon, Ber. Bunsenges. Physik. Chem., 1966, **70**, 562.

37. Vasserberg, V.E., J.R. Davydova, and T.V. Georgievskaya, Kinet. Catal., 1961, **2**, 696.

38. Schwab, G. M. and L. Lassak, Kolloid Z. Z. Polymere, 1965, **206**, 37.

39. Wolkenstein, F.F.: The Electronic Theory of Catalysis on Semiconductors; Pergamon Press, Oxford, 1963.

40. Wolkenstein, F.F., Advances Catalysis Related

Subjects, 1960, **12**, 189.

41. Garner, W.E., Advances Catalysis Related Subjects, 1956, **9**, 169.
42. Hauffe, K., Advances Catalysis Related Subjects, 1956, **9**, 187.
43. Pines, H. and C.N. Pillai, J. Amer. Chem. Soc., 1961, **83**, 3270.
44. Schwab, G. M. and E. Schwab-Agallidis, J. Amer. Chem. Soc., 1949, **71**, 1806.
45. Watanabe, K., C. N. Pillai, and H. Pines, J. Amer. Chem. Soc., 1962, **84**, 3934.
46. Herling, J. and H. Pines, Chem. and Ind., 1963, **2**, 984.
47. Pines, H. and J. Manassen, Advances Catalysis Related Subjects, 1966, **16**, 49.
48. Jain, J. R. and C.N. Pillai, Tetrahedron Lett, 1965, **11**, 675.
49. Balaceanu, J.C. and J.C. Jungers, Bull.Soc. Chem. Belges, 1951, **60**, 476.
50. Stauffer,J.E. and W.L. Kranich, Ind. Eng. Chem., Fundamentals, 1962, **1**, 107.
51. Knözinger, H. and R. Köhne, J. Catal., 1964, **3**, 559.
52. Knözinger, H. and R. Köhne, J. Catal., 1966, **5**, 264.

53. Jambor, J. and L. Berånek, Collection Czechaslav Chem. Commun., 1975, **40**, 1374.

54. Mars, P., "Proceedings of the Symposium on the Mechanism of Heterogeneous Catalysis," Amsterdam, 1959, (J.H. DeBoer, Ed.), Amsterdam:Elsevier(1960), 48.

55. Eucken, A. and H. Heur, Z. Phys. Chem.(Leipzig), 1950, **40**, 196.

56. Wicke, E., Z. Electrochem., 1948, **52**, 86.

57. Wicke, E., Z. Electrochem., 1949, **53**, 279.

58. Moffat, J.B., Catal. Rev. Sci. Eng., 1978, **18** (2), 199.

59. Kibby, C.L. and W.K. Hall, J. Catal., 1973, **31**, 65.

60. Kibby, C.L. and W.K. Hall, J. Catal., 1973, **29**, 144.

61. Tada, A., H. Itoh, Y. Kawasaki, and J. Nara, Chem. Letters Chemical Soc. of Japan, **28**, 1975, 517.

62. Davis, B.H., J. Catal., 1972, **26**, 348.

63. Pepe, F., C. Angeletti, S. DeRossi, and M. LoJacono, J. Catal., 1985, **91**, 69.

64. Cornelius, E.B., T.H. Milliken, G.A.Mills, and A.G. Oblad, J. Phys. Chem., 1955, **59**, 809.

65. Hindin, S.G. and S.W. Weller, Advances Catalysis Related Subjects, 1957, **9**, 70.

66. Peri, J.B., J. Phys. Chem., 1965, **69**, 220.

67. Knözinger, H., P. Ratnasamy, Catal. Rev.Sci.Eng., 1983, **17**, 31.

68. Kagel, R.O., J. Phys. Chem., 1967, **71**, 844.

69. De la Hardrouyere, G., Arch. Sci., 1960, **13**, 1.

70. Geschke, D. and H.Pfeifer, Z. Physik. Chem., 1966, **232**, 127.

71. Knözinger,H., E.Ress, and H.Buhl, Naturwissenschaften, 1967, **54**, 516.

72. Hammett, L.P., and A.J. Deyrup, J. Amer. Chem. Soc., 1932, **54**, 2721.

73. Lewis, G.N. and J. Bigeleisen, J. Amer. Chem. Soc., 1943, **65**, 1144.

74. Walling, C., J. Amer. Chem. Soc., 1950, **72**, 1164.

75. Benesi, H.A., J. Amer. Chem. Soc., 1956, **78**, 5490.

76. Yamanaka, T. and K. Tanabe, J. Phys. Chem., 1975, **79**, 2409.

77. Yamanaka, T. and K.Tanabe, J. Phys. Chem., 1976, **80**, 1723.

78. Mason, J.G. ,R. Siriwardane, and J.P. Wightman, J. Adhesion, 1981, **11**, 315.

79. Mapes, J.E. and R. P. Eischens, J. Phys. Chem., 1954, **58**, 1059.

80. Thomas, C. L., Ind. Eng. Chem., 1949, **41**, 2564.

81. Milliken, T.H., G.H. Mills, and A.G. Oblad, Faraday Soc. Discs., 1950, **8**, 279.

82. Tamele, M.W., Faraday Soc. Discs., 1950, **8**, 270.

83. Hansford, R.C., "Advances in Catalysis", Vol. IV, Academic Press, Inc., New York, N.Y., 1952, 1.

84. Peri, J.B., J. Phys. Chem., 1965, **69**, 231.

85. Tsyganenko, A.A., D.V. Pozdnyakov and V.N. Filimonov, J. Mol. Struc., 1975, **29**, 399.

86. Kiviat, F.E. and L. Petrakis, J. Phys. Chem., 1973, **77**, 1232.

87. Morterra, C., S. Coluccia, A. Chiorino, and F. Boccuzzi, J. Catal., 1978, **54**, 348.

88. Ward, J.W., J. Catal., 1968, **10**, 34.

89. Cvetanovic, R.J. and Y. Amenomiya, Catal. Rev., 1972, **6**, 21.

90. Falconer, J.L. and J.A. Schwartz, Catal. Rev.Sci Eng., 1983, **25**, 141.

91. Scholle, K.F.M.G.J., A.P.M.Kentgens, W.S. Veeman, P. Frenken, and G.P.M.Van der Velden, J. Phys.Chem., 1984, **88**, 5.

92. Hodnett, B.K. and J.B. Moffat, J. Catal., 1984, **88**, 253.

93. Koubek, J., J.Volf, and J. Pasek, J. Catal., 1975, **38**, 385.

94. Mieville,R.L., and B.L. Meyers, J. Catal., 1982, **74**,

196.

95. Takahashi, M., Y. Iwasawa, and S. Ogasawara, J.Catal., 1976, **45**, 1976.

96. Diggle, J. W., T.C. Downie, and C.W. Goulding, Chem. Rev, 1969, **69**, 365.

97. Keller, F., M.S. Hunter, and D.L. Robinson, J. Electrochem. Soc., 1953, **100**, 411.

98. Wood, G.C., J.P. O'Sullivan, and B. Vaszko, J. Electrochem. Soc., 1968, **112**, 618.

99. Franklin, R.W. and D. J. Stirland, J. Electrochem.Soc., 1963, **110**, 262.

100. Csokan, P., Electroplat. and Metal Fin., 1962, **15**, 75.

101. Ginsberg, H. and K. Wefers, Metall(Berlin), 1962, **16**, 173.

102. Murphy, J.F. and C.E. Michelson, Proceedings of the Conference on Anodizing, 1962, 83.

103. Hoar, T.P. and N.F. Mott, J. Phys. Chem. Solids, 1959, **9**, 97.

104. Bogoyavlenski, A.T., Anodic Protection of Metals, Paper presented at the First Interuniversity Conference, Moscow, 1964, Reported by Diggle(96).

105. Schreider, A.V., J. Appl. Chem. USSR, 1966, **39**, 2533.

106. Setoh, S. and A. Miyata, Sci. Pap. Inst. Phys.

Chem. Res. (Tokyo), 1932, **19**, 237.

107.Setoh, S. and A. Miyata, Bull. Inst. Phys. Chem. Res. (Tokyo), 1932, **11**, 317.

108.Wernick, S. J. Electrodepositors' Tech. Soc., 1934, **9**, 153.

109.Baumann, W. Z. Phys., 1939, **111**, 708.

110.Akahoni, H., J. Electron Microscopy(Japan), 1961, **10**, 175.

111.Barrett, M.A., IVth Scandinavian Corrosion Congress, Helsinki, 1964, 41.

112.Hunter, M.S. and P.F. Towner, J. Electrochem. Soc., 1961, **108**, 139.

113.Dunn, C.G., Extended Abstracts,Electrochemical Society Meeting, Dallas, Texas, Spring, 1967, p. 54, reported by Diggle(96).

114.Kissan, G.H., "Anodized Aluminum", ASTM Special Technical Publication No. 388 (1965).

115.Murphy, J.F., Plating, 1967, **54**, 1241.

116.Morfopoulos, V.C.P. and H. C. Parruva, Corrosion Sci., 1967, **7**, 241.

117.Yokata, H., Denki-Kagaku, 1967, **35**, 14.

118.Tajima, S., N. Baba, and M. Shimura, Electrochim. Acta, 1967, **12**, 955.

119.Brock, A.J. and G.C. Wood, Electrochim. Acta, 1967, **12**, 395.

120.Franklin, R.W., Nature, 1957, **180**, 1470.

121.Hoar, T.P. and J. Yakalom, J. Electrochem. Soc., 1954, **101**, 389.

122.Emmer, I., Z. Hajek, and P. Repa, Surface Sci., 1985, **162**, 303.

123.Kudo, T., R.S. Alwitt, Electrochim. Acta, 1978, **23**, 341.

124.O'Sullivan, J.P., J. A. Hockey, and G.C. Wood, Trans. Faraday Soc., 1969, **65**, 535.

125.Dorsey, G. A., J. Electrochem. Soc., 1966, **113**, 169.

126.Dorsey, G. A., J. Electrochem. Soc., 1966, **113**, 172.

127.Belov, V. T., E. N. Shlyapkina, Y. A. Fomichev, Translated from Zhurnal Prikiadnoi Khimu, 1986, **59**, 424.

128.Konno, H., S. Kobayashi, H. Takahashi, and M. Nagayama, Electrochim. Acta, 1980, **26**, 1167.

129.Treverton, J. A. and N. C. Davies, Electrochim. Acta, 1980, **25**, 1571.

130.Micromeritics Accusorb 2100E; Physical Adsorption Analyzer Manual, 1979.

131.Dr. Larry Wieserman, Alcoa Technical Center, Alcoa Center, PA.

132.Scofield, J.H., J. Electron Spectrosc, Relat.

Phenom., 1975, **5**, 129.

133.Dillard J.G., C.V. Schenck, and M.H. Koppelman, Clays Clay Miner., 1983, **31**, 69.

134.Alcoa Technical Center, Alcoa Center, PA.

135.Micropore Analysis by T-plot Method, Micromeretics Instrument Corporation, Norcross, GA.

136.Wefers,K and G. M. Bell, Alcoa Technical publication no. 19., 1972.

137.Alpert, N.L., W.E. Keiser, and H.A. Szymanski, Theory and Practice of Infrared Spectroscopy, Plenum Press: New York, 1964, p. 337.

138.Matulewicz, E.R., I.P.J.M. Kerkhof, J.A. Moulin, and H.J. Reitsma, J.Colloid Interface Sci., 1980, **77**, 110.

139.Hughes, T.R. and H.M. White, J. Phys. Chem., 1967, **71**, 2192.

140.Ramquivist, L., K. Hamrin, G. Johansson, A. Fahlman, C. Nording, J. Phys. Chem., 1969, **30**, 1835.

Appendix 1

Basic program for calculation of volume of Krypton or Nitrogen adsorbed.

```
3 DIM V(100)
4 CLEAR
5 REM program name: surface areal.ba
6 OPEN "o", #3, "surface"
7 PRINT "Identification number";
8 INPUT A$
9 LPRINT CHR$(17); A$
10 PRINT "Enter w1";
20 INPUT W1
30 PRINT "Enter w2";
40 INPUT W2
50 LET W3=W1-W2
60 LET X=132.57
70 PRINT "Enter H1";
80 INPUT H1
90 PRINT "Enter H2";
100 INPUT H2
110 PRINT "Enter Ts";
120 INPUT T1
130 LET V1= 30.94
140 PRINT "Nitrogen or Krypton(1,2)";
150 INPUT Y
160 IF Y<>1 THEN 210
170 LET P4=729.398
180 LET A1=6.6*10^-5
190 LET S=16.2
200 GOTO 280
210 IF Y=2 THEN 240
220 PRINT "must be 1 or 2"
230 GOTO 140
240 LET P4=2.297
250 LET A1=3!*10^-5
260 LET S=21
280 LET T2=(307.2+T1)/2
290 LET V2=(T1/H2)*(((V1*(H1-H2))/307.2)-((3.65*
H2)/T2))
300 LET B=((.3593*V2)/(T1*W3))+(1.311/(T2*W3))
310 LET C=(.3593*V2*A1)/(W3*T1)
340 PRINT "Enter p1 and p2, to stop enter 1 for
both"
```

```
341 DIM P1(100)
342 DIM P2(100)
343 DIM P3(100)
344 DIM D(100)
345 DIM E(100)
346 DIM F(100)
347 DIM G(100)
348 DIM H(100)
349 DIM J(100)
350 DIM Z(100)
352 DIM P(100)
353 FOR N=1 TO 100
360 PRINT "P1(";N;"):";
370 INPUT P1(N)
380 PRINT "P2(";N;"):";
390 INPUT P2(N)
400 IF P1(N)=1 AND P2(N)=1 THEN 575
401 PRINT "extra volume used yes(1) or no(2)";
402 INPUT C1
403 IF C1=1 THEN 406
404 LET A=.001169*V1/W3
405 GOTO 410
406 LET A=.001169*(V1+X)/W3
410 IF N<>1 THEN 440
420 P3(N)=0
430 GOTO 450
440 P3(N)=P2(N-1)
450 LET D(N)=P1(N)-P2(N)
460 LET E(N)=P2(N)-P3(N)
470 LET F(N)=(P2(N)^2)-(P3(N)^2)
480 LET G(N)=A*D(N)
490 LET H(N)=B*E(N)
500 LET J(N)=C*F(N)
510 LET Z(N)=G(N)-H(N)-J(N)
520 LET V(N)=V(N-1)+Z(N)
530 PRINT "Volume adsorbed (";N;")=";V(N)
535 LPRINT CHR$(17);"Volume adsorbed(";N;")=";V(
N)
540 LET P(N)=P2(N)/P4
550 PRINT "P(";N;")=";P(N)
555 LPRINT CHR$(17); "P(";N;")=";P(N)
560 NEXT N
570 CLOSE #3
575 PRINT "Do you want to continue yes(1) or No(
2)";
580 INPUT C2
585 CLOSE #3
590 IF C2=1  GOTO 6
595 IF C2=2 GOTO 9999
9999 END
```

The vita has been removed from the scanned document